

University of Montana

## ScholarWorks at University of Montana

---

Graduate Student Theses, Dissertations, &  
Professional Papers

Graduate School

---

1997

### Probing and cleaving the 16S rRNA : structural studies of the small ribosomal subunit

Brennan S. Sawyer  
*The University of Montana*

Follow this and additional works at: <https://scholarworks.umt.edu/etd>

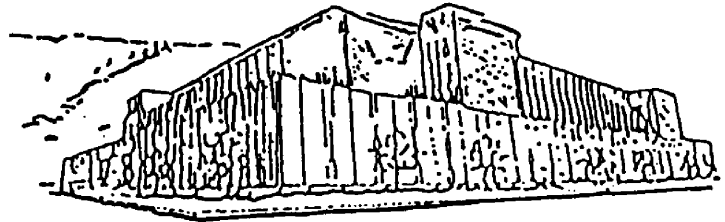
**Let us know how access to this document benefits you.**

---

#### Recommended Citation

Sawyer, Brennan S., "Probing and cleaving the 16S rRNA : structural studies of the small ribosomal subunit" (1997). *Graduate Student Theses, Dissertations, & Professional Papers*. 6636.  
<https://scholarworks.umt.edu/etd/6636>

This Thesis is brought to you for free and open access by the Graduate School at ScholarWorks at University of Montana. It has been accepted for inclusion in Graduate Student Theses, Dissertations, & Professional Papers by an authorized administrator of ScholarWorks at University of Montana. For more information, please contact [scholarworks@mso.umt.edu](mailto:scholarworks@mso.umt.edu).



Maureen and Mike  
**MANSFIELD LIBRARY**

The University of **MONTANA**

---

Permission is granted by the author to reproduce this material in its entirety, provided that this material is used for scholarly purposes and is properly cited in published works and reports.

*\*\* Please check "Yes" or "No" and provide signature \*\**

Yes, I grant permission  \_\_\_\_\_  
No, I do not grant permission  \_\_\_\_\_

Author's Signature Burman Sawyer

Date 5/8/97

Any copying for commercial purposes or financial gain may be undertaken only with the author's explicit consent.



**Probing and cleaving the 16S rRNA:  
structural studies of the small  
ribosomal subunit**

by  
**Brennan S. Sawyer**  
B.S., University of Montana 1993


Presented in partial fulfilment of the  
requirements for the degree of

**Master of Sciences**

**The University of Montana**  
1997

Approved by:

  
Chairman, Board of Examiners

  
Dean, Graduate School

8-12-97

Date



UMI Number: EP37437

All rights reserved

**INFORMATION TO ALL USERS**

The quality of this reproduction is dependent upon the quality of the copy submitted.

In the unlikely event that the author did not send a complete manuscript and there are missing pages, these will be noted. Also, if material had to be removed, a note will indicate the deletion.



UMI EP37437

Published by ProQuest LLC (2013). Copyright in the Dissertation held by the Author.

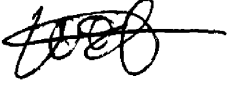
Microform Edition © ProQuest LLC.

All rights reserved. This work is protected against unauthorized copying under Title 17, United States Code



ProQuest LLC.  
789 East Eisenhower Parkway  
P.O. Box 1346  
Ann Arbor, MI 48106 - 1346

Probing and cleaving the 16S rRNA: structural studies of the small ribosomal subunit

Director: Walter E. Hill 

ABSTRACT

DNA probes complementary to the 1050 and 1200 regions were used to determine the accessibility of helix 34. The lack of probe binding and difficulties in obtaining digestion by ribonuclease H suggest this region of the 16S rRNA is not available. The addition of a messenger RNA analog, poly-U, or a crude mixture of translational factors, S150 fraction, did not increase probe binding, suggesting again that helix 34 is yet unavailable for probe binding.

T7 RNA polymerase was used to generate analogs of the anticodon loop of *E. coli* tRNA<sup>Phe</sup>. These microhelices were modified to contain thiol groups either by the addition of 4-thiouridine to the transcription reaction or by thiophosphorylating the 5' end of the microhelix. Phenanthroline could be tethered to the microhelices via the thiol groups. When bound to the P-site on programmed 30S ribosomal subunits phenanthroline could cause the cleavage of nearby nucleic acids if copper ions and a reducing agent are present. Sufficient quantities of thiol-modified microhelix could not be generated and cleavage reactions could not be performed.

Phenanthroline was used to map the tRNA binding site on programmed 30S ribosomal subunits by tethering it to positions 8 and 32 of tRNA<sup>Arg</sup>, position 8 of tRNA<sup>Phe</sup>, and position 34 of tRNA<sup>Glu</sup>. Under one set of reaction conditions cleavages were seen corresponding to nucleotides 198, 199, 840, 846, and 923-930 of the 16S ribosomal RNA, but under various other conditions cleavages were not observed. Definitive conclusions stating the cleavages are generated by phenanthroline tethered to tRNA can not be drawn.

## **Acknowledgements**

I wish to thank my family and friends for their support throughout my academic career. I would also like to thank Dr. Hill for giving me the opportunity to work in his lab. This has been one of the great learning experiences of my life. Thank you all.

## Table of contents

Abstract.....	ii
Acknowledgements.....	iii
Table of contents.....	iv
List of tables.....	vi
List of figures.....	vii
Abbreviations.....	viii
Introduction.....	1
1.0 General ribosome structure.....	1
1.1 Translation.....	7
1.2 Initiation of translation.....	7
1.3 Elongation.....	9
1.3.1 Classical model of elongation.....	9
1.3.2 Allosteric three-site model of elongation.....	10
1.3.3 Hybrid states model of elongation.....	12
1.3.4 The waggle model.....	12
1.3.5 The $\alpha/\epsilon$ model of elongation.....	14
1.4 Termination of protein synthesis.....	16
1.5 Important rRNAs.....	16
1.5.1 Helix 34.....	17
1.5.2 Helix 18 (the 530 loop).....	17
1.5.3 The 3' minor domain.....	18
1.6 The tRNA nest.....	20
1.7 tRNA structure.....	21
1.8 Phenanthroline-mediated cleavage.....	23
1.8.1 Disadvantages of other mapping techniques.....	23
1.8.2 Problems with tethered phenanthroline.....	25
1.9 Experimental designs.....	25
1.9.1 Probing helix 34.....	26
1.9.2 Mapping the anticodon loop binding site.....	26
1.9.3 Mapping the tRNA binding site on 30S subunits.....	28
Materials and methods	
2.1 Ribosome preparation.....	32
2.2 DNA synthesis and purification.....	33
2.3 Oligomer binding specificity.....	33
2.3.1 RNase H assays on ribosomes of 30S subunits.....	33
2.3.2 RNase H assays on extracted rRNA.....	34
2.4 5' end labeling of DNA oligomers.....	35
2.4.1 Phosphorylation.....	35

2.4.2	Autoradiography.....	35
2.5	Filter-binding assays (with DNA oligomers).....	35
2.6	4-thio-UTP synthesis.....	36
2.7	Microhelix template preparation.....	37
2.8	Microhelix transcription and purification.....	37
2.9	Thiophosphorylation of microhelices.....	38
2.10	5' end labeling of microhelices.....	39
2.11	Phenanthroline attachment to microhelices in an organic medium.....	39
2.12	Enzymatic sequencing of mhRNA.....	40
2.13	Filter-binding assays with mhRNA.....	40
2.14	tRNA sulfhydryl removal.....	40
2.15	Phenanthroline attachment to tRNAs.....	41
2.15.1	IOP tethering in an organic medium.....	41
2.15.2	IOP tethering in an aqueous medium.....	41
2.16	5' end labeling of OP-tRNAs.....	41
2.17	Filter-binding assays with OP-tRNAs.....	42
2.18	Cleavage reactions with OP-tRNAs.....	43
2.18.1	Cleavage reaction.....	43
2.18.2	template preparation.....	43
2.19	Primer-extension analysis.....	45

## Results

3.1	RNase H assays.....	48
3.2	Oligomer end labeling.....	48
3.3	Oligomer filter-binding assays.....	50
3.4	Microhelix template annealing.....	54
3.5	Microhelix transcriptions.....	56
3.5.1	Thio transcriptions.....	58
3.6	End labeling of microhelices.....	58
3.7	Enzymatic sequencing of mhRNA.....	60
3.8	Thiophosphorylation of mhRNA.....	60
3.9	Phenanthroline attachment of microhelices.....	62
3.10	Microhelix filter-binding assays.....	62
3.11	tRNA sulfhydryl removal.....	66
3.12	Phenanthroline tethering of tRNAs.....	70
3.12.1	OP attachment in an organic medium.....	70
3.12.2	OP attachment in an aqueous medium.....	72
3.13	End labeling of OP-tRNAs.....	74
3.14	OP-tRNA binding studies.....	74
3.15	OP-tRNA cleavage experiments.....	77
3.15.1	Cleavage experiments, using free IOP as a control.....	80
3.15.2	Cleavage experiments using NOP mock controls.....	80
3.15.3	Cleavage experiments with dialyzed tRNAs.....	82
3.15.4	Cleavage experiments with updated controls.....	84

## Discussion

4.1	Helix 34 probing study.....	87
-----	-----------------------------	----

4.2 Anticodon loop analog (microhelix) studies.....90  
4.3 Natural E. coli tRNA studies.....93  
References.....106

**List of tables**

Table 1.1 Summary of small subunit cross-links and chemical protections from mRNA and tRNA.....19

Table 2.1 List of primers used in primer-extension assays.....46

Table 3.1 Summary of DNA oligomer binding results.....53

Table 3.2 Summary of MHS<sup>+</sup> binding results in various buffer conditions.....69

## List of figures

Figure 1.1	Secondary structure of the 23S rRNA.....	2
Figure 1.2	Secondary structure of the 16S rRNA.....	4
Figure 1.3	Line drawings of the 30S ribosomal subunit.....	6
Figure 1.4	Cryoelectron micrographs of the 70S ribosome.....	8
Figure 1.5	3-site allosteric model of elongation.....	11
Figure 1.6	Hybrid states model of elongation.....	13
Figure 1.7	The $\alpha/\epsilon$ model of elongation.....	15
Figure 1.8	Tertiary structure of yeast tRNA <sup>Phe</sup> .....	22
Figure 1.9	Chemical structures of OP, IoP, NoP, AoP, and neocuproine.....	24
Figure 1.10	DNA oligomers used in the helix 34 probing study.....	27
Figure 1.11	Secondary structure of microhelices.....	29
Figure 1.12	Secondary structures of tRNA <sup>Gle</sup> , tRNA <sup>Phe</sup> , and tRNA <sup>Arg</sup> .....	31
Figure 2.1	Structure of mRNA-A1.....	44
Figure 3.1	RNase H assay.....	49
Figure 3.2	Oligomer autoradiogram.....	51
Figure 3.3	Probe binding curve.....	52
Figure 3.4	Microhelix template hybridization.....	55
Figure 3.5	Transcription of MHS <sup>+</sup> .....	57
Figure 3.6	MHS <sup>+</sup> autoradiogram.....	59
Figure 3.7	MHS <sup>+</sup> sequencing.....	61
Figure 3.8	Thiophosphorylation and OP tethering of MHS <sup>+</sup> .....	63
Figure 3.9	OP tethering to thiolated MH39U.....	64
Figure 3.10	FBA: MHS <sup>+</sup> competition with excess MHS <sup>+</sup> .....	65
Figure 3.11	FBA: MHS <sup>+</sup> competition with yeast tRNA <sup>Phe</sup> .....	67
Figure 3.12	FBA: MHS <sup>+</sup> binding at various ratios.....	68
Figure 3.13	Sulfhydryl destruction and OP tethering to tRNA.....	71
Figure 3.14	OP tethering to tRNA <sup>Glu</sup> .....	73
Figure 3.15	tRNA autoradiogram.....	75
Figure 3.16	FBA: OP-tRNA <sup>Glu</sup> .....	76
Figure 3.17	FBA: OP-tRNA <sup>Arg</sup> .....	78
Figure 3.18	FBA: unmodified-tRNA <sup>Phe</sup> .....	79
Figure 3.19	OP-tRNA <sup>Arg</sup> cleavage.....	81
Figure 3.20	3' end cleavages.....	83
Figure 3.21	Cleavage with dialyzed tRNA <sup>Phe</sup> .....	85
Figure 4.1	16S rRNA map with tRNA <sup>Arg</sup> cleavages.....	100



## Abbreviations

aatRNA.....	amino acyl transfer ribonucleic acid
AoP.....	Acetamido-1,10-phenanthroline
APM.....	[(N-acryloylamino)phenyl]mercuric chloride
Arg.....	arginine
ATP.....	adenosine triphosphate
A-site.....	acceptor site of ribosome
BABE.....	1-(p-bromacetamidobenzyl)-EDTA
BSA.....	bovine serum albumin
C.....	celsius
cDNA.....	complementary deoxyribonucleic acid
Ci.....	curie
cm.....	centimeter
CPM.....	counts per minute
dATP.....	deoxyadenosine triphosphate
dCTP.....	deoxycytosine triphosphate
ddNTP.....	dideoxynucleoside triphosphate
dGTP.....	deoxyguanosine triphosphate
DNA.....	deoxyribonucleic acid
dTTP.....	deoxythymine triphosphate
DTT.....	dithiothreitol
<u>E. coli</u> .....	<i>Escherichia coli</i>
EDTA.....	ethylenediamine tetra-acetic acid
EF-G.....	elongation factor G
EF-Tu.....	elongation factor Tu
E-site.....	exit site of the ribosome
fMet-tRNA...	formylmethionine transfer ribonucleic acid
g.....	gram
GDP.....	guanosine diphosphate
Glu.....	glutamic acid
GTP.....	guanosine triphosphate
HEPES.....	[N-2-hydroxyethylpiperazine-N'-Ethanesulfonic Acid]
HPLC.....	high pressure liquid chromatography
IF1.....	initiation factor 1
IF2.....	initiation factor 2
IF3.....	initiation factor 3
IoP.....	5-iodoacetamido-1,10-phenanthroline
PEG.....	polyethylene glycol
Phe.....	Phenylalanine
L.....	liter
mA.....	milliamperes
mhRNA.....	microhelix ribonucleic acid
min.....	minute
mL.....	milliliter
mM.....	millimolar
MPA.....	mercapto propionic acid
mRNA.....	messenger ribonucleic acid
NoP.....	5-nitro-1,10-phenanthroline
nt.....	nucleotide
NTP.....	nucleotide triphosphate

oP.....1,10-phenanthroline  
oP-mhRNA.....phenanthroline-microhelix ribonucleic acid  
                  complex  
oP-tRNA.....phenanthroline-transfer ribonucleic acid  
                  complex  
PAGE.....polyacrylamide gel electrophoresis  
pmol.....picomol  
PNK.....polynucleotide kinase  
P-site.....peptidyl site of the ribosome  
RF1.....release factor 1  
RF2.....release factor 2  
RF3.....release factor 3  
RNA.....ribonucleic acid  
RNase H.....ribonuclease H  
rpm.....revolutions per minute  
rRNA.....ribosomal ribonucleic acid  
S.....Svedberg units  
SAP.....shrimp alkaline phosphatase  
sP-mhRNA.....thiophosphorylated microhelix ribonucleic acid  
TEB.....transient electric birefringence  
tRNA.....transfer ribonucleic acid  
tRNA-SH.....dethiolated transfer ribonucleic acid  
xg.....times gravity  
UDP.....uridine diphosphate  
µg.....microgram  
µL.....microliter  
µM.....micromolar  
µm.....micrometer  
UTP.....uridine triphosphate  
UV.....ultraviolet  
vac.....vacuum  
vol.....volume  
v/v.....volume per volume  
W.....watts  
w/v.....weight per volume

## **INTRODUCTION**

The ability to synthesize proteins is vital to all life forms. It is these proteins which are utilized by all living organisms as structural components and metabolism. Ribosomes are the essential responsible for protein synthesis. A copy of the genetic code in the form of a messenger RNA (mRNA) is decoded on the ribosome using transfer RNA (tRNA) molecules which carry specific amino acids. One of life's great questions is how, exactly, does the ribosome orchestrate the interactions of the vast array of molecules involved in protein biosynthesis. As a model system, the Escherichia coli ribosome is studied to gain an understanding of this complex subcellular ballet.

### **1.0 General ribosome structure**

The Escherichia coli ribosome is the macromolecular ribonucleoprotein complex which carries out protein synthesis within the bacteria's cell. The E. coli ribosome, which has a sedimentation coefficient of 70S, is composed of two unequal subunits. The large subunit sediments at 50S and is made up of 34 proteins and two RNA molecules, the 23S rRNA (Fig 1.1) and the 5S rRNA (2904 nt and 120 nt, respectively). The small subunit, which sediments at 30S, contains only one strand of RNA, the 16S rRNA (1594 nt) (Fig. 1.2), along with 21 proteins. By looking at the conserved bases among various organisms secondary structure maps of the various rRNAs were proposed (29,31,72,109) and their helical segments numbered (3).

With the inability to grow crystals for x-ray crystallography, electron micrographs of E. coli ribosomes and ribosomal subunits provided some of the first physical

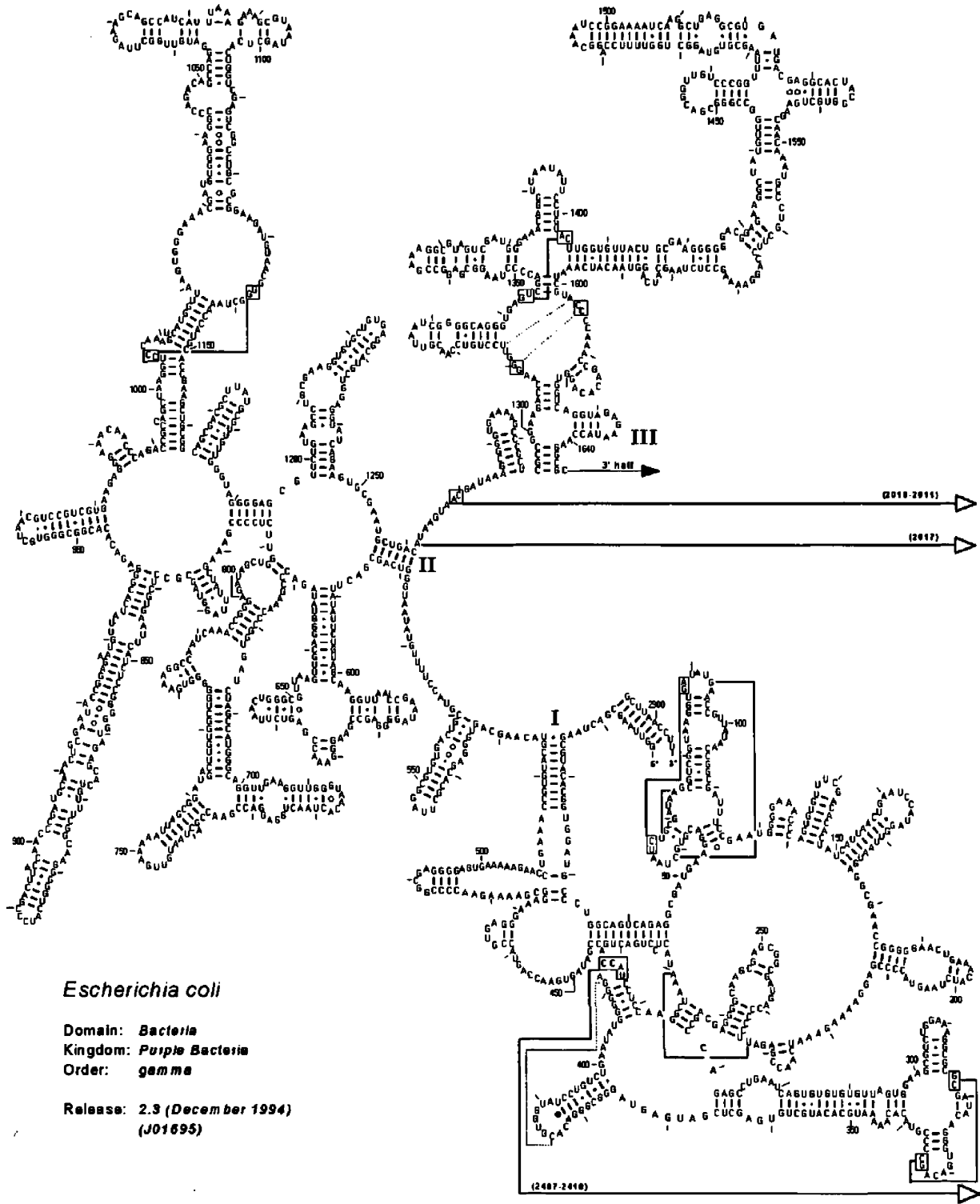
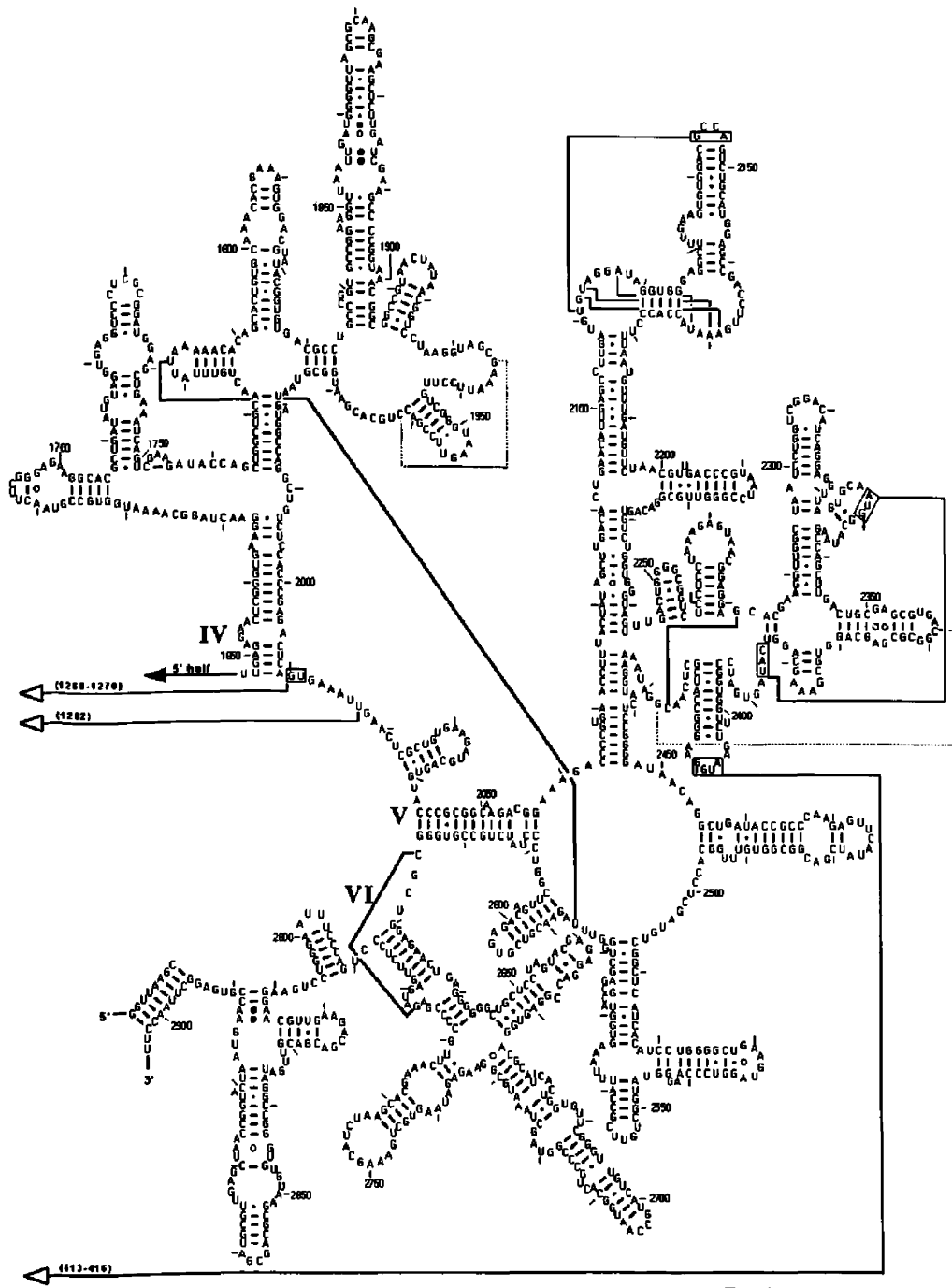


Figure 1.1 Secondary structure of the 5' half of the *E. coli* 23S rRNA as proposed by Gutell (28,71). Figure taken from the ribosomal data base in the world wide web.



*Escherichia coli*

Domain: *Bacteria*  
 Kingdom: *Purple Bacteria*  
 Order: *gamma*

Release: 2.3 (December 1994)  
 (J01695)

Figure 1.1 continued. The 3' half of the 23S rRNA from *E. coli*.

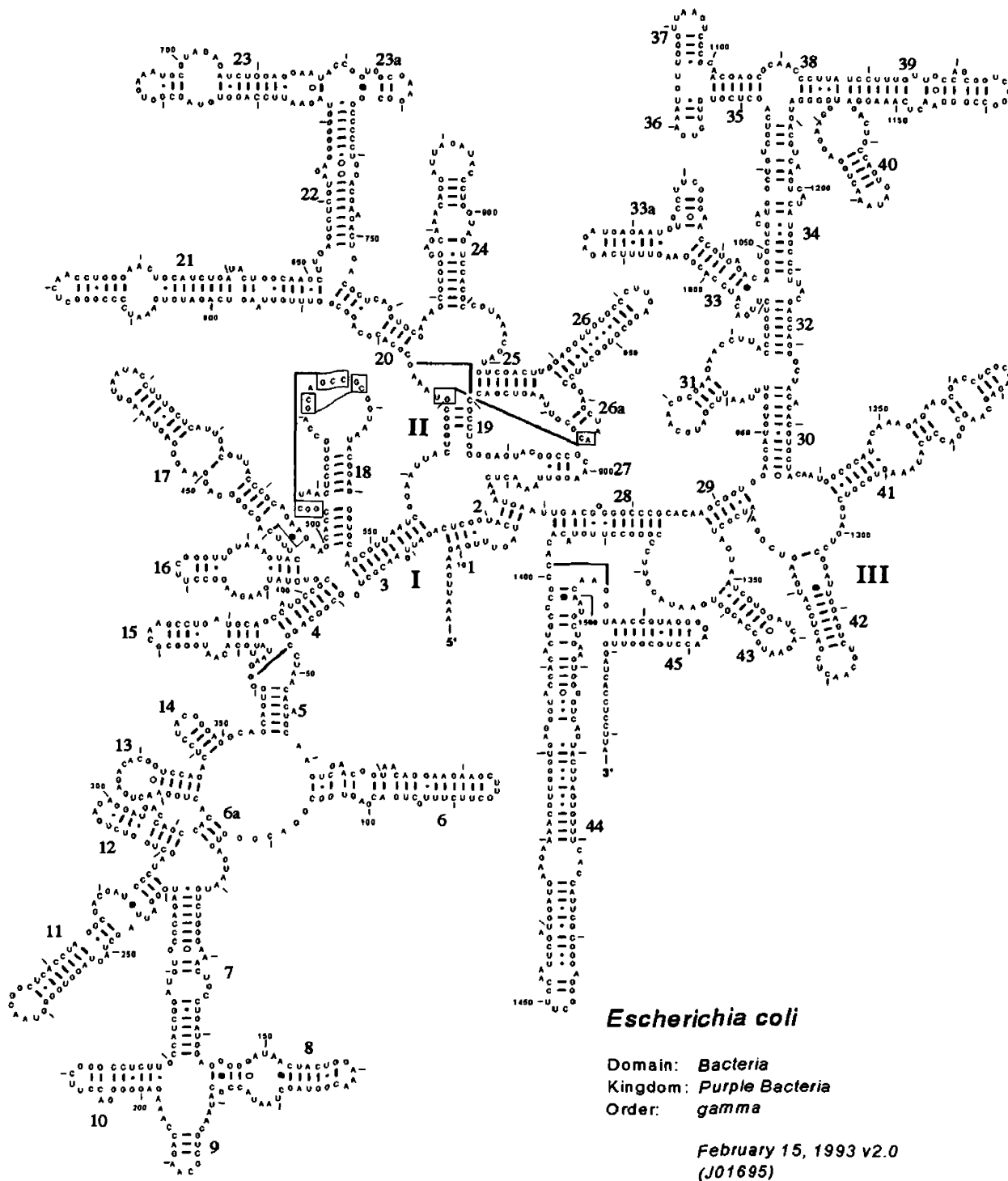


Figure 1.2 Secondary structure of the 16S rRNA as proposed by Gutell (28,30) with helix numbers based on Brimacombe (2). Figure taken from the ribosomal database in the world wide web.

descriptions of the ribosome (48,49). The ribosome was found to be roughly a 200Å diameter sphere. The observed dimensions of the ribosome varied depending on the method of ribosome preparation and the method of study (38). The small subunit was found to have several characteristic structural features including a distinct head, neck, body, and platform (Fig 1.3) (47). These early electron microscopy studies were met with both excitement and criticism. There was a great deal of excitement at actually having a visual representation of the ribosome. This technique was not perfect, with the greatest concern being some of the steps required in the preparation of the ribosome samples for the electron microscope. Samples had to be fixed, typically in glutaraldehyde, which may have locked the ribosome in an unnatural conformation. Additionally, any water in the transmission electron microscope's chamber would have caused blurring of the image along with other imaging problems. Therefore, samples had to be completely dehydrated. For this reason some researchers did not put as much faith in these pictures saying "you are looking at the raisin rather than the grape". In recent years, ribosomes prepared in vitreous ice have yielded high resolution electron micrographs of the 70S ribosome and the ribosomal subunits (20,95). These new pictures of the ribosome showed most of the familiar structures first described by Lake (47), but the new images showed these elements in greater detail and identified new structural features (50). This latest work has even shown slight structural differences between activated and unactivated 30S ribosomal subunits (Fig 1.4). Moreover, this new technique has reduced the problems of fixation and dehydration.

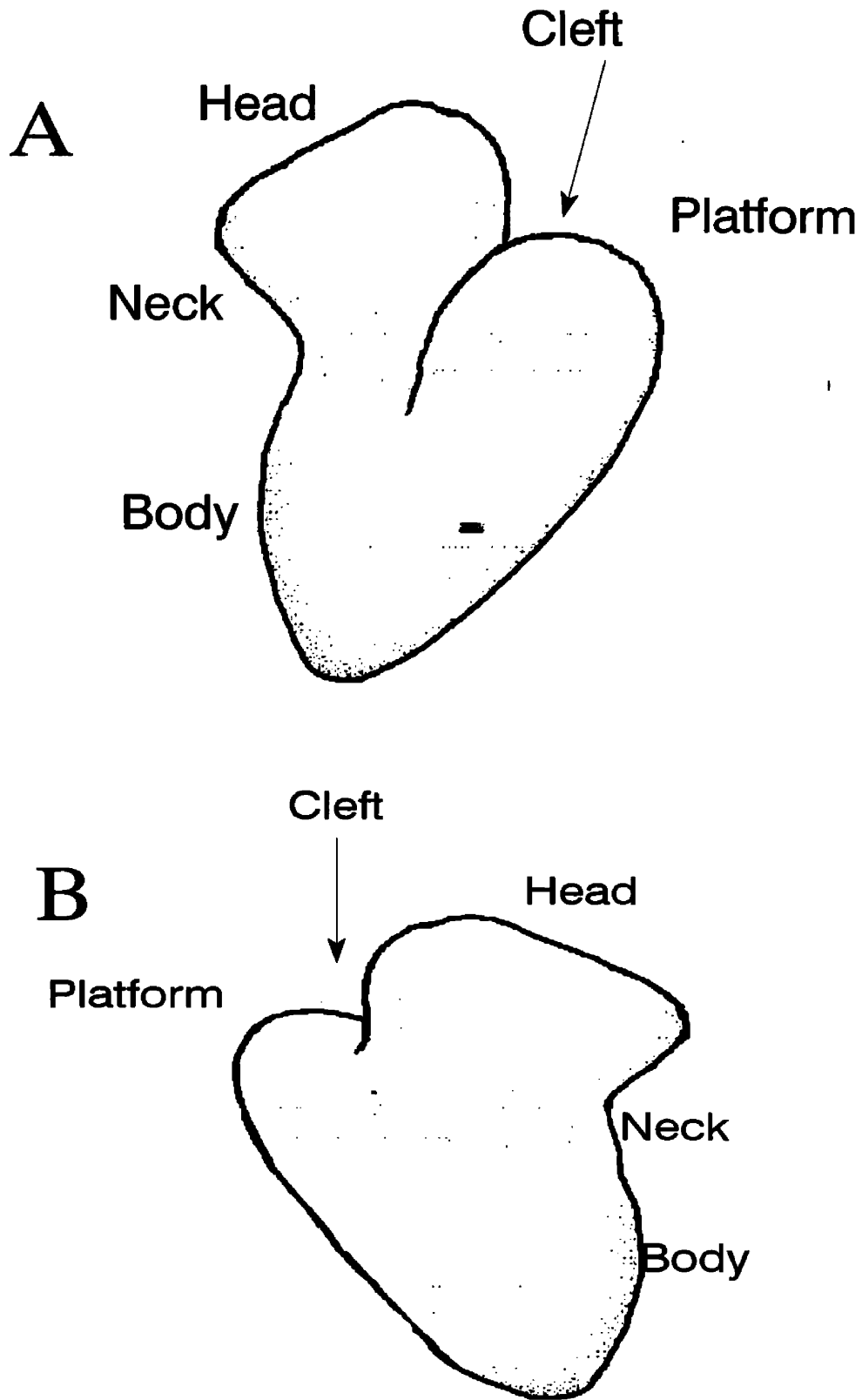


Figure 1.3 Line drawings of: A) the 50S face, and B) the cytoplasmic face of the small subunit adapted from Lake (46).



Neutron scattering has been used to measure the distance between two deuterated proteins in the small ribosomal subunit (62). From this, the center of mass for each of the 21 small ribosomal subunit proteins has been placed on a three-dimensional matrix within the outline of the 30S subunit (10) (Fig 1.5). Immunoelectron microscopy has also been used to map the location of the ribosomal proteins on the surface on the small subunit through the use of antibodies. Antibodies raised against specific ribosomal proteins were added to the ribosomes in the staining procedure. The antibody visualized in the electron micrographs indicated the location of a specific ribosomal protein. Surprisingly, there is very good agreement between the "neutron map" and the placement of the small subunit proteins as determined by immunoelectron microscopy (99). The few minor discrepancies have been attributed to inherent differences in the two techniques. Since its publication, the neutron map has become the gold standard when it comes to placement of proteins within the 30S subunit.

### **1.1 Translation**

Translation is the process by which a multitude of cellular components must sequentially interact in order for the ribosome to synthesize a protein. Transfer RNAs carrying specific amino acids are the first accessory molecule one thinks of when dealing with the ribosome, but several accessory proteins are required at all stages of protein synthesis.

### **1.2 Initiation of translation**

The fine details of initiation remain a mystery, as do most stages of protein

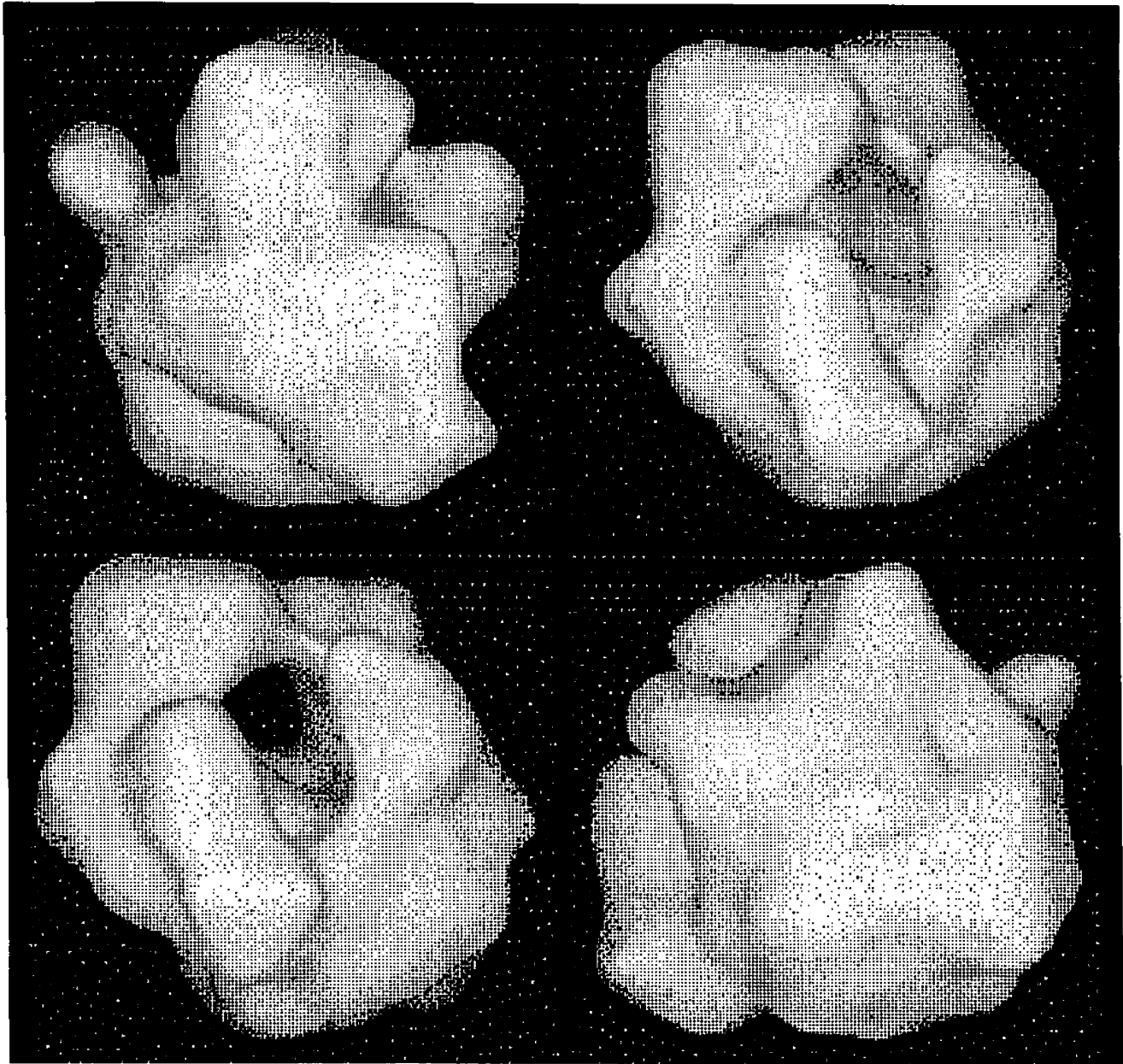


Figure 1.4 Cryoelectron micrographs of the 70S ribosome from E. coli adapted from Frank (19). Figure taken from the Wadsworth electron microscopy database in the world wide web.

synthesis. The initiation of protein synthesis involves three initiation factors (IF-1, IF 2, and IF-3), initiator tRNA acylated with formyl-methionine (fMET-tRNA<sup>fMET</sup>), the mRNA and of course the 30S subunit. The first step to begin the formation of a new protein is to disassociate the 70S ribosome into its two subunits, if they are not already free. The next stage is the association of the mRNA to the 30S subunit. This interaction is aided by base-pairing a segment of the mRNA (Shine-Dalgarno region) to a segment of the 16S rRNA (anti-Shine-Dalgarno region) (86,87). Once the mRNA is in place, the initiator tRNA can be escorted to the peptidyl site (P-site) by IF-2 carrying GTP to form the initiation complex (32,52). The interaction of IF2 and the initiator tRNA seems to be aided by IF3 (33). The 50S subunit now binds to the 30S subunit, displacing all of the accessory proteins, and the ribosome is now ready to enter the elongation stage of protein synthesis.

### **1.3 Elongation**

During this stage of protein synthesis, charged tRNAs carrying amino acids (aa-tRNAs) along with two elongation factors (EF-G and EF-Tu) are used to lengthen the nascent peptide.

#### **1.3.1 Classical model of elongation**

The classical model for ribosome function was first proposed by Watson in 1964 (106). This model was based mostly in theory since little information about ribosomes or tRNAs was available at the time, and in a general manner it was surprisingly accurate. This model proposed an incoming tRNA carrying an amino acid undergoes a codon-anticodon recognition with the mRNA. Later evidence showed the acylated

(amino acid carrying) tRNA binds to EF-Tu and GTP to form a ternary complex. An acylated tRNA having an anticodon that can base pair exactly with the codon of the mRNA (cognate tRNAs), while still within the ternary complex, will stay in this first active site called the aminoacyl site (A-site). The bound GTP is hydrolyzed and EF-Tu/GDP is released from the ribosome. In the cytoplasm, EF-Tu is recharged with GTP and is now ready to bind another tRNA and continue the cycle. Kinetic data suggested a second copy of EF-Tu is involved in the elongation step, but where and how are not known (10). When the peptide bond is formed, the A-site tRNA moves to the peptidyl site (P-site) through a process called translocation. In addition, the mRNA is thought to move a distance of three bases so the next codon is correctly positioned in the A-site. After GTP hydrolysis, EF-G/GDP is released and recycled in the cytoplasm. In the translocation step, the growing peptide chain is transferred from the 3' terminus of the P-site tRNA to the A-site tRNA. The P-site tRNA is now ejected from the ribosome.

### **1.3.2 Allosteric three-site model of elongation**

As a refinement of the classical model of elongation the allosteric three-site model of elongation (Fig 1.6) has been proposed by Nierhaus. In this model a third tRNA binding site, the exit site (E-site), exists adjacent to the P-site. As the A-site tRNA is translocated to the P-site, the now deacylated P-site tRNA is translocated to the E-site. One of the major tenets of this model is that the A-site and E-site are linked in a negative cooperativity (79). After translocation, the tRNAs are in the P and E-sites and the A-site has a very low affinity for tRNA. When aminoacyl tRNA occupies the

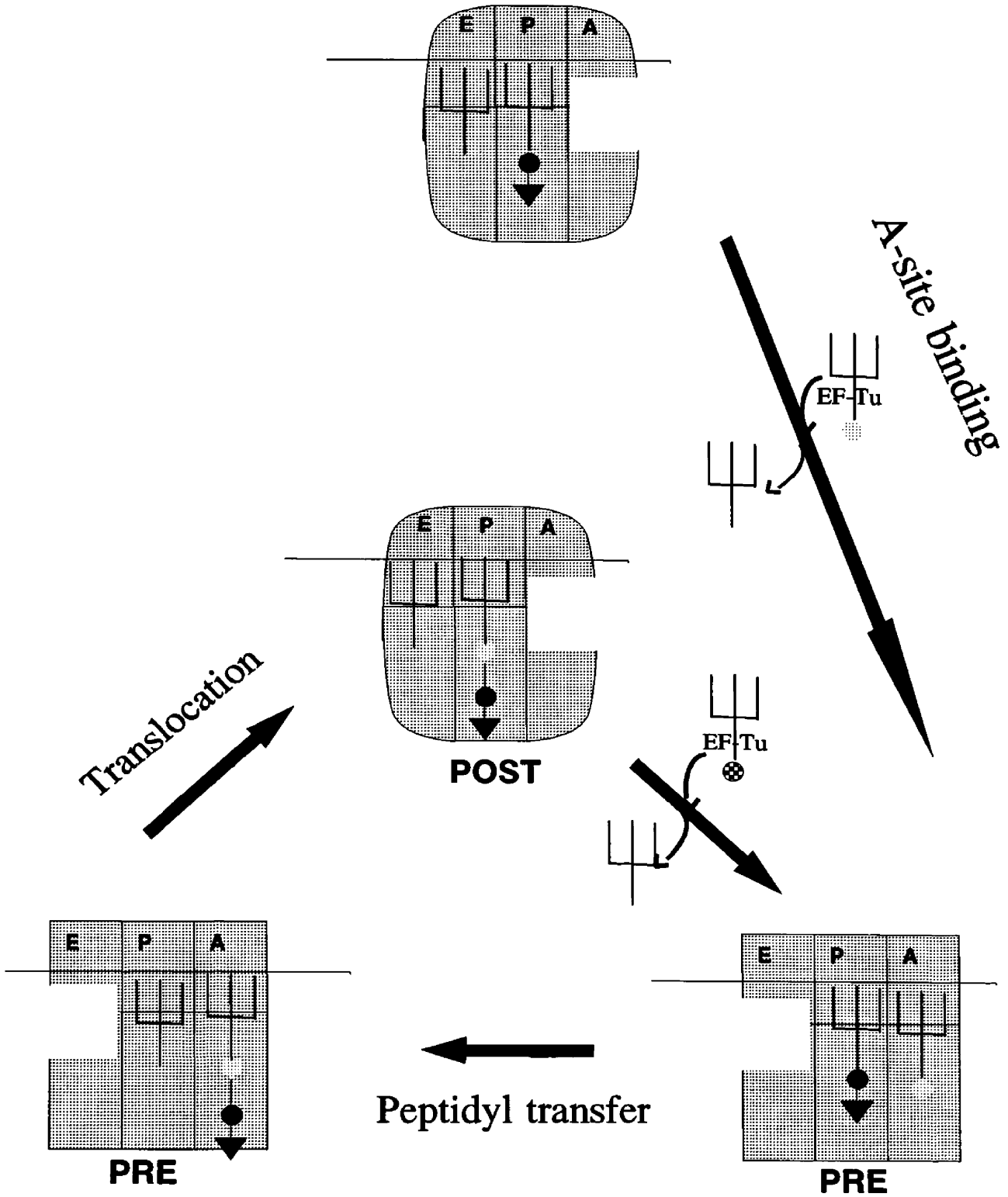


Figure 1.5 The 3-site allosteric model of elongation adapted from Nierhaus (65,66).

A-site, the A-site now has a high affinity for tRNA giving the E-site low affinity for its deacyl tRNA, which causes its release. Additionally, this model proposes two ribosomal conformations, the pretranslocational state and the posttranslocational state. In the pretranslocation state the A and P-sites are occupied and the now low affinity E-site is empty. After translocation the ribosome is in the posttranslocation state, and the P and E-site are occupied. The A-site has a low affinity for tRNA and is empty (24,66,78).

### **1.3.3 Hybrid states model of elongation**

The hybrid states model of elongation has gained popularity with many researchers. At its core, this model suggests that mRNA/tRNA movement through the ribosome occurs in two discrete steps (Fig 1.7). It is easiest to think of the tRNAs as ratcheting their way through the ribosome rather than jumping sites entirely, as in the allosteric three sites model above. In the first stage, the anticodon loops of the tRNAs remain fixed while the acceptor stems cog to the next site on the large subunit. The A-site tRNA goes from an A/A site to a A/P site, and the P-site tRNA goes from P/P to P/E. The first letter denotes the binding site occupied on the 30S subunit, and the second letter denotes the tRNA binding site occupied on the 50S subunit. In the second stage the mRNA along with the anticodon loops of the tRNAs move with respect to the small subunit. The tRNA in the A/P site goes to a P/P site and the P/E site tRNA goes to the E-site (57-59).

### **1.3.4 The Waggle model**

The waggle theory of tRNA movement through the ribosome was proposed by

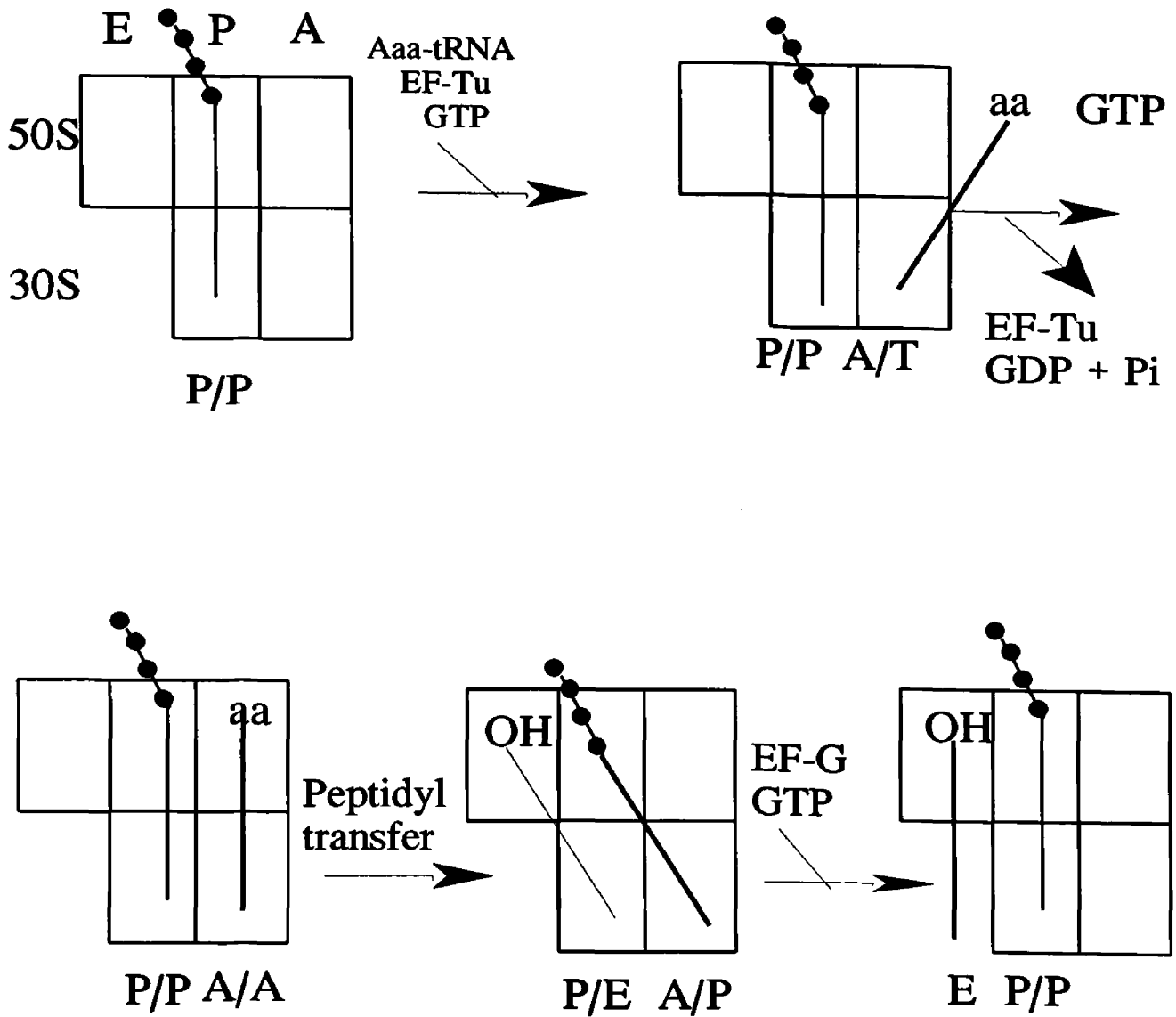


Figure 1.6 Hybrid states model of elongation adapted from Noller (58).

Yarus (91,92,112). The waggle hypothesis tries to draw a compromise between the hybrid states model of elongation and the 3-site allosteric model of elongation. According to the model, during decoding tRNAs undergo small but energetically significant shape changes as the ribosome also undergoes small but energetically significant conformational changes. This model also makes an attempt to explain how proof reading can occur on the rapidly translating ribosome. Slowed cognate tRNA disassociation is caused by a conformational change (waggle) in the tRNAs anticodon domain. This model is based primarily on energetic arguments with little direct evidence to support it. Furthermore, the waggle hypothesis adds little to the understanding of ribosome function.

### **1.3.5 The $\alpha/\epsilon$ model of elongation**

The newest model describing the elongation stage of protein synthesis is the  $\alpha/\epsilon$  model of elongation (Fig 1.8). This model was sparked by the observation that patterns of phosphorothioate-tRNA cleavage using iodine did not change during translocation. From this the existence of movable tRNA binding domains on the ribosome, with two adjacent tRNA binding sites, was proposed. The domain at the A-site (now the A-region) prior to translocation is referred to as the  $\alpha$ -site. The domain at the E-site (now E-region) after translocation is called the  $\epsilon$ -site. The P-site (now P-region) has no defined site, but rather it contains the  $\epsilon$ -site in the pretranslocational state and the  $\alpha$ -site in the posttranslocational state. The A-region contains a nonmovable decoding center named the  $\sigma$ -site. The  $\alpha$  and  $\epsilon$  domains move together with the tRNA and mRNA during translocation from the A and P regions to the P and



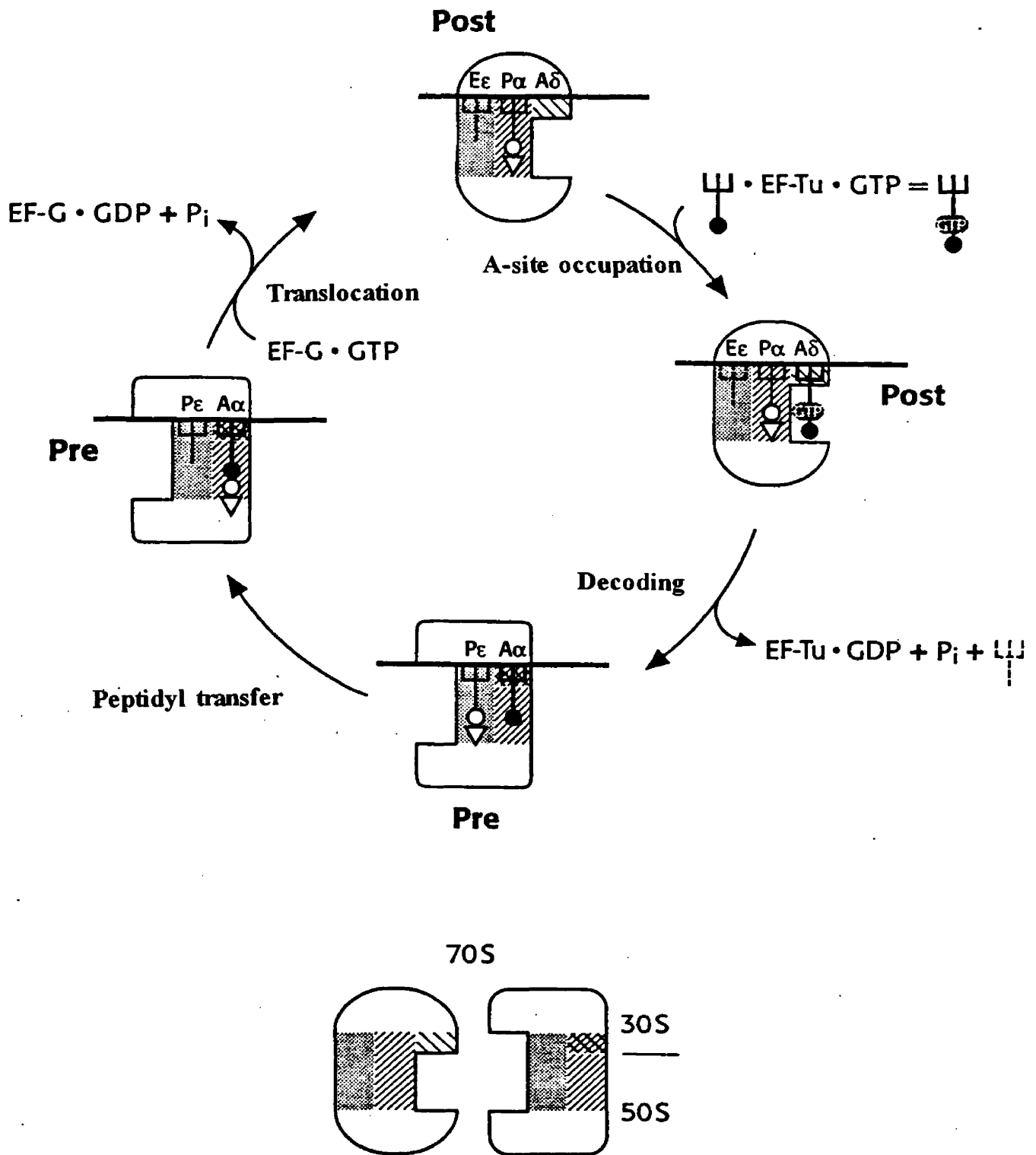


Figure 1.7 The  $\alpha/\epsilon$  model of elongation adapted from Nierhaus (66).

E regions respectively (67). This model is based primarily on the observed patterns of protection of phosphorothioate-substituted tRNAs on the ribosome in different binding sites. The model does seem to correlate well with previous data. However, the patterns of tRNA protection by the ribosome were not very great when the raw data were examined.

#### **1.4 Termination of protein synthesis**

The termination of protein synthesis leads to the hydrolysis of the ester bond between the carboxyl terminus to the nascent peptide and the 3' hydroxyl of the tRNA. Termination of protein synthesis begins when an in-frame stop codon enters the ribosomal A-site. Unlike sense codons that are decoded by specific tRNAs via RNA-RNA interactions, there are no tRNAs to decode the stop codons. Proteins called release factors (RFs) play a crucial role in the termination of protein synthesis. RF1 terminates UAA and UAG stop codons, and RF2 terminates UAA and UGA stop codons. A third protein (RF3) stimulates termination, but apparently it is not required for termination (14,102).

#### **1.5 Important rRNAs**

In the past, it was thought that the ribosomal RNAs served as a scaffolding to hold the ribosomal proteins in place, allowing them to carry out translation. It has become increasingly clear that the ribosomal RNAs themselves play an active role in translation, and the proteins act in part, to keep the rRNA in the proper conformation throughout the translational process (15,69). Recent studies have demonstrated the ability of the 23S rRNA to catalyze the formation of the peptide bond in the absence

of all ribosomal proteins, with the possibility of only a few peptide fragments remaining associated with the rRNA (71)).

### **1.5.1 Helix 34**

There are several regions of the 16S rRNA thought to play major roles in the translational process. Helix 34 (bases 1046-1067 and 1189-1211) was thought to play a dominant role in the termination of protein synthesis (25,63). It was once believed this helix participated in termination by physically base pairing with the stop codon of the mRNA (16,26). Recent studies have shown that this region of the 16S rRNA plays a more generalized role in termination (65). The function of helix 34 is not clearly defined, but mutations in this region profoundly affected the function of the ribosome; specifically the ability to terminate translation, and the overall health of the cell (61). Corroborating these functional studies, physical studies have assigned some importance to helix 34 in the translational process. A zero-length cross-link has been reported between base U1052 and the third base of the A-site codon of the mRNA (mRNA position +6) (17).

### **1.5.2 Helix 18 (the 530 loop)**

The 530 loop of the 16S rRNA is one of the most highly conserved of all rRNA domains (30). Again the exact function of this segment of rRNA is not known, but it appears to be crucial to ribosome function. The modification of G530 has been shown to decrease the binding of EF-Tu/tRNA (74). It is believed that the 530 loop undergoes conformational changes during the process of translation, presumably alternating between a pseudoknot and an open loop (109). This apparent

conformational change, combined with the implications of the EF-Tu binding studies, has led some ribosomologists to believe the 530 loop may serve as a switching mechanism which allows for movement of the tRNA through the ribosome (74).

### **1.5.3 The 3' minor domain**

The 3' minor domain of the 16S rRNA encompasses the 3' 150 nucleotides of the small subunit rRNA. This domain contains the 1400 and 1500 regions, both of which are highly conserved (86,87). As compared to most regions of the 16S rRNA, the structure and function of the 3' minor domain has been defined in greater detail. This region is the site of interaction of many ligands involved in translation. To begin with, this domain contains the anti-Shine-Dalgarno sequence (nucleotides 1535-1540), which is important for proper mRNA positioning on the 30S subunit. Protections due to P-site tRNA and A-site tRNA have also been observed in the 1400 and 1500 regions (56,60) (Table 1.1). This domain has also been implicated in IF3 binding and 50S subunit associations. Additionally, mutations or modifications in the 1400 and 1500 regions conferred resistance to many antibiotics (reviewed by Zimmermann) (115). Since so many molecules involved in the decoding process interact with the 3' minor domain, it has come to be commonly referred to as the decoding site.

The three regions of the 16S rRNA discussed here (helix 18, helix 34, and the 1400 region) have been cross-linked from mRNA analogs thereby localizing them to the decoding site (17). These results were recently duplicated using phenanthroline tethered to the +5 position of a mRNA analog (7). Cleavages were seen in the 530

### tRNA/16S rRNA cross-links

tRNA species	position in tRNA	site on ribosome	cross-linked nucleotide
E. coli Phe	8	P	1338, 1339
lupin Met	20	A	649, 711, 1335
		P	649, 711, 1342
E. coli Arg	32	A	936, 1378
		P	693, 957, 966, 1338
		E	693, 1376, 1378
E. coli Val	34	P	1400
E. coli Phe	47	P	701, 717, 1345, 1348
		E	701, 717

### mRNA/16S rRNA cross-links

position of mRNA	cross-linked nucleotide
5' end (-20 to -12)	523, 693, 723, 818, 845, 1167
+4	1402, 1408
+6	1052
+7	1395
+11	532
middle (-3 to +6)	532, 693, 723, 818, 845, 1167, 1381
3' end (+20 to 26)	412, 523, 723, 1381

### 16S rRNA protections by tRNA

A-site	529-531, 892, 1405, 1408, 1492-1498
P-site	532, 693, 794-795, 926, 966, 1338-1339, 1381, 1399-1401

Table 1.1 Summary of small subunit cross-links and chemical protections from tRNA and mRNA.

loop (528-532), helix 34 (1053-1055, and A1196) and in the 1400 region (A1396 and C1397). These segments of the rRNA have been implicated in participating in the decoding process (see below).

## **1.6 The tRNA nest**

The tRNAs move through a large channel between the 50S and 30S subunits of the ribosome (20,114), in which they temporarily reside in defined sites. Much of the work from other laboratories to more thoroughly define the tRNA binding sites has consisted of chemical protection and cross-linking studies. Chemical protection studies have demonstrated that A-site and P-site tRNAs protect specific bases of the 16S rRNA from chemical modification (56,59). There is some overlap in the 530 region (60). Protections caused by bound tRNAs or fragments thereof are summarized in Table 1.1.

Cross-linking from various positions of tRNAs has provided a wealth of information (Table 1.1) implicating interactions between several segments of the 16S rRNA and ribosome-bound tRNAs (19,73,81). When looking at the secondary structure of the 16S rRNA, the vast majority of tRNA cross links appeared to be confined to two domains. The 700 region of helix 23 was cross-linked by A, P, and E-site tRNAs from positions 20, 32, and 47. Cross-links from these positions of the tRNA to nucleotides in the 1300 region and neighboring segments of the 16S have been observed. This tight grouping of tRNA cross-links does well to define a tRNA nest, however there are concerns. At times the groupings seem to be too tight. Often the same bases of the 16S rRNA are cross-linked from the same modified tRNA

bound to various sites on the ribosome suggesting possible overlapping binding sites. Cross-linking of identical bases by A-site and E-site tRNAs suggest some of the cross-links may be due to nonspecific tRNA binding. In addition, base 34 of P-site-bound tRNA<sup>Val</sup> has been cross-linked to base C1400 of the 16S rRNA (76). Nucleotides 1394-1399 have been cross-linked to the mRNA analog poly-A (98), and many other cross-links have been seen between the mRNA and the 1400 region (17,80). Several other segments of the 16S rRNA have been cross-linked to mRNAs (110). Obviously the mRNA is in close proximity to the tRNA so the bases cross-linked to mRNA are likely part of the tRNA nest within the ribosome.

### **1.7 tRNA structure**

It is well established that almost all tRNAs have similar cloverleaf secondary structures (40,93,94), which are folded into the common L-shaped tertiary structure (Fig 1.9). This L-shaped structure has been seen by nuclease digestion studies with tRNAs in solution, but most convincingly the L-shape has been seen in crystal structures and with NMR (42,44,46,83,100,111). These studies have demonstrated that the anticodon loop is single stranded and solvent exposed (105). In addition, the two bases adjacent to the 3' end of the anticodon have been shown to form a helical stack with the anticodon stem (113), confirming the tRNA's conformation as seen in the crystal structures. It has been difficult to confirm the angle between the two arms of the tRNA in solution due to limitations inherent to the techniques used. A recent study using transient electric birefringence (TEB) has determined with some certainty



Figure 1.8 A) Crystal structure of yeast tRNA<sup>Phe</sup>, and B) the tertiary structure of yeast tRNA<sup>Phe</sup> adapted from Kim (43).



that the angle between the two arms is  $90^\circ$ , as seen in the crystal structures (21). With such strong direct and indirect evidence for the L-shaped structure of tRNA, there is little doubt as to the tertiary structure of tRNAs.

## **1.8 Phenanthroline-mediated cleavage**

Recently, researchers have begun tethering cleavage reagents to one molecule to understand how that molecule interacts with other molecules or large macromolecular complexes such as the ribosome (9,27,34,35,43,55). By tethering a cleavage reagent, such as 1-(p-bromoacetamidobenzyl)-EDTA (BABE) or 1,10-orthophenanthroline (P) (Fig 1.10), to a specific segment of a ligand, one can identify specific segments of a molecule or macromolecular complex that closely interact with a specific segment of that ligand. Phenanthroline has been shown to cause the cleavage of nucleic acids and proteins in the presence of copper ions and a reducing agent (11,88).

### **1.8.1 Disadvantages of other mapping techniques**

Tethered-phenanthroline mediated cleavage appears to have some advantages over cross-linking and chemical protection/modification studies. Cross-linking suffers from two major requirements which must be met before an actual cross-link can be formed. The cross-linking agent (donor) and the molecule to which the cross-link is formed (receptor) must be in very close proximity and in the correct steric orientation in order for a bond to form. Phenanthroline has not demonstrated a need for such requirements. Chemical protection studies suffer from the inability to distinguish protections due to a bound ligand versus protections caused by ligand-induced conformational changes. Tethered phenanthroline-mediated cleavage allows us to pick

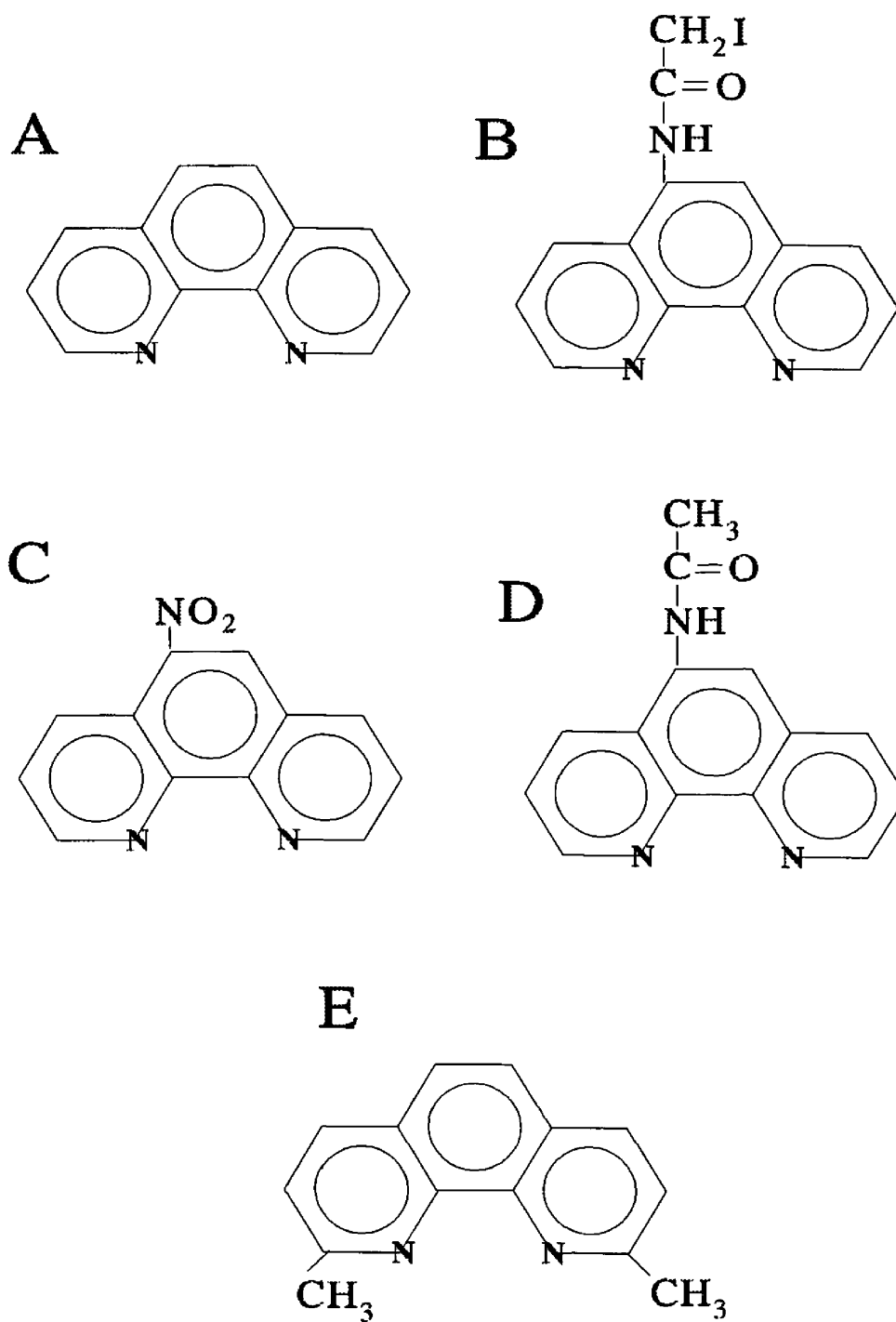


Figure 1.9 Chemical structures of A) oP, B) IoP, C) NoP, D) AoP, and E) neocuproine.

up short to mid-range and possibly transient interactions. The three carbon tether we use to link phenanthroline to the tRNA allows phenanthroline approximately a 10Å sweep so only nearby nucleic acids are cleaved.

### **1.8.2 Problems with tethered phenanthroline**

There are two major problems with phenanthroline. It is difficult to separate untethered free phenanthroline from the tethered product. Phenanthroline sticks to plastics and column resins, making the recovery of highly purified phenanthroline-tethered ligands extremely difficult. An additional drawback is that the mechanism of cleavage is not known, and the basic question of whether the *bis* complex (two phenanthroline molecules coordinated around a single copper atom) or the *mono* complex is required for cleavage is also an unknown. There has been much debate as to the mechanism of phenanthroline cleavage, but the mechanistic details are not yet known. Some believe the reaction generates a hydroxyl radical (12,89), while others describe the reactions as generating some other mysterious oxidative intermediate (22,84,89). This has confounded designing proper controls and interpreting results.

### **1.9 Experimental designs**

To understand the mechanism by which the ribosome functions, we must first identify the active sites on the ribosome. Of paramount importance is the identification and characterization of the tRNA binding sites. In addition to mapping the binding sites, the identification of rRNA in the tRNAs' vicinity may implicate some rRNAs in the movement of tRNA through the ribosome. A great deal of work has already been done to further define the active sites on the ribosome, specifically

the binding sites for tRNA, mRNA, and translation factors (discussed above).

DNA probes complementary to helix 34 of the 16S rRNA can be used to probe the structure of this segment of rRNA. Segments of the 16S rRNA proximal to the anticodon loop binding site can be mapped using oP-tethered microhelices analogous to the anticodon loop of E. coli tRNA<sup>phe</sup>. It is also possible to map segments of the 16S proximal to various regions of tRNA using oP tethered to native E. coli tRNAs.

### **1.9.1 Probing helix 34**

As mentioned above, mutational studies suggested that helix 34 is involved in the termination of proteins synthesis. A model has been proposed in which the mRNA stop codons base paired with bulges within helix 34, stalling the ribosome and initiating the termination process. According to the secondary structure maps, this region has four helical segments interrupted by the proposed stop codon binding bulges. In order for these bulges to bind stop codons, they must be solvent-exposed and single stranded. If this is the case, these regions would be available for probing with short complementary DNA oligomers (36,39). A series of short DNA oligomers (Fig 1.10) were designed and used to probe the accessibility of the bulge containing the tandem UCA repeats (bases 1199-1204).

### **1.9.2 Mapping the anticodon loop binding site using microhelices**

Interestingly, all of the same 16S rRNA chemical protections were observed when, instead of tRNA, its anticodon loop was bound to the ribosome (59). Additionally, all of the elements required for binding of the tRNA to the 30S subunit appeared to be located within the anticodon loop (64,82), and without a messenger RNA there is no

**Probes used:**

**1046-1061 5'-CAGCCATGCAGCA-3'**

**1057-1062 5'-ACAGGC-3'**

**1197-1202 5'-AUGACT-3'**

**1199-1204 5'-TGATGA-3'**

Figure 1.10 DNA probes used in the helix 34 probing studies.

tRNA binding to the small ribosomal subunit (41). One goal of this series of studies was to take advantage of the anticodon loop's ability to bind the 30S subunit and the ability of phenanthroline to cleave nucleic acids to map the anticodon loop (tRNA binding) site on the 30S ribosomal subunit. Viral T7 RNA polymerase was used to synthesize anticodon loop analogs of the anticodon loop of tRNA<sup>Phe</sup> (Fig 1.12) containing single uridines. Thiol groups were introduced into the anticodon loop analogs either by phosphorylation of the 5' end with a thiophosphate, or by adding 4-thio UTP to the T7 transcription reaction. 5-iodoacetamido-1,10-phenanthroline (IoP) underwent nucleophilic attack from the thiol group (SN2 reaction) which resulted in attachment of phenanthroline to the thiol group. The phenanthroline-microhelix complex was to be bound to the P-site on the 30S subunits where the rRNA could be cleaved in the presence of copper and under reducing conditions. After the cleavage reaction, the rRNAs were purified by phenol extractions and analyzed for cleavage by reverse transcriptase primer extension assays. One anticodon loop analog was identical to the anticodon loop of tRNA<sup>Phe</sup> (MHSG+) having three sites for the incorporation of 4-thio UTP. Two other anticodon loop analogs were designed (MH34U and MH39U), each containing only one possible site for UTP incorporation to map rRNAs proximal to different regions of the anticodon loop.

### **1.9.3 Mapping the tRNA binding site on 30S subunits**

Like the microhelix study, the aim of this study was to map the position of the anticodon loop on the 30S ribosome. Instead of utilizing synthesized anticodon loop analogs for cleavage studies, natural E. coli tRNAs were used (Fig 1.13). These

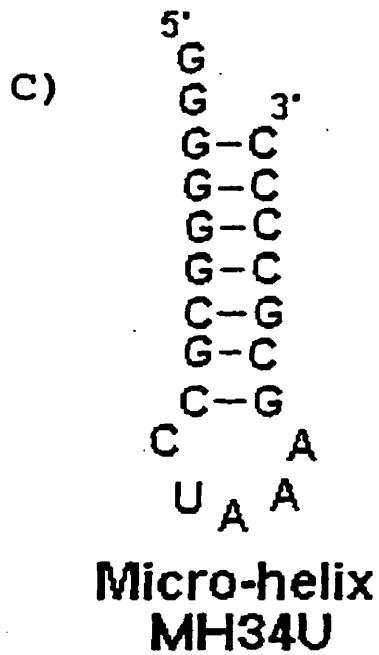
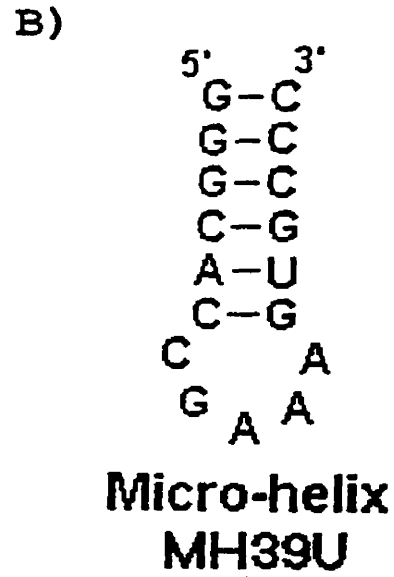
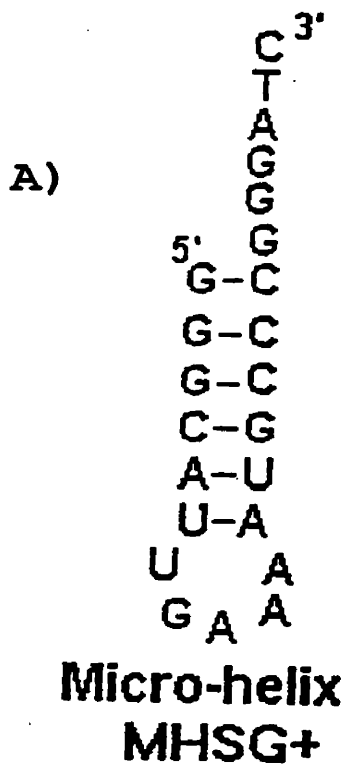


Figure 1.11 Putative secondary structure of the of micorhelices A) MHSG+, B) MH39U, and C) MH34U.

tRNAs contained naturally occurring thiol-modified bases to which phenanthroline was attached. Three tRNAs containing thiol groups in various locations were tethered to phenanthroline and used in cleavage experiments in order to map segments of rRNA proximal to various regions of P-site bound tRNAs.

The three tRNAs used in this study were:

E. coli tRNA<sup>Phe</sup> position 8 4-thiouridine (s<sup>2</sup>U)

E. coli tRNA<sup>Glu</sup> position 34 5-methylaminomethyl-2-thiouridine  
(mnm<sup>5</sup>s<sup>2</sup>U)

E. coli tRNA<sup>Arg</sup> position 8 4-thiouridine (s<sup>2</sup>U), position 32 2-thiocytisine  
(s<sup>2</sup>C)

Using tRNA<sup>Phe</sup> and tRNA<sup>Arg</sup> it would be possible to subtract one set of cleavages from the other in the process of determining cleavages specific to position 8 and position 32.

Having phenanthroline tethered to various locations on the tRNA allow the mapping of different segments of the 16S rRNA proximal to specific regions of the tRNA. This would go a long way in further defining the tRNA binding site on the E. coli 30S ribosomal subunit.

The aims of this project were to:

1. Determine the availability of helix 34 to cDNA probes.
2. Map the anticodon loop binding site on the 30S subunit.
3. Map the tRNA binding site on the 30S subunit.



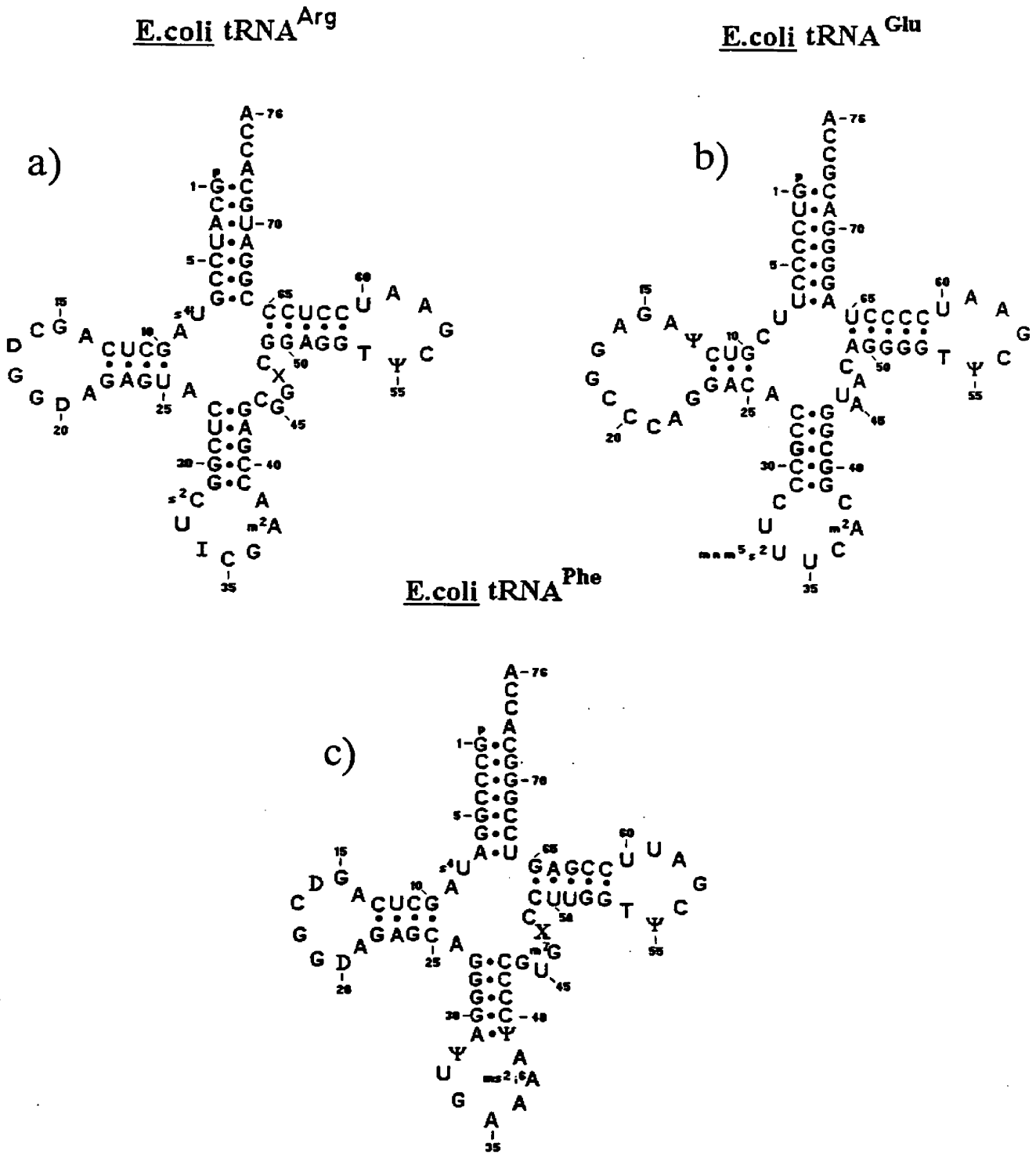


Figure 1.12 Secondary structures of A) tRNA<sup>Arg</sup>, B) tRNA<sup>Glu</sup>, C) and tRNA<sup>Phe</sup> reconstructed from Sprinzl (92).

## **MATERIALS AND METHODS**

### **2.1 Ribosome preparation**

Ribosomes and ribosomal subunits were isolated from Escherichia coli MRE600 essentially by the procedure described by Tam *et al.* (101) and Lodmel *et al.* (51). Escherichia coli was grown to early log phase in Luria broth at 37°C, and concentrated using a Millipore pellicon cassette system (Millipore, Bedford, MA). Cells were washed from the cassette with TC70 buffer (10 mM Tris-HCl pH 7.4, 100 mM KCl, 6 mM MgCl<sub>2</sub>) and concentrated further by centrifugation in a Sorval GSA rotor for five minutes at 5,000 rpm (4000 xg) at 4°C in a Sorval RC5 refrigerated centrifuge (Dupont instruments, Boston, MA). Cells were stored frozen at -80°C until use. Cells were disrupted by grinding approximately 15 g of cells for one hour at 4°C in 2x crack A buffer (20 mM Tris-HCl pH 7.4, 30 mM MgCl<sub>2</sub>, 300 mM KCl) with alumina using a mortar and pestle. Centrifugation in a Sorval SS-34 rotor at 4°C for 10 min at 10,000 rpm (12,000 xg) pelleted unlysed cells, cell debris, and alumina. The pellet was resuspended in 1x crack A buffer (10 mM Tris-HCl pH 7.4, 15 mM MgCl<sub>2</sub>, 150 mM KCl) and re-centrifuged as above. The combined supernatants were centrifuged at 28,000 rpm (72,000 xg) in a Ti70 rotor for 30 min at 4°C to pellet any remaining cell debris and alumina. The supernatant containing the ribosomes was centrifuged in a Ti70 rotor at 60,000 rpm (330,000 xg) for 2.5 hours at 4°C to pellet the ribosomes. Gently scraping the pellets removed a brown layer, and the pellets were then resuspended in 1X crack A buffer. The ribosome solution was centrifuged at 28,000 rpm (72,000 xg) in a Ti70 rotor for 30 min at 4°C, and then centrifuged in a Ti70

rotor at 60,000 rpm (330,000 xg) for 2.5 hours at 4°C to re-pellet the ribosomes. Scraping the ribosome pellets again removed any residual brown layer. The pellets were then resuspended in a total of 22.5 mL of 1X 30-50 buffer (10 mM Tris-HCl pH 7.4, 1.5 mM MgCl<sub>2</sub>, 100 mM KCl) at 4°C and left to stir gently overnight. The isolated subunits were purified from the ribosome/ribosomal subunit solution by zonal centrifugation through a 10-38% sucrose gradient in a Ti-14 rotor at 4°C for 3.5 hours at 45,000 rpm. Sucrose fractions containing ribosomal subunits, as determined by A<sub>260</sub>, were collected and the ribosomal subunits were pelleted out of the sucrose by overnight centrifugation at 60,000 rpm (330,000 xg) at 4°C in a Ti70 rotor. Ribosomal subunit pellets were resuspended in 1X 30-50 buffer and dialyzed against two 2 L volumes of 1X 30-50 buffer. The now highly-purified ribosomal subunits were aliquoted and stored at -80°C until use.

## **2.2 DNA synthesis and purification**

DNA oligomer synthesis was done on an ABI 394 automated DNA/RNA synthesizer (Applied Biosystems Inc., Foster City, CA) using standard phosphoramidite chemistry at the Murdock Molecular Biology Facility at the University of Montana. The protecting trityl groups were removed using NENprep nucleic acid purification cartridges according to the manufacturers' instructions (Dupont, Boston, MA). Purified DNA oligomers were stored at -80°C until use.

## **2.3 Oligomer binding specificity**

### **2.3.1 RNase H assays on ribosomes or 30S subunits**

In order to determine the specificity of DNA oligomer binding, ribonuclease H

(RNase H) assays were employed. 25 pmol of 70S ribosomes or 30S subunits were incubated with 100 pmol DNA probe in 15-25  $\mu$ L RNase H buffer (40 mM Tris-HCl pH 7.4, 10 mM MgCl<sub>2</sub>, 60 mM KCl) with 3 units of RNase H (Takara Shuzo Co., Shiga, Japan) for 30 min at 37°C followed by an incubation at 4°C for 2 hours. Ribosomal RNA, and fragments thereof, were separated from the ribosomal proteins by three phenol extractions, followed by two chloroform extractions (to remove the phenol). The rRNAs were precipitated by the addition of three volumes of 95% cold ethanol and 1/10 vol 3 M NaOAc and placed at -20°C for 30 to 120 min. The RNA was pelleted by centrifugation at 13000 xg for 20 min at 4°C in a Savant SFR13K refrigerated microcentrifuge (Savant Instruments Inc., Farmingdale, NY). The supernatant was aspirated and the RNA pellet was dried in a Savant SC110 speed vac. The pellet containing the purified ribosomal RNA was resuspended in 10  $\mu$ L analytical grade water and 10  $\mu$ L 1X tracking dye (7 M urea 0.025% w/v bromphenol blue, 0.025% w/v xylene cyanol in 1X TBE). Resuspended rRNA was electrophoresed on a pre-run 4% acrylamide gel (15 cm x 12 cm x 0.2 cm) in TBE buffer (45 mM Tris-borate, 1 mM EDTA) at 15 mA for 3.5 hours. Staining the gel in a 0.2% methylene blue based dye allowed the RNA to be visualized.

### **2.3.2 RNase H assay on extracted rRNA**

To obtain purified rRNA for use in RNase H assays, 30S ribosomal subunits were extracted and precipitated from ethanol as described above and resuspended in TE buffer (10 mM Tris-HCl pH 7.5, 10 mM EDTA). If necessary, rRNA was linearized by incubating at 80°C for five minutes and then quickly cooled on ice. 25 pmol

protein-free rRNA was incubated with 100 pmol probe as above. After the reaction the rRNA was dried, resuspended, and electrophoresed as above.

## **2.4 5' end labeling of DNA oligomers**

### **2.4.1 Phosphorylation**

Typically, 35 pmol DNA probe was incubated with 5-10  $\mu\text{L}$  of ( $\gamma\text{P}^{32}\text{-ATP}$  3000 Ci/mmol) (DuPont NEN) 3 units of T4 poly nucleotide kinase (PNK) (USB, Cleveland, OH) in PKMB buffer in a 20-30  $\mu\text{L}$  volume for 60 min at 37°C. The oligomer was purified using NENsorb 20 columns according to the manufacturers' directions (DuPont). The fraction containing the eluted DNA was dried in the speed vac and resuspended in 50-100  $\mu\text{L}$  TE.

### **2.4.2 Autoradiography**

Autoradiography of the end-labeled probes effectively checked probe integrity and purity. A sample of the end labeled probe was diluted with analytical grade water, and 100,000 CPM was loaded on a pre-run 10% acrylamide gel (15 cm x 12 cm x 0.2 cm). The gel ran for 45 min, probe samples were loaded again and the gel ran for an additional 5 min at 15-20 mA. The gel was removed from the electrophoresis rig and used for autoradiography. The gel was wrapped in Saran Wrap, place in an autoradiography cassette with a piece of X-OMAT AR X-ray film (Kodak, Rochester, NY ) large enough to cover the entire gel. The cassette containing the radioactive gel and the X-ray film exposed for 30-45 min at -20°C, and then the film was developed.

## **2.5 Filter-binding assays (with DNA oligomers)**

Filter-binding assays were performed essentially as described by Hill *et al.*

(36,39,54). The 30S subunits were first activated by incubating at 37°C for 30 min in FBA buffer (10 mM Tris-HCl pH 7.4, 10 mM MgCl<sub>2</sub>, 15 mM KCl). Increasing amounts of a hot-cold probe mix containing the end-labeled DNA oligomer diluted with unlabeled oligo to a specific activity of approximately 500 CPM/pmol were added to aliquots of the activated subunits. The reaction was incubated at 37°C for 30 min then incubated at 4°C for 30 or 120 min. The reactions were diluted to 1 mL in FBA buffer and filtered through presoaked 0.45 µm pore nitrocellulose filters (Millipore) at approximately 12.5 cm vac with three 1.0 mL FBA buffer washed. Radioactivity retained on the filter could be counted by liquid scintillation in a Packard Tri-carb 1500 liquid scintillation analyzer (Packard, Meriden, CT).

## **2.6 4-thio-UTP synthesis**

Phosphorylating 4-thio-UDP (Sigma, St Louis, MO) generated the modified nucleotide 4-thio-UTP (68,90). Approximately, 7.8 g of 4-thio UDP and 16.9 g of phosphoenolpyruvate were resuspended in a 5.0 mL volume of UDP-phosphorylation buffer (100 mM Tris-HCl pH 6.9, 20 mM MgCl<sub>2</sub>, 30 mM KCl, 0.1 mM DTT) in a foil-wrapped pear-shaped boiling flask. Purging the flask with helium for two hours removed atmospheric oxygen from the reaction vessel. The addition of 40 units of pyruvate kinase in PK buffer (10 mM tris-HCl pH 7.5, 50% v/v glycerol, stored at -20°C) initiated the reaction. The atmosphere was again flushed with helium for 15 min, and the reaction stirred in the sealed vessel overnight (20 hours) in the dark. Adding enough EDTA to chelate all of the magnesium quenched the phosphorylation reaction. The reaction was aliquoted into brown eppendorf tubes and the volume of

each tube was reduced by half in the speed vac. The product was recovered by ethanol precipitating with three volumes of cold 95% ethanol, centrifuging and drying as before. The pellet was resuspended with 160  $\mu$ L 10 mM Tris-HCl pH 7.5, 80  $\mu$ L 0.1 M EDTA, and 10 $\mu$ L 1 M DTT. Two phenol extractions removed remaining proteins, and the purified 4-thio UTP was again ethanol precipitated. The final product was resuspended in 10 mM Tris-HCl pH 8.0. The concentration of the product was determined by  $A_{260}$  readings, and the purity was determined by reverse phase HPLC on a C18 column using a 0-10% acetonitrile/water gradient.

## **2.7 Microhelix template preparation**

Microhelix template DNAs were synthesized and purified as outlined above for DNA oligomers. Double-stranded templates were prepared by adding equal molar amounts of coding and non-coding strands to an Eppendorf tube. The tube containing the template was placed in 100 mL beaker containing boiling water which was slowly cooled to room temperature allowing the two strands to hybridize. Electrophoresis on a 10% nondenaturing-acrylamide gel (15 cm x 12 cm x 0.2 cm) run for 30 min at 30 mA verified template DNA hybridization.

## **2.8 Microhelix transcription and purification**

Typically, a 0.5 mL transcription reaction contained 2000 pmol of microhelix template DNA in MEB Buffer (40 mM Tris-HCl pH 8.0, 25 mM DTT, 1 mM spermidine, 25 mM  $MgCl_2$ , 0.01% v/v Triton-X 100, 8% w/v PEG-8000, 50  $\mu$ g/mL BSA) with 0.1 unit of inorganic pyrophosphatase (Sigma), 4 mM NTPs (Pharmacia), and 15,000 units of T7 RNA polymerase (courtesy of Jim Bullard). If thiolated

microhelix was required, 4-thiol UTP ( $s^4$ -UTP) was added to the reaction at a ratio of 9:1 ( $s^4$ -UTP to UTP) where the combined concentration of  $s^4$ -UTP and UTP equaled 4 mM. The reaction was incubated for 4-5 hours at 37°C, and quenched by the addition 10  $\mu$ L 0.5 M EDTA pH 8.0, which removed the flocculent white precipitate (though to be magnesium pyrophosphate). The product was precipitated by adding three volumes of ethanol. The product was resuspended in tracking dye, and gel-purified on a pre-run 10% acrylamide gel (15 cm x 12 cm x 0.2 cm) run at 20-30 mA until the bromphenol blue dye was 1-2 cm from the bottom edge of the gel. If the gel was run for analytical purposes, it was stained as noted previously. If the gel was preoperative, the full-length product was visualized by UV shadowing. Full-length product bands were excised from the gel, diced with a new razor blade (VWR, Media, PA), and the RNA eluted with 500  $\mu$ L high-salt elution buffer (500 mM  $\text{NH}_4\text{OAc}$ , 10 mM  $\text{MgOAc}$ , 1 mM EDTA pH 8.0, 0.1% v/v SDS) overnight at 4°C with gentle agitation. Purified full length microhelix RNA was ethanol precipitated as above, resuspended in TE, and Bio-spin 6 column purified using TE according to the manufacturer's instructions. Final concentration was determined by  $A_{260}$  readings, and final product purity was checked by denaturing PAGE.

## **2.9 Thiophosphorylation of microhelices**

Optimally, 2000-4000 pmol of microhelix RNA (mhRNA) was dephosphorylated using shrimp alkaline phosphatase (SAP) according to the manufacturer's instructions (USB). Incubating the reaction at 65°C for 15 min denatured the SAP. 3-6 units of T4 PNK, PNK buffer, and 1  $\mu$ L 10 mM ATP- $\gamma$ s were added to the SAP reaction,



following which the reaction incubated for 1 hour at 37°C. The mhRNA was precipitated using three volumes of 95% ethanol as before. The dried mhRNA was resuspended in TE, and column purified on a biospin 6 column as before.

### **2.10 5' end labeling of microhelices**

Microhelices were dephosphorylated as above. Phosphorylation also proceeded as above, except that instead of adding ATP- $\gamma$ S to the reaction, 5-10  $\mu$ L ATP $\gamma$ P<sup>32</sup> (3000 Ci/mmol) was added. The end labeled mhRNA was NENsorb column purified as described above, and the integrity of the final product was checked by autoradiography as above.

### **2.11 Phenanthroline attachment to microhelices in an organic medium**

The typical phenanthroline attachment reaction contained mhRNA at a concentration of 5-10  $\mu$ M in 10 mM Tris-HCl pH 7.5, 25% v/v acetonitrile, 3 mM IoP (a kind gift from Dr. David Sigman, UCLA), and 10-20  $\mu$ M DTT. The components were added to a brown or a foil-wrapped Eppendorf tube at room temperature, followed by a two hour incubation at 37°C in the dark. The aqueous volume was increased by the addition of 0.25-0.5 vol analytical grade water, and some free IoP was removed by a series of five extractions with 1 vol 1:1 n-butanol-chloroform. The extracted aqueous phases were centrifuged at 13,000 xg for 30 min at 4°C to pellet any remaining IoP. The aqueous phase was transferred to a new tube, leaving the IoP pellet behind, and dried in the speed vac. The oP-mhRNA complexes were resuspended in TE. To confirm the attachment of IoP to the microhelix, a sample of the oP-mhRNA complex was electrophoresed at 10-15 mA on a 10% acrylamide mini

gel (10 cm x 8 cm x 0.08 cm) containing 10-25 µg/mL [(N-acryloylamino)phenyl] mercuric chloride (APM) (courtesy of Jim Bullard) until the bromphenol blue appeared to be 1-2 cm from the bottom of the gel. Gels were stained as described above.

### **2.12 Enzymatic sequencing of mhRNA**

Radio-labeled microhelices were sequenced using a RNA sequencing kit (USB) according to the manufacturers' instructions. In an attempt to obtain complete digestion of the mhRNA, it was necessary to incubate the digestions at 75°C, which would linearize the microhelix, making the double-stranded regions accessible to the sequencing nucleases.

### **2.13 Filter-binding assays with mhRNA**

Filter-binding assays were performed essentially as described above in section 2.5 using various buffer conditions. The molar ratio of microhelix to 30S subunit was kept constant at 4:1. Poly-U was added to a final concentration of 0.8 mg/mL in the binding reaction, with the 4°C incubation being limited to 30 min. Various buffers were tested to see which allowed optimal microhelix binding.

### **2.14 tRNA sulfhydryl removal**

Incubation of 1600 pmol tRNA in a reaction containing 100 mM Tris-HCl pH 7.5, 4.4 mM MgCl<sub>2</sub>, 0.83% H<sub>2</sub>O<sub>2</sub> for one hour at room temperature oxidized and subsequently deactivated the sulfhydryl groups from the various tRNAs (85). The tRNA was recovered by ethanol precipitation with 2.2 vol 95% ethanol. Prior to drying in the speed vac, the pellet was washed with 500 µL 70% cold ethanol, and centrifuged as above. The speed vac-dried tRNA pellet was resuspended in analytical

grade water and stored at -20°C until used.

## **2.15 Phenanthroline attachment to tRNAs**

### **2.15.1 IoP tethering to tRNAs in an organic medium**

IoP was tethered to the various tRNAs in an organic environment and purified by extraction as described above in section 2.11. In addition to extractions, several other methods of purification were attempted. In attempts to remove excess unreacted IoP a 4.0 mL sephadex G-10 column (20 cm x 0.5 cm) (BIO RAD, Hercules, CA) buffered with TE was used. Fractions of 1.0 mL were collected and fractions containing tRNA as determined by  $A_{260}$  readings were combined and ethanol precipitated. Biospin 6 columns (BIO RAD) were also used with TE to remove free IoP. Dialysis in spectrapore membrane tubing #08-667A (Fischer Scientific, Pittsburgh, PA) against two 500 mL volumes TE was also used in an attempt to eliminate free IoP.

### **2.15.2 IoP tethering to tRNAs in an aqueous medium**

In a typical tethering reaction, 500 pmol tRNA or dethiolated tRNA (tRNA-SH) was incubated in a 50  $\mu$ L reaction volume containing 20 mM Tris-HCl pH 7.5, and 1 mM IoP at 37°C for 2 hours in the dark. The tRNA was ethanol precipitated as above, using 9 volumes of primer extension precipitation buffer (68% EtOH, 83.5 mM NaOAc pH 6.5, 0.8 mM EDTA). The dried tRNA was resuspended in analytical grade water. IoP attachment was checked on an APM gel as described above.

## **2.16 5' end-labeling of oP-tRNAs**

SAP was used to dephosphorylate 50 pmol of oP-tRNA as described above in section 2.9. Instead of heat inactivation to denature the SAP, the enzyme was

removed by extracting with 1 vol chloroform, extracting with 1 vol phenol, extracting again with 1 vol chloroform, and finally ethanol precipitating with 3-4 volumes of cold 95% ethanol. The dephosphorylated oP-tRNA was resuspended and end labeled using PNK as described above. Phosphorylated oP-tRNA was dried down in the speed vac, then resuspended in 25  $\mu$ L tracking dye. The tRNA was separated from degradation products by denaturing PAGE on a 10% acrylamide gel (15 cm x 12 cm x 0.2 cm) run at 30-35 mA until the bromphenol blue was just starting to run off the gel. Bands containing end-labeled tRNA or fragments thereof were visualized by autoradiography as described above. Using the autoradiogram as a guide, the full-length and the first degradation product bands were excised from the gel using a new razor blade. The gel bands were cut into small cubes, placed in an Eppendorf tube and the tRNA eluted with 500  $\mu$ L tRNA elution buffer (300 mM NaOAc pH 6.5, 5 mM EDTA). Elutions took place for either 2 hours at 37°C or overnight at 4°C. The supernatant was removed and fresh elution buffer added and the tRNA was eluted as above. The second supernatant was removed and the tRNA was precipitated with 2 vol cold 95% ethanol. The tRNA was resuspended in analytical grade water.

### **2.17 Filter-binding assays with oP-tRNAs**

Filter-binding assays proceeded essentially as described in section 2.13 with a few minor changes. The buffer used was BC buffer, and after the incubations at 37°C the samples were not incubated at 4°C. Five 1.0 mL buffer washes were used to wash the filters to reduce the high background radiation retained on the filters seen with oP tethered ligands.

## **2.18 Cleavage reactions with oP-tRNAs**

### **2.18.1 Cleavage reactions**

Small ribosomal subunits or 70S ribosomes were activated in 1X binding-cleavage (BC) buffer (35 mM Tris-HCl pH 7.5, 15 mM MgCl<sub>2</sub>, 150 mM KCl) for 30 min at 37°C. Ligand mixes for the cleavage reaction and the appropriate controls (discussed below in section 3.15) were added to the activated subunits or ribosomes and incubated at 37°C for 30 min to allow the ligands to bind (Fig 2.1).

Mercaptopropionic acid (MPA) was added to initiate cleavage with final concentrations in the cleavage reaction being: 1 μM 30S, 4 μM tRNA, 4 μM mRNA (Oligos Etc.) (0.4 mg/mL poly-AG or poly-U in place of the designed message), 200 μM CuSO<sub>4</sub>, 2 mM MPA. The cleavage reaction proceeded for 30 min at 37°C in the dark. In some experiments a small amount of free IoP or 5-acetamido-1,10-phenanthroline (AoP) was added back to the cleavage reaction (details below). After the cleavage, the addition of 1.0 μL of a 10 mM neocuproine solution quenched the reaction by chelating the copper.

### **2.18.2 Template preparation**

To the completed cleavage reaction, ribosomes or ribosomal subunits were precipitated by the addition of three volumes of cold 95% ethanol and stored at -20°C for 30-60 min. Ribosomes or ribosomal subunits were pelleted by centrifugation at 13,000 xg for 20 min at 4°C. The ethanol was poured off and the pellet was dried in the speed vac for 2.5 min. The pellet was resuspended in 100 μL sequencing resuspension buffer (0.3 M NaOAc pH 6.5, 0.5% w/v SDS, 5 mM EDTA). The rRNA

**mRNA-A1**

**5'-GGGAGAAAGAAAGCGUUAAAAAAAAAA-3'**

Figure 2.1 Structure of mRNA-A1 with the anticodon for tRNA<sup>Glu</sup> underlined.

was phenol extracted three times with acid phenol. The first extraction was shaken vigorously by hand for 5 min, but the next two extractions were mechanically vortexed briefly. The protein-free rRNA was extracted twice with 1 vol chloroform to remove any remaining phenol. Three volumes of cold 95% ethanol were added and the tube was stored at -20°C for 30-60 min. The rRNA was pelleted by centrifugation at 13,000 xg for 20 min at 4°C. The ethanol was decanted and the pellet was dried in the speed vac for 2.5 min. Assuming a recovery of 90%, the RNA pellet was resuspended in analytical grade water to a final concentration of 0.2 pmol/μL. Purified template for sequencing was stored at -20°C when not in use.

### **2.19 Primer extension analysis**

To identify the sites of cleavage, the purified templates were analyzed by reverse-transcriptase primer extension assays first described by H. F. Noller (18,97). Primers needed to be titrated to determine the concentration of primer which provided gels with optimal definition prior to actual analysis. To begin the primer extension "sequencing" assay, 2.0 μL of one of the diluted primers (Table 2.1) in 2.25X hybridization buffer (112.5 mM K-HEPES pH 7.0, 375 mM KCl) was added to 2.5 μL purified cleavage template (0.2 pmol/μL). The primer was annealed to the template by heating the mixture at 90°C for 2.0 min and allowing the mixture to cool to 45°C slowly (about 28 min). During the annealing cool-down the extension mix (E-mix) (780 mM Tris-HCl pH 8.5, 60 mM MgCl<sub>2</sub>, 60 mM DTT, 102 μM dATP, 102 μM dCTP, 102 μM dGTP, 5.6 μM dTTP, and 0.66 U/μL AMV-RT (Seikagaku USA, Rockville, MD) was prepared with α<sup>32</sup>P-TTP (NEN) at an activity of 215 Ci/mmol.

<b>16S primer 161</b>	<b>5'-GCG GTA TTA GCT ACC GT-3'</b>
<b>16S primer 232</b>	<b>5'-AGT CTG GAC CGT GTC TC-3'</b>
<b>16S primer 480</b>	<b>5'-CTT CTG CGG GTA ACG TC-3'</b>
<b>16S primer 683</b>	<b>5'-CGC ATT TCA CCG CTA CA-3'</b>
<b>16S primer 837</b>	<b>5'-ACG CAC GCC TCA AGG GC-3'</b>
<b>16S primer 906</b>	<b>5'-CCG TCA ATT CA(orC)T TTA(orG) AGT TT-3'</b>
<b>16S primer 1046</b>	<b>5'-GAC ACG CAT GCA GCA CC-3'</b>
<b>16S primer 1199</b>	<b>5'-TCG TAA GGG CCA TGA TG-3'</b>
<b>16S primer 1391</b>	<b>5'-ACG GGC GGT GTG TA(orG)C-3'</b>
<b>16S primer 1490</b>	<b>5'-TAC CTT GTT ACG ACT TC-3'</b>
<b>23S primer 235</b>	<b>5'-ACT CTC GGT TGA TTT CT-3'</b>

**Table 2.1** List of primers used in primers-extension assays.



Tubes containing the hybridized template and primer were briefly centrifuged to remove the water from the outside of the tubes, then 2.0  $\mu$ L E-mix was added to each tube. The appropriate 1.5 mM ddNTPs were added to the sequencing reactions. The reactions were gently vortexed, briefly centrifuged, and incubated at 40-45°C for 30 min. For the chase reactions, 1.0  $\mu$ L chase mix (200  $\mu$ M NTPs) was added to each tube, and 1.0  $\mu$ L of the appropriate 67 $\mu$ M ddNTP was added to each sequencing reaction. The tubes were gently vortexed, briefly centrifuged, and incubated at 40-45°C for 15 min. After the chase reaction, the addition of 75  $\mu$ L sequencing precipitation buffer (70% ethanol, 84 mM NaOAc pH 6.5, 0.8 mM EDTA) to each reaction tube precipitated the newly synthesized DNA. After standing for 10 min at room temperature the reactions were centrifuged at 13,000 xg for 20 min at 4°C. The ethanol was carefully aspirated off and the tubes were dried in the speed vac for exactly 3.0 min. The DNA was resuspended in 7 or 10  $\mu$ L tracking dye, depending on the number of samples to be run and the comb used. The tubes were vortexed, and the resuspended DNA was denatured by incubating at 90°C for 90 seconds. Samples were quick-cooled on ice and loaded on a pre-run 6% denaturing acrylamide gel (60 cm x 20 cm x 0.022 cm) electrophoresed at 55 W for 3 hours. The gel was removed from the electrophoresis rig, transferred to chromatography paper (Whatman, Hillsboro, OR), and dried under vacuum in a BIO-RAD 583 gel dryer at 70°C for 30 min. The dried gel was used for autoradiography.

## **RESULTS**

### **3.1 RNase H assays**

Ribonuclease H assays with the short DNA oligomers were accomplished with some trial and error. Ribonuclease H assays with any of the probes (1049-1061, 1057-1061, 1197-1202, and 1199-1204) and 30S subunits resulted in no specific cleavage. Attempts with phenol-extracted, purified, naked 16S rRNA also yielded no cleavage. Only after linearizing the rRNA by heating it and then performing the assay were cleavages seen (Fig 3.1). Hexameric probes to the 1200 region (1197-1202, and 1199-1204) showed the expected digestion pattern. Using these probes, two fragments of rRNA were seen, one about 1200 bases in length and the other about 300 bases in length. The hexameric probe (1057-1061) to the 1050 region located opposite the 1200 bulge also gave the expected digestion products, fragments of roughly 1000 and 500 bases in length. RNase H assays with the 13-base probe (1049-1061) on protein-free 16S rRNA showed two sets of cleavage. It showed the expected 1000 and about 500 base fragments, but it also showed fragments of 1200 bases and 300 bases. When the primary structure of the 16S rRNA was looked at more closely, a partial sequence complementarity between the 13-base probe and the 300 region was discovered.

### **3.2 Oligomer end labeling**

The end labeling of the various DNA oligomers used in the helix 34 probing study was accomplished with ease. Following the labeling procedure outlined in the preceding section, two fractions were collected off the Nensorb column according to the manufacturers' instructions. The first fraction contained the end-labeled DNA

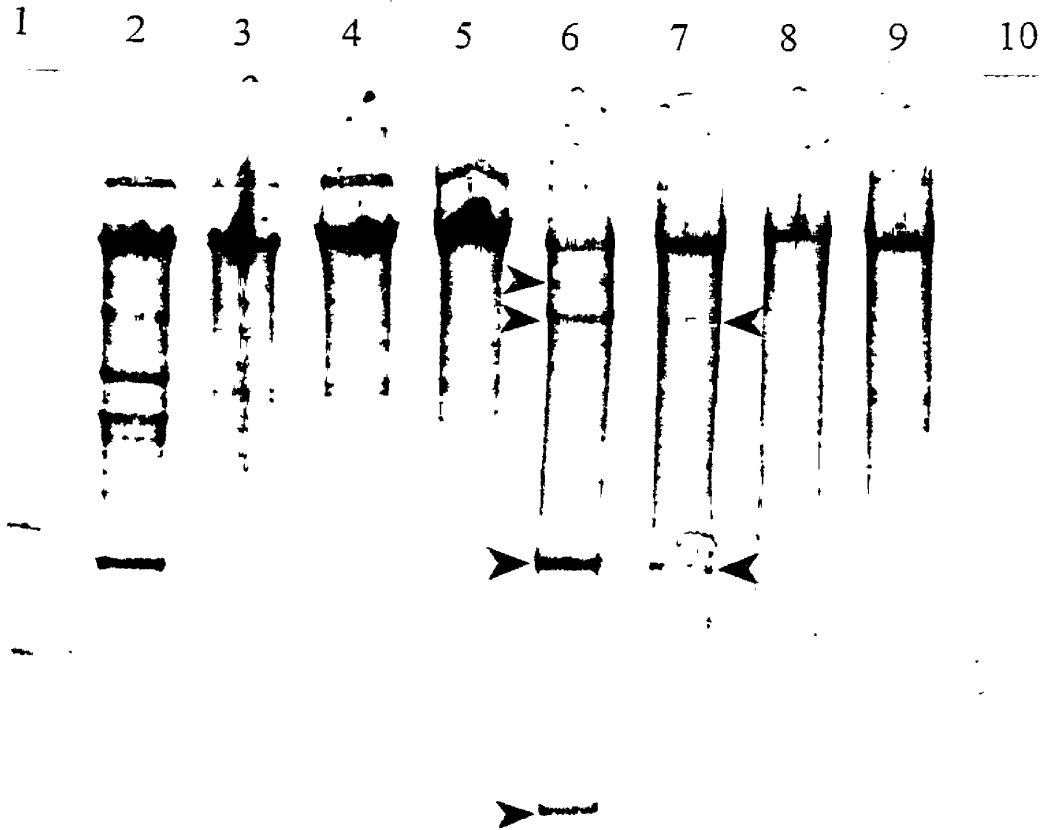


Figure 3.1 RNase H assay showing the binding specificity of cDNA probes to protein-free rRNA performed as described in section 2.3.2. Lanes 1 and 10) 1.77 kb RNA molecular weight ladder (BRL). Lanes: 2) RNase H assay using probe 1049-1061, 3) RNase H assay using probe 1057-1062, 4) control minus probe, 5) control minus enzyme. Lanes 6, 7, 8, and 9, are identical to lanes 2, 3, 4, and 5 except that the rRNA had been linearized by heating. Arrows denote digestion products.

oligomer, and the level of radiation determined by liquid scintillation was typically about  $1 \times 10^6$  CPM/ $\mu$ L for hexameric probes. The labeling of longer probes (9-13 bases) was slightly less efficient, with the levels of radioactivity being 30-50% lower. The second fraction collected did not contain the DNA oligomer, and accordingly the level of radiation in this fraction was greatly reduced. Often when the radioactivity of the tube containing the entire second fraction was measured by a Geiger counter (Technical Associates, Canoga Park, CA) the readings were less than  $1 \times 10^6$  CPM for the entire sample.

Autoradiography showed that after the labeling process, DNA probes contained the radioactive phosphate group and were not degraded in the labeling process. The autoradiograms (Fig 3.2) have two lanes for each sample. In one lane the sample has been electrophoresed for about 45 minutes, and in the other lane the same sample electrophoresed for about 5 minutes. In the 45 minute lanes there was one major band corresponding to the end-labeled oligomer. In the 5 minute lane there was also one major band again corresponding to the DNA oligomer. There were no bands seen below this major band indicating the absence of degradation products, free  $\gamma$ P<sup>32</sup>-ATP, or acid hydrolyzed P<sup>32</sup> phosphate (PO<sub>4</sub>). As one would expect, probes nine bases in length migrated at a slower rate than did hexameric probes. This migrational difference was clearly seen on autoradiograms of 10% gels on which 6-mers and 9-mers were run side by side (Fig 3.2).

### **3.3 Oligomer filter-binding assays**

None of the three hexameric probes used bound to 30S ribosomal subunits at any



Figure 3.2. Autoradiogram of end-labeled cDNA probes performed as described in section 2.4.2. Lanes: 1) probe 1049-1061 electrophoresed for 45 min, 2) probe 1049-1061 electrophoresed for 5 min, 3) probe 1057-1062 electrophoresed for 5 min, 4) probe 1057-1062 electrophoresed for 45 min.

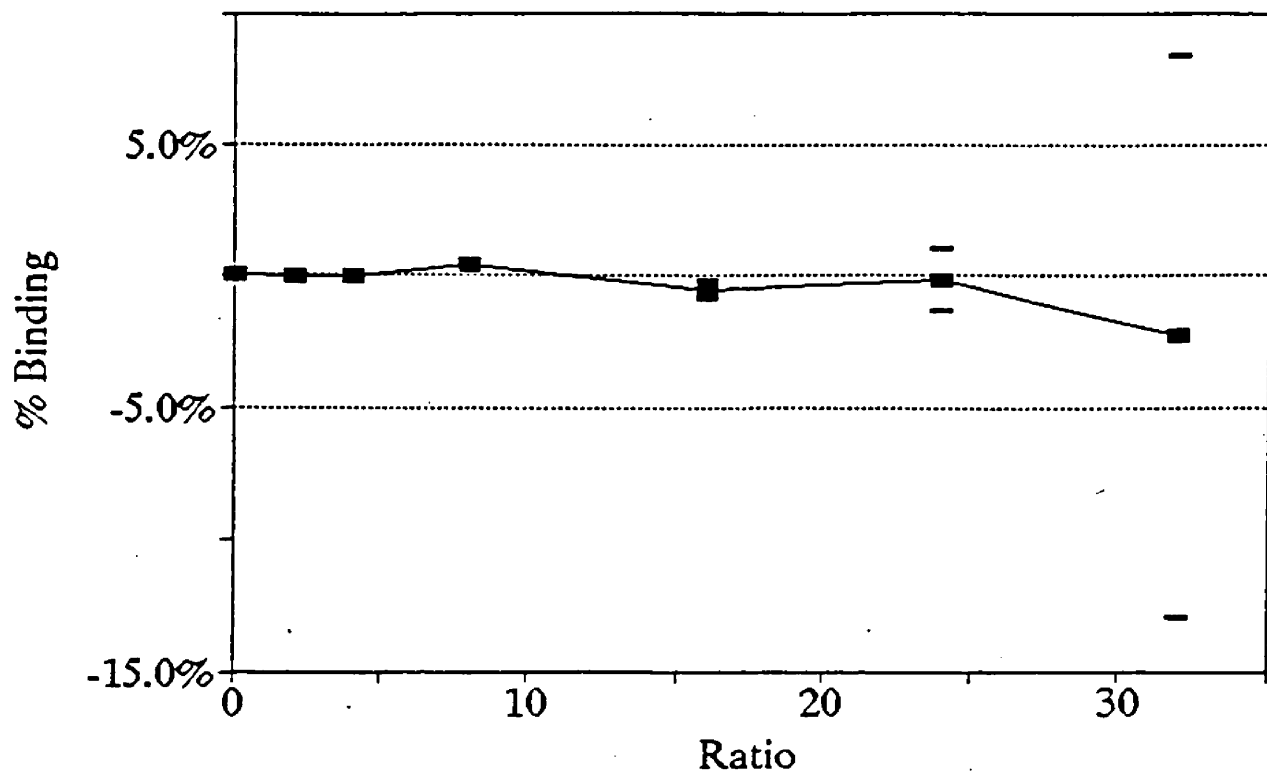


Figure 3.3 Filter-binding assay performed as described in section 2.5. Probe 1199-1204 was bound to 30S at increasing ratios of probe to subunits.

Probe	percent binding		
	alone	w/ poly-U	w/ S150
1049-1062	4.2	5	14.2
1057-1061	0.1	0.2	0.2
1197-1202	0.2	0.2	0.1
1199-1204	0.2	0.4	0.3

Table 3.1 Summary of cDNA oligomer binding results to 30S.

probe to subunit ratio. The values for the percent of subunits bound were consistently near 0.1% (Fig 3.3). The addition of the messenger RNA analog poly-U did not increase or decrease observed probe binding. Likewise, the addition of S150, a crude mixture of tRNAs and translation factors, did little to affect probe binding (Table 3.1).

The filter-binding studies with the 13-base probe had slightly different results. At low probe to subunit ratios the probe did not bind, but at high probe to subunit ratios (32:1, 40:1) the probe bound very weakly; about 4%. The addition of poly-U had no significant effect on binding of the 13-base probe. The addition of S150 to the binding reaction, however, had a slight affect increasing probe binding from 4% to 14%. This increased binding occurred only at high probe ratios (Table 3.1). The results of these studies led us to use other means to probe 30S ribosomal subunit structure and function

### **3.4 Microhelix template annealing**

Double-stranded microhelix templates were generated by annealing the appropriate coding and noncoding DNA oligomers. A template was also generated by hybridizing the P3 oligonucleotide, DNA complementary to the T7 RNA polymerase promoter, and the appropriate non-coding strand. The template hybridization was clearly visible on nondenaturing gels. Each oligonucleotide by itself typically gave one band. The only oligomer that showed two bands when run by itself was the P3 oligomer. It was latter found that incomplete deprotection of the P3 oligomer resulted in the two bands. However, when any two complementary oligomers were hybridized to form the double-stranded template, only one band with a slower migration rate corresponding to



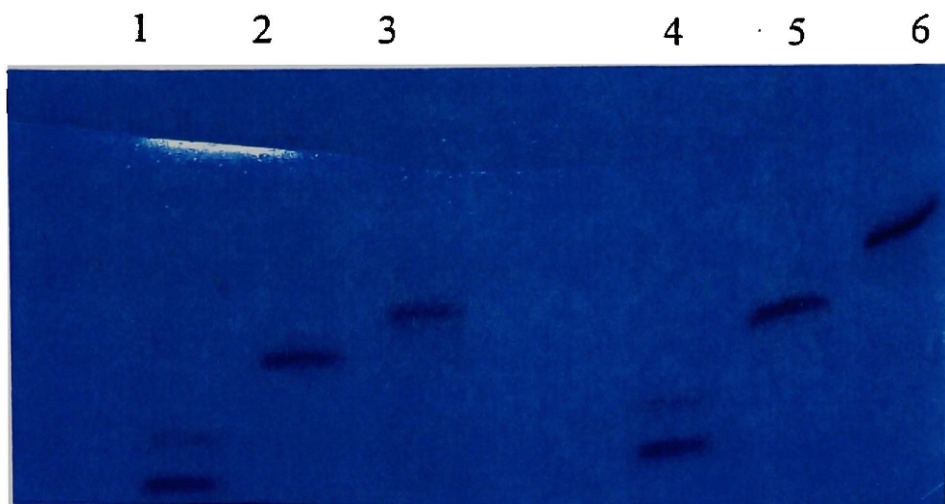


**Figure 3.4** 10% nondenaturing acrylamide gel showing microhelix template hybridization performed as described in section 2.7. Lanes 1) and 4) P3 oligonucleotide (complement to the T7 RNA polymerase promoter), 2) MH39U noncoding strand, 3) double-stranded MH39U template, 5) MHSG+ noncoding strand, 6) double-stranded MHSG+ template.

the double stranded template was seen (Fig 3.4).

Nuclease-digestion studies with the single-strand specific nuclease S1 and the all purpose DNA nuclease RQ1 nuclease also demonstrated proper hybridization. Each of the oligos by itself was susceptible to digestion by nuclease S1 and RQ1 DNase. The hybridized template could be digested with RQ1 DNase but not nuclease S1 (data not shown).

### **3.5 Microhelix transcriptions**

Of the three microhelices designed, only two, MHS<sup>+</sup> and MH39U, were transcribed and used for study. After the transcription reaction incubation period had concluded, a white flocculent precipitate typically appeared. A relationship between the presence of this precipitate and the amount of RNA product was discovered. Typically, if there was no white precipitate there was little or no RNA product. If the precipitate was present in copious amounts, a high product yield was often observed. This flocculent white precipitate was thought to be magnesium pyrophosphate. At the end of the transcription reaction incubation period, the addition of enough EDTA to chelate all of the magnesium had several positive effects. First, it quenched the transcription reaction. Second, it removed the white precipitate, which hastened migration through the purification gel. Without the addition of EDTA, migration on an acrylamide gel was greatly retarded, and excess salts in the sample were believed to be the cause of this migrational retardation.

Whether the transcription reaction was visualized by UV shadowing (preparative) or by methylene blue staining (analytical), the same pattern was typically seen. At the

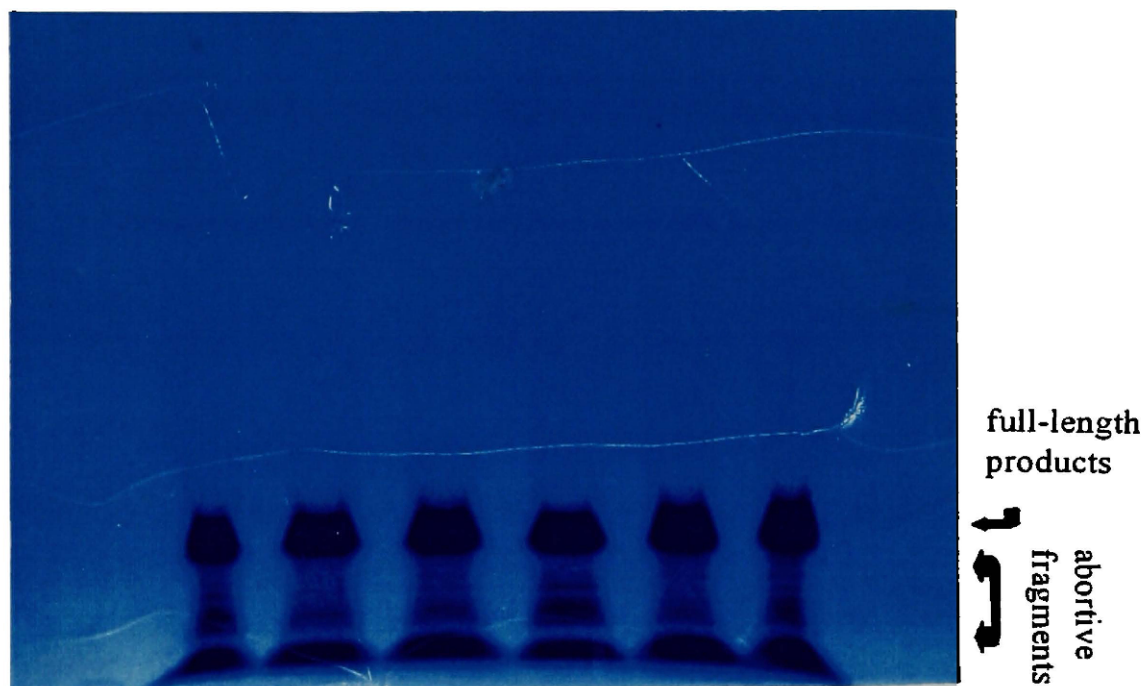


Figure 3.5 10% denaturing methylene blue-stained polyacrylamide gel showing T7 RNA polymerase transcription products of MHS G+ performed as described in section 2.8. All lanes contain a 50 $\mu$ L aliquot of the 500  $\mu$ L transcription reaction. Arrows indicate full-length product and abortive fragments.

bottom of the gel there was a large smear of unresolved abortive products. The full-length product was separated from the abortive smear by a small gap (Fig 3.5). Often one observed faint bands above the major full-length product band. Since many polymerases, including T7 RNA polymerase, add bases in a nonspecific or undirected manner to the 3' end of the newly synthesized oligo, these bands, when seen, were not excised from the gel or used for further study.

### **3.5.1 Thio transcriptions**

In theory, obtaining thiolated microhelix (MH39U) seemed to be an easy proposition, but turned out to be rather difficult. A transcription reaction containing only 4-thio UTP yielded no product. It was necessary to include at least some unthiolated UTP in the transcription reaction to make the reaction proceed. Even when RNA product was produced, the yield was significantly lower as compared to the same size transcription reaction using only normal UTP. Nearly all of the purified thio-transcribed MH39U contained the thiouridine as evidenced on an APM gel. The retarded thiol-containing microhelix band appeared as a doublet. There was a faint band at the bottom of the APM gel representing unthiolated transcript (data not shown).

### **3.6 End labeling of microhelices**

Only one microhelix (MHSG+) was end labeled and subsequently used for sequencing and binding studies Fig (3.6). End labeling of mhRNA was not as consistent or efficient as the labeling of DNA oligos. Counts taken on 1 $\mu$ L spots of different labeled preparations would range between 100,000 and 600,000 CPM/ $\mu$ L.

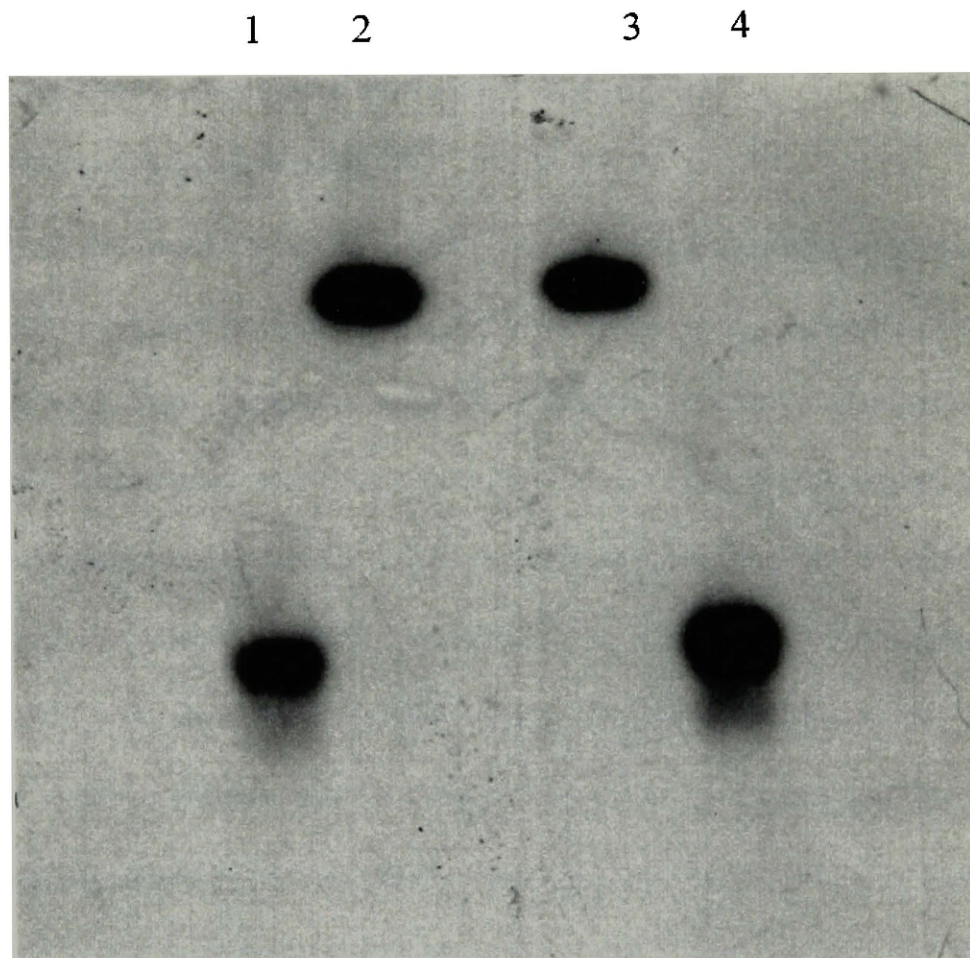


Figure 3.6 Autoradiogram of end-labeled MHSg<sup>+</sup> obtained as described in section 2.10. Lanes 1) and 4) MHSg<sup>+</sup> electrophoresed for 45 min, 2) and 3) MHSg<sup>+</sup> electrophoresed for 5 min.

Autoradiograms typically had two lanes as before. The 45 minute lane had one band corresponding to the full length microhelix. No dimers were seen above the full-length band, and no degradation products were seen below the full length band. The 5 minute lane also had one band corresponding to the full length MHSG+ and no free phosphate band was seen below the full-length band. MH39U was not used in binding and sequencing studies, and therefore was not end labeled.

### **3.7 Enzymatic sequencing of mhRNA**

To confirm the sequence of the mhRNA transcripts, enzymatic sequencing of end-labeled microhelices was employed. Of the two microhelices transcribed, only MHSG+ was sequenced. Sequencing of the end-labeled mhRNA according to the manufacturers' instructions met with limited results because the nucleases used will only cleave single-stranded RNAs. The sequence of the tail on the 3' end and the anticodon loop was seen repeatedly, but the sequence of the double-stranded stem was never seen (Fig 3.7). In an attempt to linearize the microhelix during the sequencing reaction, the reaction temperature was ramped up to 75°C. Increasing the temperature of the sequencing reaction did not change the sequence pattern seen on previous autoradiograms of lower temperature sequencing reactions (data not shown). MH39U was not used in enzymatic-sequencing assays since the only region to appear should have been the anticodon loop. Obtaining the sequence of just the anticodon loop would not provide adequate information to determine if MH39U was produced correctly.

### **3.8 Thiophosphorylation of mhRNA**

Since incorporation of s<sup>4</sup>U via transcription reactions proved to be so difficult,



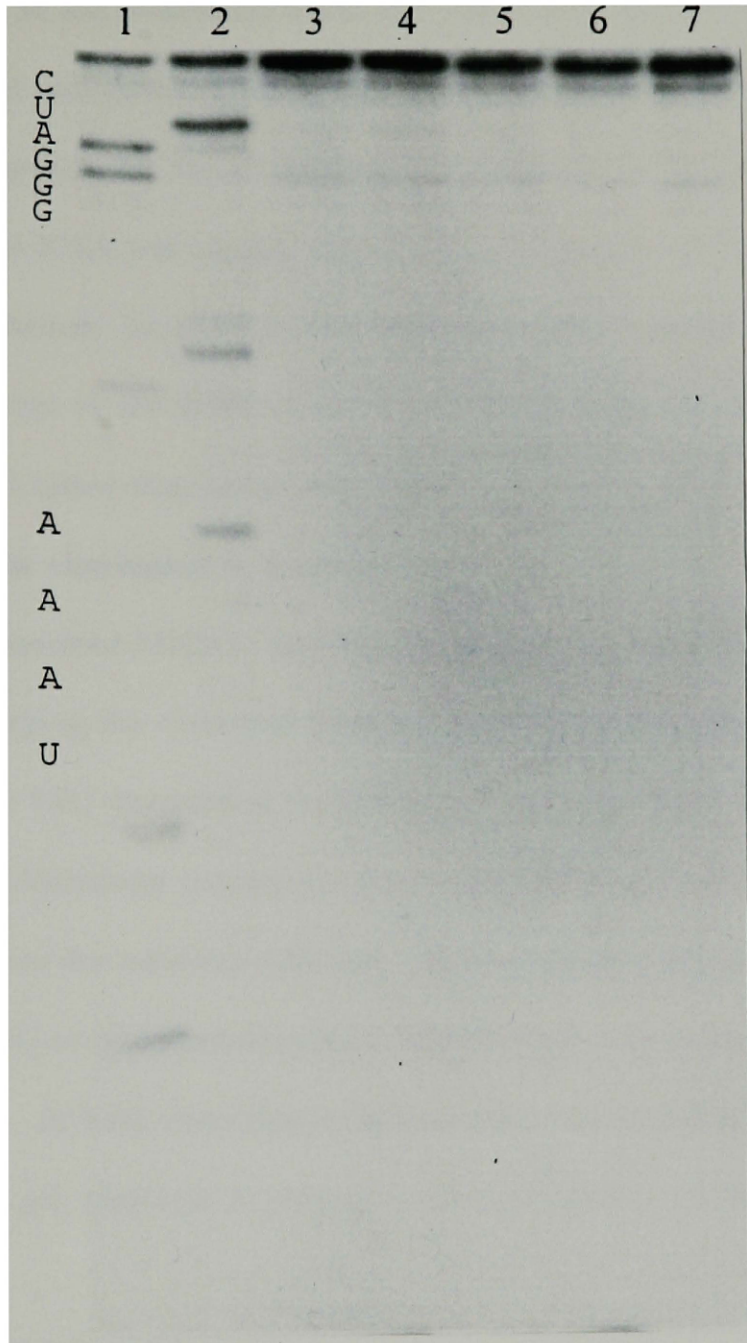


Figure 3.7 Autoradiogram showing the enzymatic sequencing of MHSg+ obtained as described in section 2.12. Microhelix was digested by a different nuclease in each reaction. Lanes are: 1) nuclease T1, 2) nuclease U2, 3) nuclease C13, 4) nuclease Phy M, 5) nuclease from B. cerus, 6) base hydrolysis. Lane 7 is a control mRNA lane. Base sequence is indicate along side the figure.

thiophosphorylation was also attempted. Thiophosphorylation of the microhelices could be carried out. However, the reaction could not be forced to completion. After slight adjustments in the incubation times and conditions, the best yield of thiophosphorylated microhelix RNA (sP-mhRNA) was approximately 15% as seen on an APM gel. Migration of the sP-mhRNA was retarded on an APM gel. The thiophosphorylated RNA was readily distinguished from the unmodified mhRNA which was not retarded. In addition, the large quantity of salts left in the reaction caused a deformation in the shape of the unmodified mhRNA band making it appear almost egg-shaped rather than linear (Fig. 3.8).

### **3.9 Phenanthroline attachment to microhelices**

Both thio-transcribed MHS<sup>G+</sup> and thiophosphorylated MHS<sup>G+</sup> tethered readily to oP. After centrifuging the extracted tethering reactions for 30 min, a small brown pellet, presumably IoP, was seen at the bottom of the tube. This indicated that the series of butanol/chloroform extractions clearly did not remove all of the free phenanthroline from the tethering reaction. As seen on an APM gel, 100% of the thio-transcribed MH39U or thiophosphorylated MHS<sup>G+</sup> was conjugated to oP in the tethering reaction. In both cases the entire retarded thiol-modified band was shifted to the bottom of the gel, identical in position to the unmodified mhRNA (Fig. 3.8 and Fig 3.9).

### **3.10 Microhelix filter-binding assays**

Filter-binding assays were used to quantify MHS<sup>G+</sup> binding to programmed 30S subunits under various conditions. MHS<sup>G+</sup> presumably binds to the P-site on



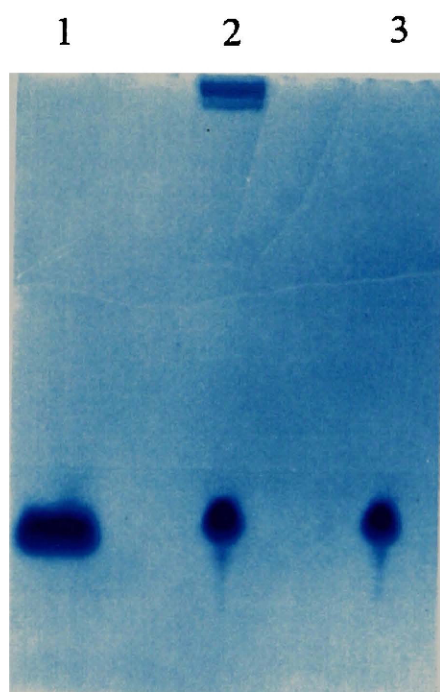
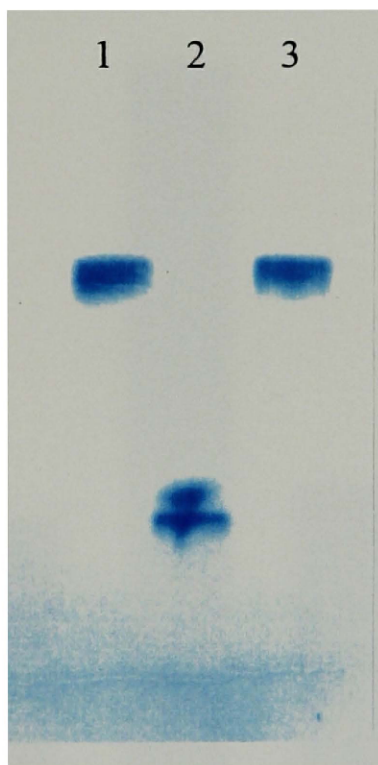


Figure 3.8 10% APM gel showing MHSg<sup>+</sup> modification performed as described in section 2.11. Lanes: 1) MHSg<sup>+</sup>, 2) thiophosphorylated MHSg<sup>+</sup>, 3) oP-tethered thiophosphorylated MHSg<sup>+</sup>.



**Figure 3.9** 10% APM gel showing MH39U modification performed as described in section 2.11. Lanes: 1) MH39U, 2) thio-transcribed MH39U, 3) oP-tethered thio-transcribed MH39U.

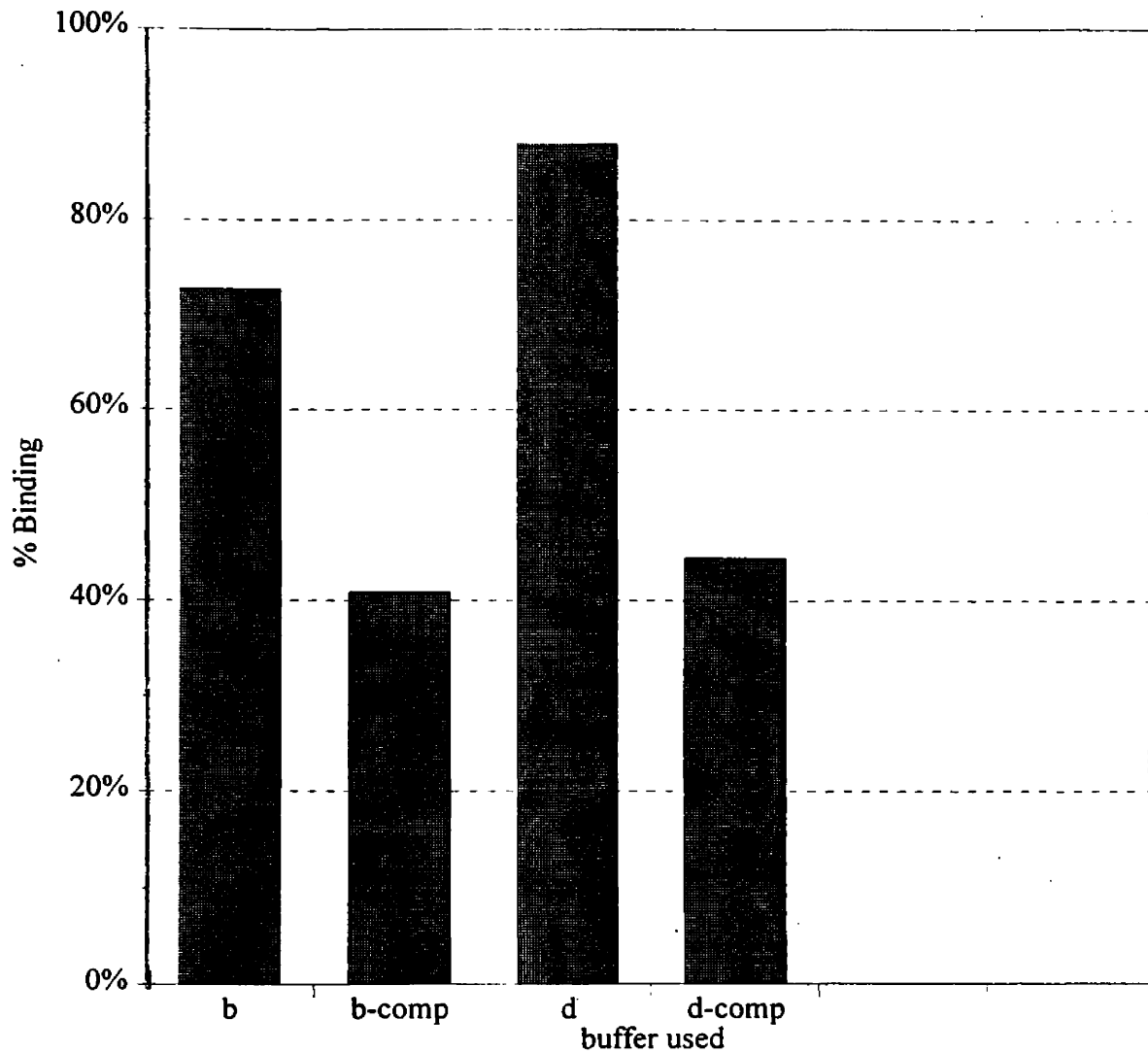


Figure 3.10 Filter-binding assay MHS<sup>+</sup> competition with excess MHS<sup>+</sup>. For buffer information see table 3.2. Reaction: b) MHS<sup>+</sup> binding in activation buffer, b-comp) competition with a 2-fold excess MHS<sup>+</sup>. d) and d-comp) same as b and b-comp) except that helix-binding buffer was used.

programmed 30S subunits. One key set of experiments performed was a series of binding assays using different buffers in an attempt to find a buffer that demonstrated efficient mhRNA binding, but not artifactual binding (Table 3.2). In the standardized cleavage (SC) buffer the microhelix bound at 50%. In a standard activation buffer MHSG+ bound 111%. In a buffer used by the Noller lab, the microhelix bound at a consistent 85%. Extremely high binding, more than 150%, was seen with the high-magnesium buffer and the high-salt buffer. The activation buffer and the Noller buffer were selected for use in competition assays. In the competition assay, a 2-fold excess of unlabeled MHSG+ was added to compete with the labeled MHSG+ for the binding site on the programmed 30S subunit. The expected two-fold reduction in microhelix binding in both buffers was observed (Fig 3.10). The activation buffer and the Noller buffer were used in competition assays with yeast tRNA<sup>Phe</sup>. The presence of an equal molar amount of yeast tRNA<sup>Phe</sup> reduced the binding by the expected 50% in both buffers (Fig 3.11). Binding of MHSG+ at various helix to subunit ratios was examined. The helix bound at a consistent 70% at the three ratios examined (Fig 3.12). Since MH39U and MHSG+ should have had the same hairpin secondary structure and had the same anticodon, it was believed that the binding of MH39U would be very similar to that of MHSG+. It was also necessary to conserve thiolated MH39U for tethering to IoP. For these reasons, only MHSG+ was used in filter-binding studies.

### **3.11 tRNA sulfhydryl removal**

The availability of naturally-occurring thiol-modifications in several *E. coli* tRNAs

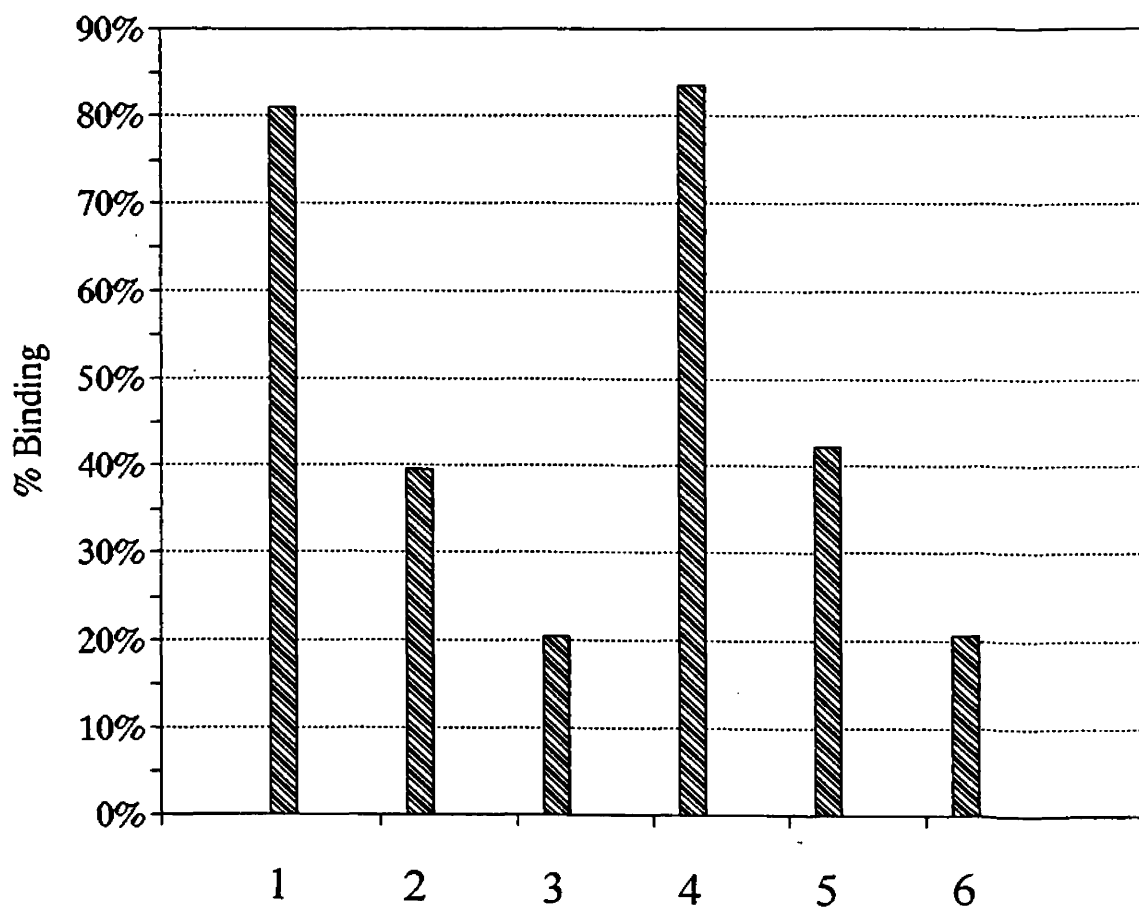


Figure 3.11 Filter-binding assay MHS<sup>+</sup> competition with yeast tRNA<sup>Phe</sup>. For buffer information see table 3.2. Reaction: 1) MHS<sup>+</sup> binding in activation buffer, 2) competition of MHS<sup>+</sup> with an equal molar amount of tRNA in activation buffer, competition with a 10-fold excess tRNA. Reactions 4, 5, and 6 are identical to 1, 2, and 3 except that helix-binding buffer was used.

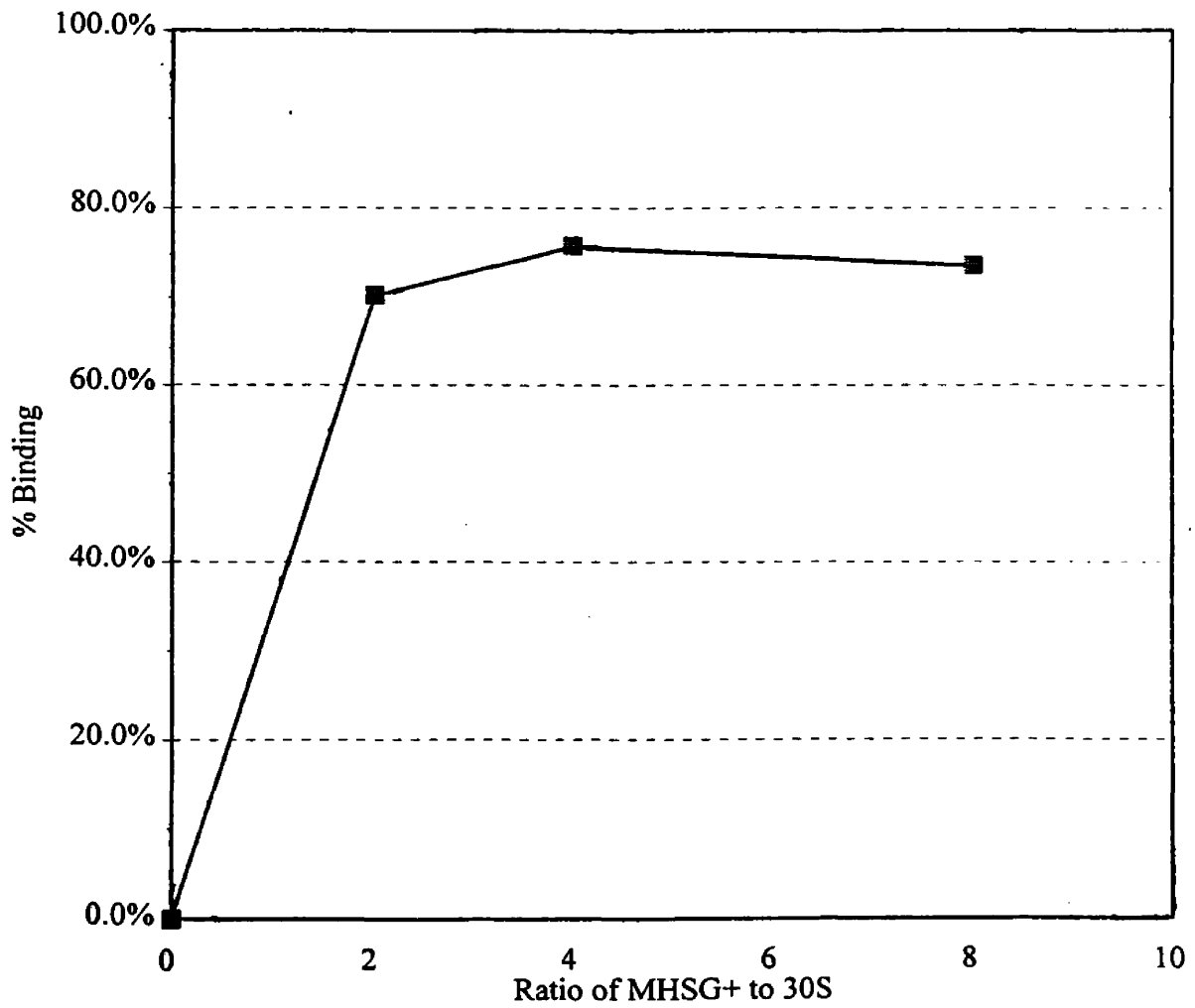
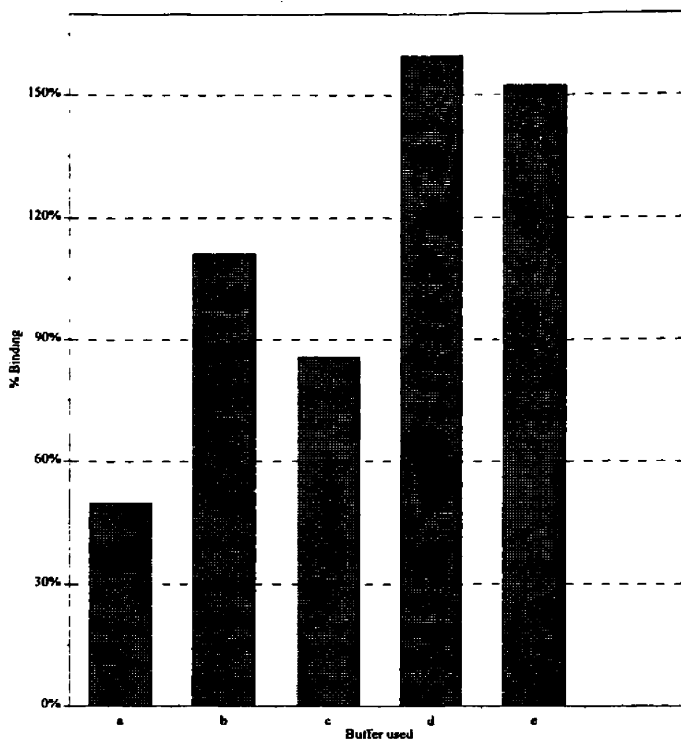


Figure 3.12 Filter-binding assay showing the binding at increasing ratios of MHSg+ to 30S in activation buffer. Assay was performed as described in section 2.13.



Buffer Letter	Buffer name	1X buffer recipe	percent binding
A	standardized Hill lab buffer	40 mM Tris-HCl pH 7.4 6 mM MgCl 60 mM KCl	50%
B	activation buffer	40 mM Tris -HCl pH 7.4 15 mM MgCl <sub>2</sub> 150 mM KCl	111%
C	Noller lab heix binding buffer	80 mM K-cacodylate pH 7.2 25 mM MgCl <sub>2</sub> 100 mM NH <sub>4</sub> Cl	85%
D	Hi Mag buffer	40 mM Tris-HCl pH 7.4 20 mM MgCl <sub>2</sub> 150 mM KCl	159%
E	High salt buffer	40 mM Tris-HCl pH 7.4 25 mM MgCl <sub>2</sub> 250 mM KCl	152%

Table 3.2 Summary of MHS<sup>+</sup> binding results in various buffers.

made their use as a tool to map the tRNA binding site on the 30S ribosome quite attractive. By removing the thiol group and then sending the dethiolated tRNA through the tethering reaction, an excellent mock control reaction was made. The naturally-occurring sulfhydryl groups on the tRNAs were completely removed by the peroxide treatment as seen on an APM gel. The untreated tRNA was retarded in its migration, appearing as a band at the top of the gel. Treatment of the tRNA with hydrogen peroxide removed the sulfhydryl group, with the reaction going to completion. The entire tRNA band was shifted from the top of the gel to the bottom of the APM gel with no trace of any unreacted tRNA at the top of the gel (Fig 3.13). In the natural tRNAs there appeared to be a very small fraction of the tRNA which lost its thio group, as evidenced by a band corresponding to the sulfhydryl-destroyed tRNA (-SH tRNA) at the bottom of the APM gel. The migrational difference between tRNA<sup>Phe</sup> and -SH tRNA<sup>Phe</sup> as well as tRNA<sup>Arg</sup> and -SH tRNA<sup>Arg</sup> was very significant. The unmodified tRNA band was typically at the top of the gel, and the -SH tRNAs were in the bottom of the gel. This pattern was not seen with tRNA<sup>Glu</sup>. Modified tRNA migrated to the bottom of the gel as expected. However, the unmodified tRNA<sup>Glu</sup> band migrated much further than expected. Typically, the tRNA<sup>Glu</sup> band was about 1 cm above the -SH-tRNA<sup>Glu</sup> band in a standard minigel. With tRNA<sup>Phe</sup> or tRNA<sup>Arg</sup> this difference could be 5(+) cm on the same size gel.

### **3.12 Phenanthroline tethering to tRNAs**

#### **3.12.1 oP attachment in an organic medium**

As seen with the microhelices, phenanthroline was readily tethered to all three



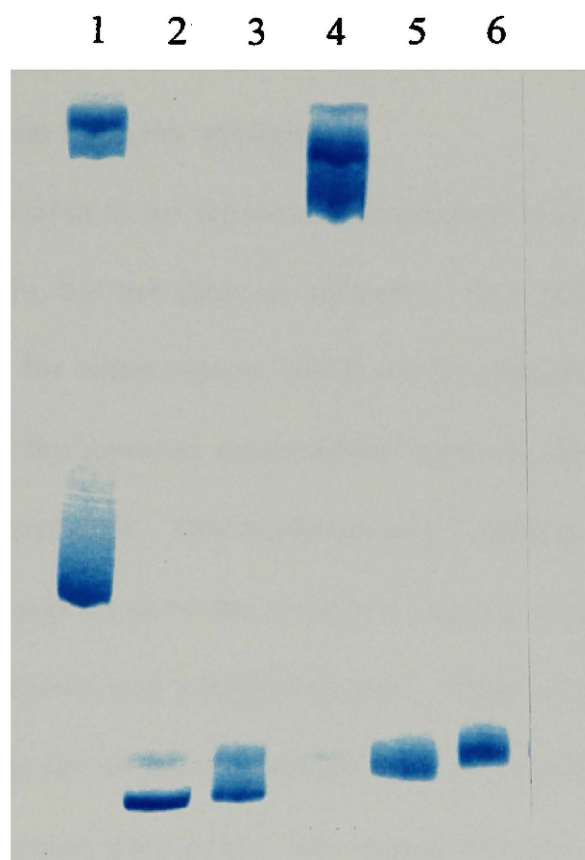


Figure 3.13 10% APM gel showing modification of tRNA performed as described in section 2.15.2. Lanes: 1) tRNA<sup>Glu</sup>, 2) sulfhydryl destroyed tRNA<sup>Glu</sup>, 3) oP-tRNA<sup>Glu</sup>, 4) tRNA<sup>Arg</sup>, 5) sulfhydryl destroyed tRNA<sup>Arg</sup>, 6) oP-tRNA<sup>Arg</sup>.

tRNAs. Again, the centrifugation step produced a small brown pellet at the bottom of the tube. This indicated that the series of butanol/chloroform extractions clearly did not remove all of the free phenanthroline from the tethering reaction. A complete band shift was seen on the APM gel. The entire thiolated band at the top of the gel was shifted to the bottom of the gel (Fig 3.14), providing indirect evidence for the tethering of oP to the tRNA.

### **3.12.2 oP attachment in an aqueous medium**

Phenanthroline attachment in an aqueous environment was much more straightforward and simple, but not quite as efficient. The tRNAs tethered to IoP in the organic environment, for some reason, could not be ethanol precipitated. The tRNAs tethered to IoP in the aqueous environment behaved more like native tRNA and could be ethanol precipitated. Spectrophotometer readings taken 260 nm on oP-tRNA samples gave readings close to the expected readings indicating the presence of little or no free phenanthroline and a high recovery. When a known quantity of unmodified tRNA was run on an acrylamide gel next to a similar quantity of oP-tRNA, similar band intensities were seen. This meant that the spectrophotometer readings were reliable and again suggested the absence of free phenanthroline. When analyzed on an APM gel, there was usually a very faint band at the top of the gel. This indicated the tethering reaction did not go to completion, but the amount of untethered tRNA appeared to be less than 5% of the sample. The migration of oP-tRNAs prepared in organic or aqueous environments were the same, both migrated to the bottom of an APM gel.

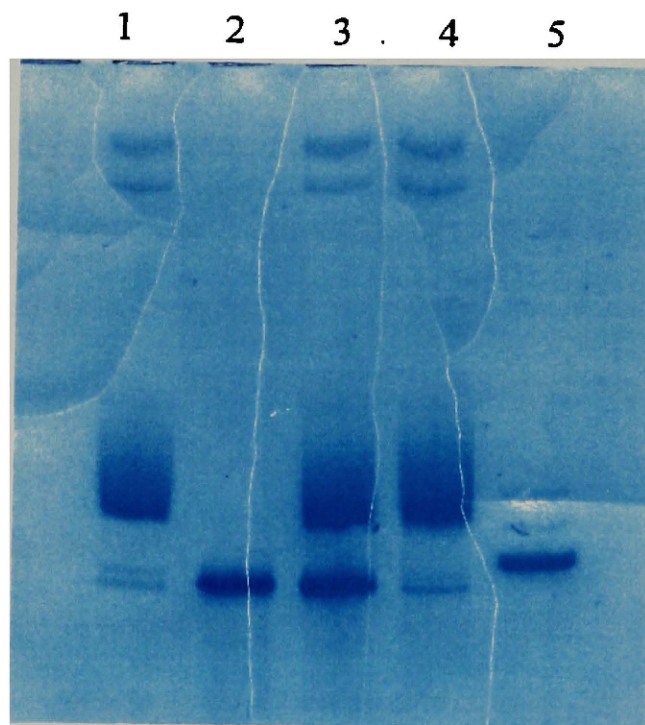


Figure 3.14 10% APM gel showing the modification of tRNA<sup>Glu</sup> performed as described in section 2.15.1. Lanes: 1) tRNA<sup>Glu</sup>, 2) oP-tRNA<sup>Glu</sup>, 3) mixture of samples from lanes 1 and 2, 4) NoP mock control tRNA<sup>Glu</sup>, 5) yeast tRNA<sup>Phe</sup>.

### **3.13 End labeling of oP-tRNAs**

The long process of 5' end labeling the tRNAs was made especially difficult by massive amounts of tRNA degradation throughout the process and by the fact that these smaller fragments of tRNA were labeled more readily. The amount of radioactive material in the purification gel was always extremely high as evidenced by the extremely short exposure times (5-30 seconds) required for quality autoradiograms. Massive amounts of degradation produced tRNA fragments which were visualized on the autoradiograms as bands below the full-length tRNA band. The full-length band was separated from what was presumed to be a tRNA degradation product wherein three bases had been removed (N-3). Oddly, no single-base or two-base degradation products were seen. Below the N-3 band, each degradation product could be seen if the exposure time was reduced as to not overexpose the film (Fig 3.15)

### **3.14 oP-tRNA binding studies**

Binding of the various end-labeled tRNAs to the P-site of programmed 30S ribosomal subunits was quantified by filter-binding assays. The first attempts at quantifying tRNA binding via filter-binding assays met with limited success, due to high backgrounds and uninterpretable results, presumably caused by high amounts of residual free IoP. Previous studies in our lab demonstrated that gel purification of ligands tethered to oP in an organic environment was required if the ligand was to be used in filter-binding assays. This set of experiments included a mock control in which a sample of the tRNA was sent through the IoP tethering reaction with 5-nitrophenanthroline (NoP) instead of IoP. Since NoP has no tethering group it would

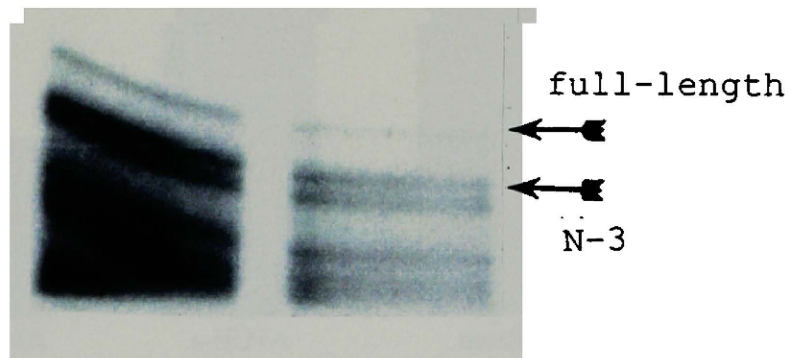


Figure 3.15 Autoradiogram showing the end labeling of tRNA<sup>Phe</sup> obtained as described in section 2.16. Each lane contains an aliquot of the labeling reaction. Arrows indicate full-length and N-3 products.

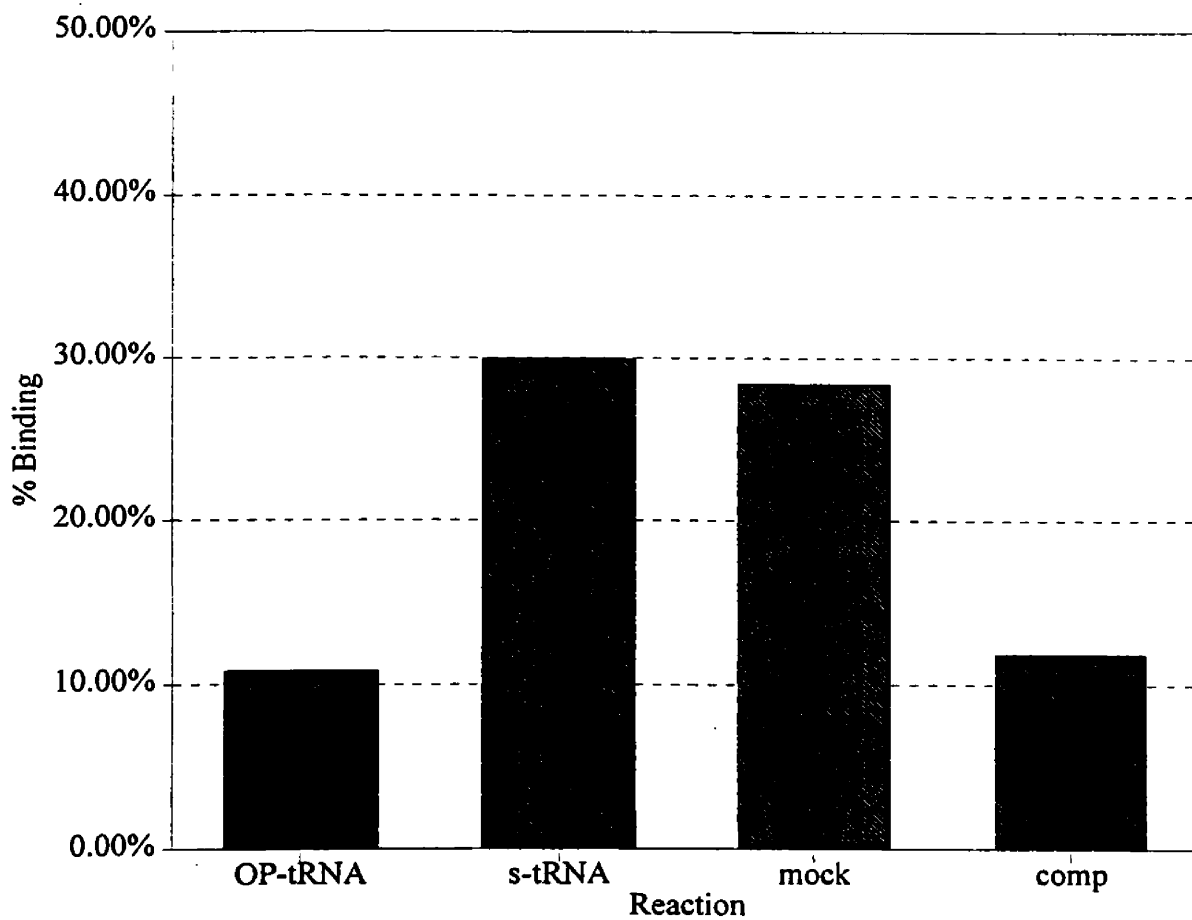


Figure 3.16 Filter-binding assay showing the binding of modified tRNA<sup>Glu</sup> in BC buffer. Reactions: 1) oP-tRNA<sup>Glu</sup>, 2) unmodified tRNA<sup>Glu</sup>, 3) NoP mock control tRNA<sup>Glu</sup>, 4) oP-tRNA<sup>Glu</sup> competed with a 5-fold excess unmodified tRNA<sup>Glu</sup>.

not attach to a thiol-containing tRNA, thereby controlling out any affects caused by the tethering reaction itself.

The first "successful" binding experiment was done with tRNA<sup>Glu</sup> and poly-AG programmed 30S ribosomal subunits. The unmodified tRNA bound weakly as did the mock control tRNA<sup>Glu</sup>, both about 30%. The oP-tethered tRNA<sup>Glu</sup> bound very weakly, slightly more than 10%. Competition of oP-tethered tRNA<sup>Glu</sup> with a five-fold excess of unmodified tRNA<sup>Glu</sup> did not show the expected reduction in binding of oP-tRNA<sup>Glu</sup> (Fig 3.16).

The binding studies with tRNA<sup>Arg</sup> and mRNA-A1 programmed 30S subunits told a different story. Binding of the unmodified, oP-tethered, and mock forms of tRNA<sup>Arg</sup> were all near 45%. Competition of oP-tethered tRNA<sup>Arg</sup> with a five-fold excess of unmodified tRNA<sup>Arg</sup> did, in fact, show the expected reduction in binding of oP-tRNA<sup>Arg</sup>. In the competition reaction, the binding dropped to 8%, almost the expected value (Fig 3.17).

Filter-binding studies with unmodified tRNA<sup>Phe</sup> were done in BC buffer, previously used for cleavage experiments. In this buffer, tRNA<sup>Phe</sup> was found to bind at about 73% at a 4:1 tRNA to subunit ratio (Fig 3.18). No binding studies were performed with oP-tRNA<sup>Phe</sup>.

### **3.15 oP-tRNA cleavage experiments**

Knowing that oP could be tethered to the various E. coli tRNAs, and that these oP-tRNAs could bind to programmed 30S ribosomal subunits, cleavage reactions were carried out.

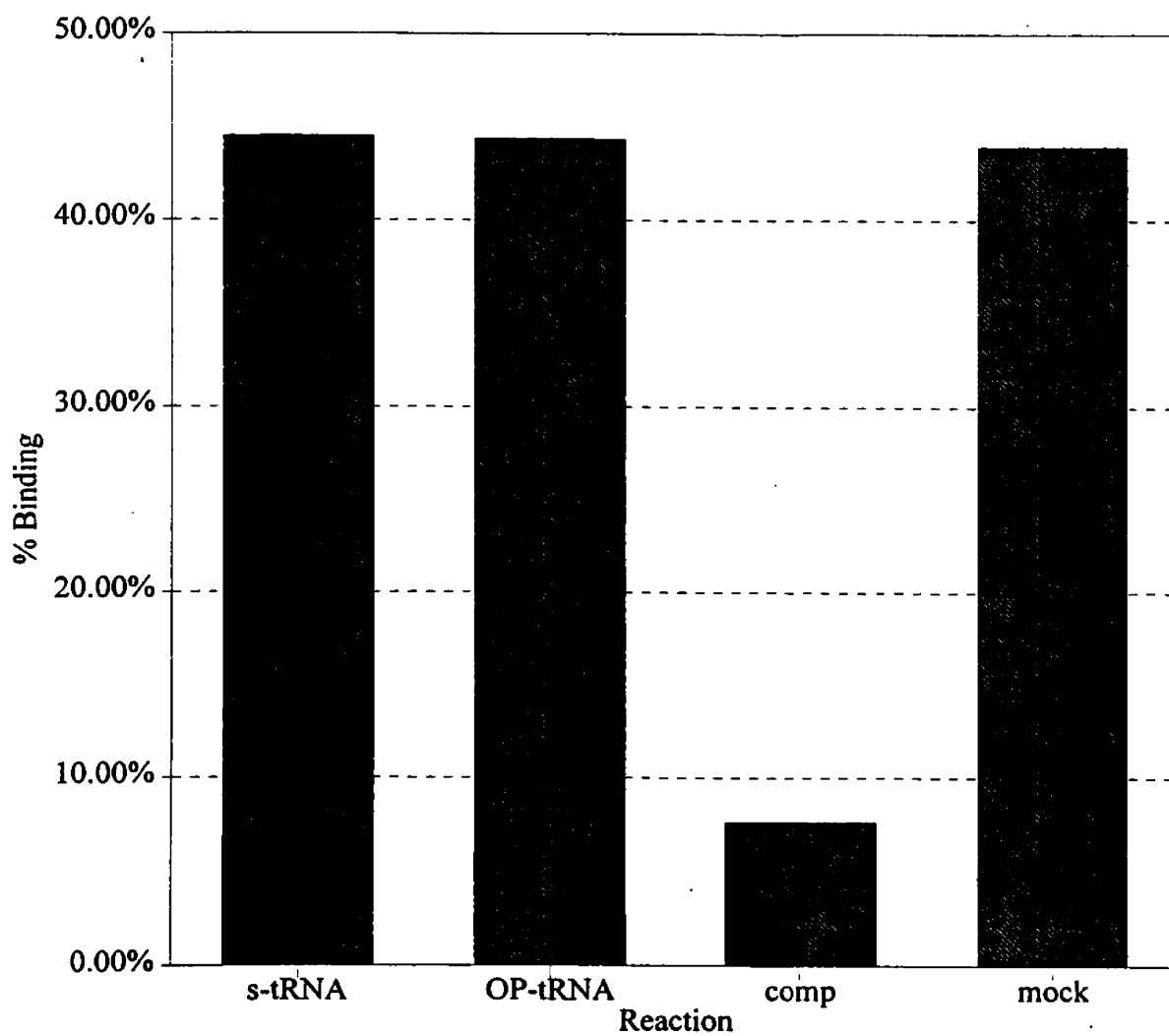


Figure 3.17 Filter-binding assay showing the binding of modified tRNA<sup>Arg</sup> in BC buffer. Reactions: 1) unmodified tRNA<sup>Arg</sup>, 2) oP-tRNA<sup>Arg</sup>, 3) oP-tRNA<sup>Arg</sup> competed with a 5-fold excess unmodified tRNA<sup>Arg</sup>, 4) NoP mock control tRNA<sup>Arg</sup>.



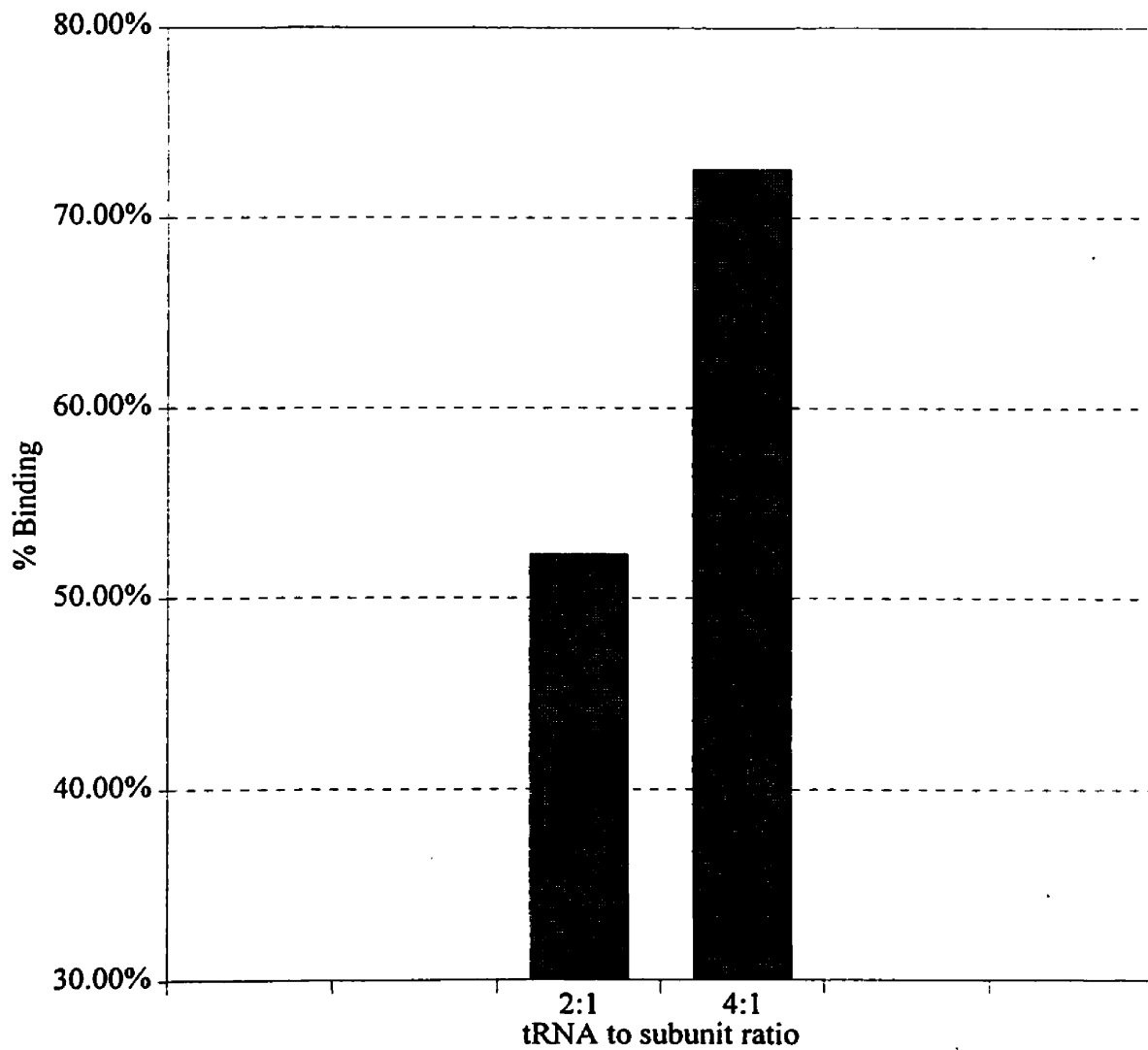


Figure 3.18 Filter binding assay showing the binding of *E. coli* tRNA<sup>Phe</sup> to programmed 30S in bC buffer at 2:1 and 4:1 tRNA to subunit ratios.

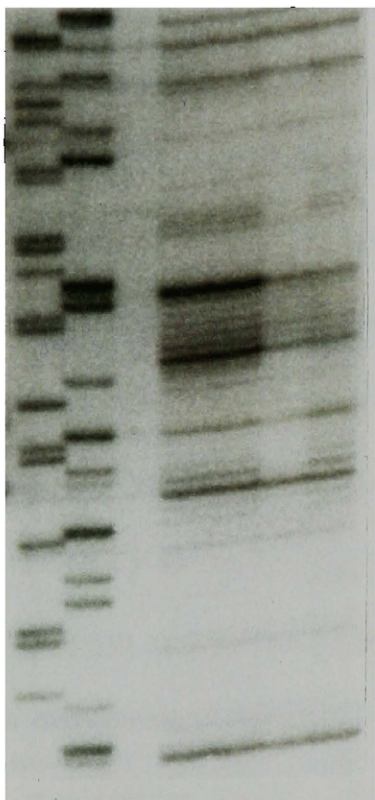
### **3.15.1 Cleavage experiments, using free IoP as a control**

In this cleavage reaction using oP-tRNA<sup>Glu</sup>, an attempt was made to duplicate the conditions used by Noller in his chemical protection studies, yet allowing binding of oP-tRNA<sup>Glu</sup> and cleavage by oP. Subunit concentration was 1.0 μM with the molar tRNA to subunit ratio being 4:1 in binding buffer with 40 μM copper<sup>+2</sup> and 0.4 μg/μL poly-U. After the activation incubation and binding incubation, the cleavage reaction was initiated by the addition of MPA to a final concentration of 2.5 mM. In the free IoP control, 1.0 μL of 1.0 mM IoP was added to the reaction with the final volume being 75 μL bringing the final ratio of free IoP to 30S subunits to 13.3:1. No tRNA was added to the free IoP control reaction. As always, a competition control reaction was included in which a five-fold excess of unmodified tRNA was added to the reaction. Extensive primer extension analysis revealed no cleavages of the 16S rRNA specifically from oP-tRNA<sup>Glu</sup> (data not shown).

### **3.15.2 Cleavage experiments using NoP mock controls**

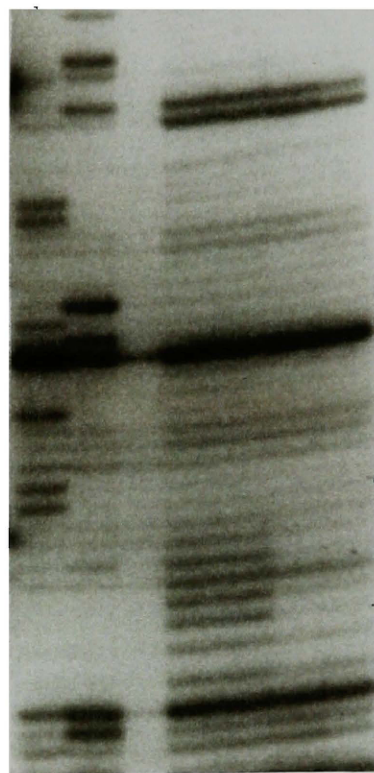
This second set of cleavage experiments contained two basic controls, the NoP mock and the competition controls, both described in section 3.14. One minor change was made in the conditions of this set of cleavage reactions: the copper concentration was increased to 100 μM. Cleavage experiments using tRNA<sup>Arg</sup> used the designed mRNA analog mRNA-A1 at a molar concentration equal to that of the tRNA in the cleavage reaction. Cleavage experiments with oP-tRNA<sup>Arg</sup> and subsequent primer extension analysis revealed three potential sites of cleavage. Stops were seen on the films corresponding to nucleotides G198/A199, C840/G846, and 923-930 of

U C K 1 2 3 4



840 region

U C K 1 2 3 4



920 region

Figure 3.19 Autoradiogram of primer-extension assays showing cleavages generated by oP-tRNA<sup>Arg</sup>. Gel was run as described in section 2.19. Lane designations are the same for panels A and B since they are segments of the same autoradiogram. Lanes U) and C) are sequencing lanes using ddATP and ddGTP respectively. Lanes K) is a control extension lane. Lanes 1) and 2) are cleavage reactions using oP-tRNA<sup>Arg</sup> at 4:1 tRNA to subunit ratio. Lanes 3) is competition reaction using a five-fold excess unmodified tRNA<sup>Arg</sup>. Lane 4) is a reaction using NoP mock control tRNA<sup>Arg</sup>. Arrows indicate the sites of cleavage.

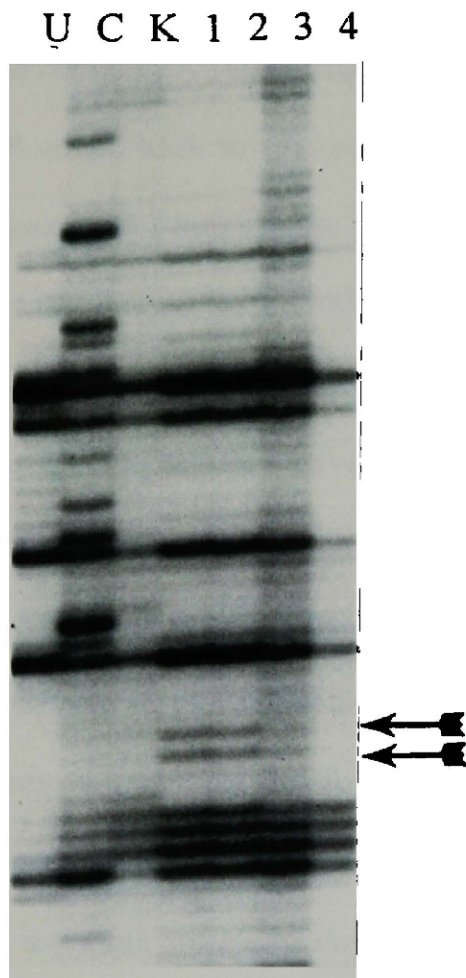
16S rRNA. This experiment was repeated with the addition of a noncognate mRNA control. In this control, a mRNA that would not form a codon-anticodon interaction was included to a final concentration equal to the concentration of that mRNA in a cognate reaction. Cleavage experiments were done with oP-tRNA<sup>Arg</sup> and oP-tRNA<sup>Phe</sup>. Again, stops were seen on the films corresponding to nucleotides G198/A199, C840/G846, and 923-930 of oP-tRNA<sup>Arg</sup> cleaved 30S (Fig 3.19). In the experiments with oP-tRNA<sup>Phe</sup>, bands resulting from cleavage by oP-tRNA<sup>Phe</sup> were seen corresponding to bases G198/A199 (Fig 3.20).

On an interesting note, later analysis demonstrated the presence of enough 50S contamination in the 30S subunit preparations to give a signal when 23S rRNA primer 235 was used to analyze these tRNA<sup>Arg</sup> cleaved 30S. On top of this, cleavages were seen repeatedly at nucleotides 59-66 and 86-93 of the 23S rRNA. The entire 23S rRNA was not sequenced by primer extension assays. In experiments with both oP-tRNAs containing a position 8 s<sup>4</sup>-U cleavages were seen at the 5' end of the 23S rRNA, nucleotides 59-66 and 86-93.

### 3.15.3 Cleavage experiment with dialyzed tRNAs

Up to this point, cleavages at G198/A199 had always been seen when 30S were cleaved with oP-tRNA<sup>Phe</sup> or oP-tRNA<sup>Arg</sup>. To determine the affect of free IoP in the cleavage reaction, oP-tRNA<sup>Phe</sup> purified from the IoP tethering reaction by butanol/chloroform extractions was compared to oP-tRNA<sup>Phe</sup> purified by dialysis. In addition, a new cleavage reagent 5-acetamido-1,10-phenanthroline (AoP) was examined for its potential use as a replacement for NoP in the mock control reaction. The tRNA

A



B

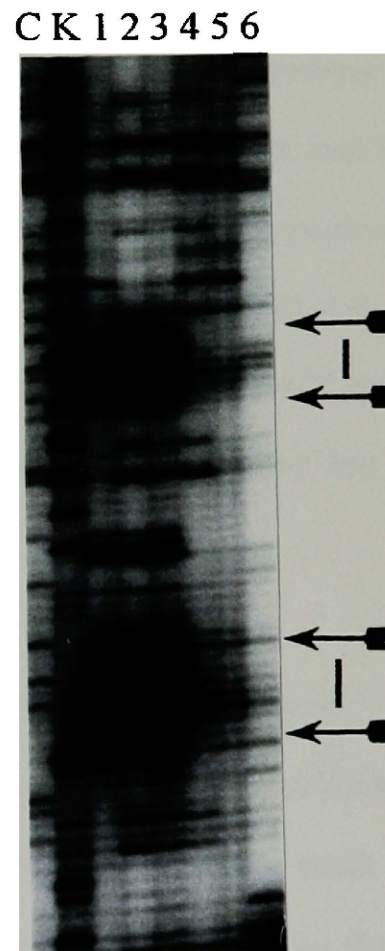


Figure 3.20 Autoradiogram of primer-extension assay showing cleavages generated by oP-tRNA<sup>Phe</sup>. Gel was run as described in section 2.19. Panel A. Lanes U) and C) are sequencing lanes using ddATP and ddGTP respectively. Lanes K) is a control extension lane. Lanes 1) and 2) are cleavage reactions using oP-tRNA<sup>Arg</sup> at 4:1 tRNA to subunit ratio. Lanes 3) is competition reaction using a five-fold excess unmodified tRNA<sup>Arg</sup>. Lane 4) is a reaction using NoP mock control tRNA<sup>Arg</sup>.

Panel B. Lanes C and K are the same in panel A. Lanes: 1) 30S with 75 μM free IoP, 2) 30S with mRNA and 75 μM free IoP, 3) Cleavage reaction with oP-tRNA<sup>Phe</sup> at a 4:1 tRNA to subunit ratio, 4) sulfhydryl destroyed mock control tRNA<sup>Phe</sup>, 5) competition with a 5-fold excess unmodified tRNA<sup>Phe</sup>, 6) cleavage reaction with non-cognate mRNA (poly-AG). Arrows indicate the sites of cleavage.

recovered from dialysis was checked on an APM gel, and this tRNA was not retarded in its migration. Standard conditions were used, with copper at 200  $\mu\text{M}$  and MPA at 2.0 mM. Six reactions were run: extracted oP-tRNA<sup>Phe</sup>, dialyzed oP-tRNA<sup>Phe</sup>, extracted AoP-tRNA<sup>Phe</sup>, and dialyzed AoP-tRNA<sup>Phe</sup>. The last two reactions contained dialyzed oP-tRNA<sup>Phe</sup> which had one molar equivalent and two molar equivalents of free IoP added back to the reaction (final IoP concentrations were 4.0  $\mu\text{M}$ , and 8.0  $\mu\text{M}$  respectively) making the final ratio of free IoP to 30S 4:1 and 8:1 respectively. Dialysis eliminated the G198/A199 cleavages, even when free IoP was added back to the reaction. Both the extracted AoP-tRNA<sup>Phe</sup> and the dialyzed AoP-tRNA<sup>Phe</sup> did not produce the 200 region cleavages. The only sample which did generate the 200 region cleavages was the extracted oP-tRNA<sup>Phe</sup> (Fig 3.21).

#### **3.15.4 Cleavage experiments with updated controls**

In this set of experiments, the tRNAs were tethered to IoP in the aqueous environment, mock control from section 3.15.2 was revamped, reaction conditions were altered slightly, and two additional controls were added. In the new mock control the thiol groups of the various tRNAs are first removed, as described above in section 2.14, before the tRNAs are sent through the aqueous environment IoP tethering reaction. The two new controls contained free IoP at a final concentration of 75 $\mu\text{M}$  with 30S subunits only and 30S subunits with the cognate mRNA for that set of experiments. Here the ratio of free IoP to 30S was 75:1, close to the ratio of free IoP 30S in the extracted tRNA samples. The copper concentration was increased to 200  $\mu\text{M}$ , and the MPA concentration was decreased to 2.0 mM.

U C K 1 2 3 4 5 6

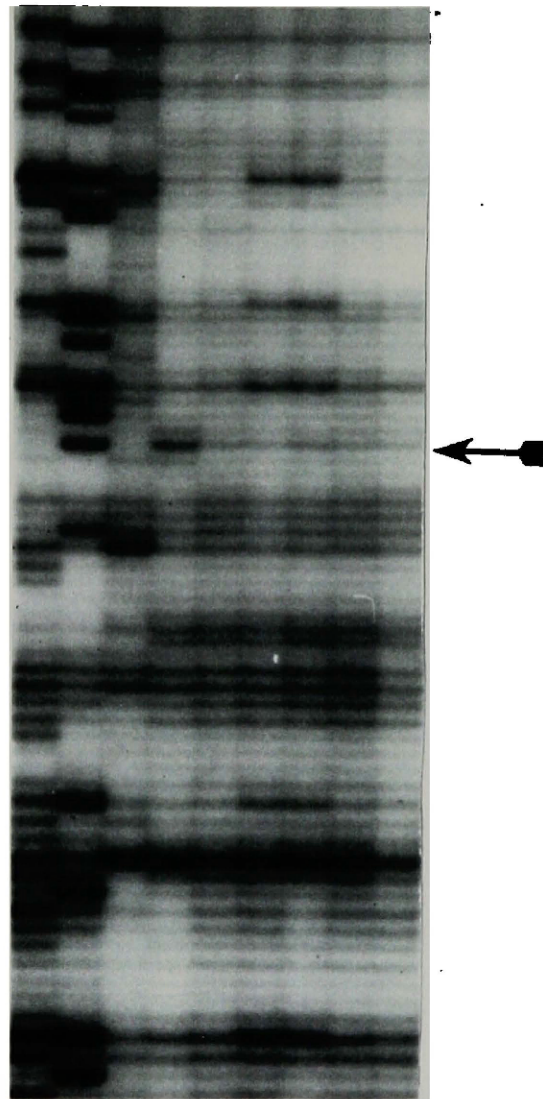


Figure 3.21 Autoradiogram of primer-extension assay from the dialysis experiment. Gel was run as described in section 2.19. Lanes U and C are sequencing lanes using ddATP and ddGTP respectively. Lane K is a control extension lane. Remaining lanes are cleavage reactions using various forms of  $tRNA^{Phe}$ . Lane: 1) butanol/chloroform extracted oP- $tRNA^{Phe}$ , 2) dialyzed oP- $tRNA^{Phe}$ , 3) and 4) dialyzed oP- $tRNA^{Phe}$  with 4.0  $\mu M$  and 8.0  $\mu M$  free IoP added back respectively, 5) butanol/chloroform extracted AoP/ $tRNA^{Phe}$ , 6) dialyzed AoP/ $tRNA^{Phe}$ . Arrow indicated the site of cleavage.



No bands due to cleavage were seen on the films of 16S rRNA from oP-tRNA<sup>Arg</sup> cleaved 30S subunits. The same was true for oP-tRNA<sup>Phe</sup> and tRNA<sup>Glu</sup>; no cleavages were seen in the 16S rRNA. However, all three oP-tRNAs did generate the same cleavages at the 5' end of the 23S rRNA (data not shown).



## **4.0 DISCUSSION**

### **4.1 Helix 34 probing study**

The goal of this part of the project was to study the structure of helix 34 of the E. coli 16S rRNA. All of the popular secondary structure maps depict helix 34 as double stranded with several small bulge regions. In the mRNA/rRNA model of termination, an opening of helix 34 is necessary to allow the mRNA access to the ribosomal RNA, if it is not already accessible (15,25,62).

Ribonuclease H studies demonstrated the binding specificity of the three hexameric probes used in this study. Each hexameric probe specifically hybridized to helix 34 when the rRNA was denatured, as evidenced by the size of the rRNA fragments seen on the RNase H assay gels. The 13-base probe bound to helix 34, as well as a second site. By examining the size of the 16S rRNA fragments generated by this probe in RNase H assays and looking at the sequence of the rRNA itself, the 300 region is thought to be the second site to which probe 1049-1061 bound. However, only if the small subunit was stripped of all proteins and the rRNA linearized was digestion by RNase H possible. The necessity for having protein-free linearized RNA indicates a tight double-stranded structure for helix 34. If the ribosomal proteins shield this region from digestion by RNase H, removing the proteins through phenol extractions should have been sufficient to make helix 34 susceptible to RNase H digestion. If this region is single stranded or has a loose structure, the highly-structured protein-free rRNA would have been susceptible to digestion by RNase H. Clearly, this was not the case. The rRNA needed to be linearized by heating after phenol extraction,

indicating a tight double-stranded structure.

Cross-linking studies revealed a zero-length cross-link between the third base of the A-site codon and base U1052 of the 16S rRNA (17). These cross-linking studies suggested helix 34 is not buried within the small subunit, but rather provided strong evidence to indicate that helix 34 may be solvent exposed (4). The cross-linking results lend support to the mRNA/rRNA base pairing model of termination by placing helix 34, the rRNA segment supposedly involved in direct mRNA/rRNA base pairing, at the decoding site on the ribosome.

Although they bound to denatured 16S rRNA, none of the hexameric probes bound to the 30S subunit at any probe to subunit ratio. The 13-base probe bound only at high probe to subunit ratios, again suggesting helix 34 is truly double stranded. If the mRNA/rRNA hypothesis of termination is correct, the addition of mRNA, or a mRNA analog, might induce structural changes within helix 34 opening up the structure to allow the mRNA/rRNA interaction. In the process helix 34 should be opened up and made available to probe binding. This did not occur. The addition of poly-U and S150, a crude mixture of translation factors, did not cause an increase in probe binding. Binding of the 13-base probe did increase from 4.2% to 14.3% upon the addition of poly-U, but this was only at the higher ratios. Previous studies by others have shown structural changes upon the addition of mRNA or mRNA analogs, but the amount of change is unknown.

Probe binding only at high probe to subunit ratios (32:1 or 40:1) is often characteristic of nonspecific or second site binding (37). Since a sequence

complementarity exists between probe 1049-1061 and the 300 region of the 16S rRNA, the binding at these high ratios is attributed to the 300 region. The addition of poly-U may induce a structural change that slightly opens up the 300 region. However, a 10% increase in binding is not usually significant. The lack of probe binding in these last sets of experiments strongly suggests helix 34 does not open up for probe binding and the region remains tightly double stranded.

The bulge at 1199-1204 contains tandem UCA triplets which could base pair with the UGA stop codon. Deletion of base C1054 was found to suppress UGA-dependent termination because this deletion changed the sequence of the 1050 region such that it is complementary to the 1200 bulge (63). With the 1200 bulge base paired, mRNAs containing the UGA stop codon could not base pair with the 16S rRNA. From this mutagenesis study and the observed conservation of the bulges within helix 34 to which the stop codons could base pair, the base pairing model of termination was proposed. A subsequent mutagenesis study found that deletion of C1054 was a general suppressor of all three stop codons (65). The suppression of all three stop codons suggests helix 34 plays a more general role in termination.

A series of site-directed mutagenesis studies showed that nucleotides (1202 and 1203) supposedly involved in the mRNA/rRNA base pairing could be mutagenized with no ill effects to the cell. Other nucleotides within the same bulge (1199 and 1200) had moderate effects. Several nucleotides on the other side of the helix (1054, 1057, 1058), not involved in base pairing to the mRNA, could not be mutagenized without drastically harming the cell. Other bases in the same region could be changed.

No clear pattern can be defined (61).

Since helix 34 is not available for binding by single-stranded DNA probes and the bulge supposedly involved in base pairing to the mRNA stop codons can be altered, it seems very unlikely that the mRNA/rRNA base pairing model for termination is valid. Helix 34 is important to ribosome function, but there may not be direct interaction with mRNA. If helix 34 plays any role in termination, it must be a more generalized role. The filter-binding data and the RNase H assay data suggest that helix 34 is not accessible to cDNA probes, suggesting that the structure remains reasonably closed.

#### **4.2 Anticodon loop analog (microhelix) studies**

Transcriptions produced the unmodified microhelix MHSG+ in quantities sufficient for study. Yields were close to the reported expected yields for a 0.5 mL T7 RNA polymerase transcription reaction. Thiol-containing transcription reactions produced small yields of thiolated MH39U. Initially, template structure was thought to be the problem. Nondenaturing gels showed that the P3 complement was hybridizing to the noncoding strand as it should. Since the template coded for a hairpin structure, it was possible for the noncoding template strand to fold back on itself. However, nuclease-digestion studies showed the template was not folding back on itself. Subsequent experiments by Nierhaus showed  $s^4$ -UTP to be a negative allosteric effector of T7 RNA polymerase (103). For this reason, a small quantity of UTP was required in the transcription reaction. If a transcription reaction contains only  $s^4$ -UTP the polymerase would be down regulated to the extent of no transcription. Shifting the reaction conditions to contain 20-30% UTP versus 10% UTP in the thio-transcription reaction

may indeed increase the product yield. However, a major problem may be created in the process. At this concentration of UTP, a substantial quantity of unthiolated MH39U would have been produced. As visualized on a APM gel, 10% UTP in the thio-transcription reaction resulted in the production of little unthiolated microhelix.

End labeling MHS<sup>G+</sup> for use in enzymatic sequencing studies and filter-binding assays was not very efficient. On occasion it was difficult to obtain a microhelix sample "hot" enough for use in enzymatic-sequencing experiments and filter-binding assays. According to the secondary structure of MHS<sup>G+</sup>, the 5' end is recessed, likely being shielded by the 3' tail. Shielding of the 5' end may render it somewhat inaccessible to modification by a kinase. For this reason, it is thought that phosphorylation (end labeling) and thiophosphorylation of MHS<sup>G+</sup> were inefficient.

Enzymatic sequencing indirectly confirmed the primary and secondary structure of MHS<sup>G+</sup>. The sequence of the single-stranded loop and the 3' tail were visualized on the autoradiograms. The lack of sequence of the supposedly base-paired segments indirectly confirmed their structure and sequence. The lack of digestion clearly showed this region to be double stranded since the nucleases in the sequencing kit only digest single-stranded RNA. In order for base pairing to occur, the sequences must be complementary, which implies MHS<sup>G+</sup> had the correct primary structure in the stem region.

What little thiol-modified mhRNA that was generated could easily be tethered to phenanthroline. In both cases the entire thiol-containing mhRNA band could be shifted to the bottom of the gel upon oP tethering, indicating complete attachment of

the microhelices to oP. However, the quantities of oP-MHSG+ or oP-MH39U needed for a cleavage reaction could not be generated.

Microhelix binding to the P-site of the 30S ribosomal subunit in the low-salt buffer was low, and for this reason, the low-salt buffer was not used in further studies. Binding in the high-salt buffer and the high-magnesium buffer was near 150%, an artifact likely created by the buffers. Helix-binding buffer allowed the microhelix to bind at about 85%. This level of binding is very close to that seen previously by the Noller lab using this buffer with the anticodon loop fragment of tRNA<sup>Phe</sup>. Microhelix binding in the activation buffer was slightly higher than 100%. The binding in excess of 100% was most likely not due to nonspecific binding. Competition studies showed that MHSG+ binding was specific (see below). Since the activation buffer has been used by many ribosome researchers for many years, it is not likely that the buffer was to blame for any artifacts of binding. Therefore, binding in excess of 100% is considered to be experimental error.

In reactions using the helix-binding buffer and the activation buffer, competition with a two-fold excess of unmodified MHSG+ decreased binding by half. This linear competition suggests the microhelix binds to a real site, presumably the P-site, in both buffers. In the competition experiment with excess MHSG+, binding of the microhelix in the activation buffer was lower: closer to 73%, a number more realistic than 111% binding previously seen with this buffer. The competition studies of MHSG+ with yeast tRNA<sup>Phe</sup> in activation buffer also showed a linear competition. This means that the microhelix not only competes with itself, which may occur at some secondary site,

but it also competes with native tRNA suggesting the microhelix binds to a functional tRNA binding site on the ribosome. A tRNA will presumably bind to the P-site of a programmed 30S subunit. Since tRNA<sup>Phe</sup> competes with MHS<sup>+</sup>, then the microhelix must also bind to the P-site of the programmed 30S. Cleavage experiments could not be carried out since sufficient quantities of thio-modified microhelix RNA could not be generated

#### **4.3 Natural E. coli tRNA studies**

Analysis on an APM gel showed unmodified tRNAs Glu, Phe, and Arg did not migrate as far as yeast tRNA<sup>Phe</sup>, which is of similar size. The difference is the presence of naturally-occurring thiol groups within these three E. coli tRNAs which caused their retarded migration. Destruction of the sulfhydryl group contained within any of the tRNAs by peroxide treatment shifted the entire tRNA band to the bottom of the gel (Fig 3.13). This indicates that the sulfhydryl destruction reaction went to completion, thus the resulting tRNA contained no thiol group to retard its migration on the APM gel. An identical band shift could be seen when the native tRNAs were tethered to IoP. Tethering oP to the thiol-modified base of the tRNA effectively shielded the thiol group and thus prevented binding and migrational retardation by the APM gel matrix. If the tRNAs were tethered to IoP in an organic environment the tethering reaction went to completion. The same reaction in an aqueous environment was not as efficient, but was used for several reasons. For an unexplained reason, tRNAs tethered to IoP in the organic environment could not be ethanol precipitated. The inability to be ethanol precipitated made the purification and

preparation of the oP-tRNAs much more difficult. In the aqueous environment the oP-tRNAs acted like native tRNAs and could be readily precipitated with ethanol. In the aqueous tethering reaction the amount of IoP used was cut drastically to ensure no free IoP would be left in the tRNA sample after purification of oP-tRNAs.

One peculiar characteristic of tRNA<sup>Glu</sup> was its migration on APM gels. If the thiol group on base 34 was shielded or destroyed, tRNA<sup>Glu</sup> migrated as an unthiolated tRNA. Unmodified thiol-containing tRNA<sup>Glu</sup> migrated much farther than expected, suggesting the sulfhydryl group is not readily accessible. Yet, IoP could be tethered to the tRNA, indicating that the sulfhydryl group was indeed present. Circular dichroism studies have shown the sulfhydryl group to be freely accessible to the solvent, not base paired or hidden within the secondary structure of the tRNA (105). The most probable explanation for this discrepancy is within base 34 of tRNA<sup>Glu</sup> itself. Base 34 is hypermodified, containing a methylaminomethyl group on the C5 position in addition to the sulfhydryl group at the C2 position. The hypermodification possibly shielded base U34 from the gel matrix, thereby not allowing the gel matrix to bind to and retard the migration of tRNA<sup>Glu</sup>.

An elaborate tRNA end-labeling procedure was required due to the high rate of tRNA degradation and by the fact that these degradation products label faster. The majority of degradation in the tRNA labeling process came from the nucleases present in the SAP. It is commonly known that even highly purified SAP contains some residual nuclease contamination which can potentially generate substantial quantities of degradation products. From experience with DNA oligomers it was found that the



shorter probes labeled better. It is believed that the shorter DNA probes have higher diffusion rates, which allow the shorter fragments to be bound by the kinase faster relative to the larger probes. Thus, shorter molecules typically label better than larger ones. It is not known why there were no N-1 or N-2 degradation products seen in the purification gels.

Binding studies performed with the various end-labeled tRNAs provided a great deal of information. As with the microhelices, tRNAs should bind to the P-site on programmed 30S subunits. Binding studies with unmodified tRNA<sup>Phe</sup> demonstrated the ability of the tRNA to bind to poly-U programmed 30S subunits at about 80%. This value is consistent with previous tRNA<sup>Phe</sup> binding studies. No binding studies were done with oP-tRNA<sup>Phe</sup>.

However, concurrent and previous experiments have shown that oP-modification of tRNA<sup>Phe</sup> does not alter its function. These previous studies showed that oP-tRNA<sup>Phe</sup> bound to programmed 70S ribosomes, and competed with excesses of yeast tRNA<sup>Phe</sup> and *E. coli* N-acylphenylalanine-tRNA<sup>Phe</sup> (N-AcPhe-tRNA<sup>Phe</sup>) as expected. Additionally, oP-tRNA<sup>Phe</sup> could be acylated, and was functional in translation (poly-Phe synthesis) and could undergo the puromycin reaction (77,104). Since oP modification of tRNA<sup>Phe</sup> seemingly does not alter its ability to participate in translation, oP-tRNA<sup>Phe</sup> should be able to bind to programmed 30S ribosomal subunits.

Binding of tRNA<sup>Glu</sup> was about 30%, as was the binding of the NoP mock control tRNA<sup>Glu</sup>. The binding of these two should have been and were nearly identical. This is due to the fact that NoP cannot attach to the thiol-modified base within the tRNA;

thus no chemical or physical modification of tRNA<sup>Glu</sup> took place. Since the binding of the mock tRNA<sup>Glu</sup> and the unmodified tRNA<sup>Glu</sup> were equal, this indicated that the tethering reaction did not alter the tRNAs ability to bind to programmed 30S ribosomal subunits.

In the competition reaction, a five-fold excess of unmodified tRNA<sup>Glu</sup> was added to the reaction also containing end-labelled oP-tRNA<sup>Glu</sup>, and binding dropped to 8%. Since the two competed in a linear fashion, the implications are that the two were competing for the same binding site on the ribosome. If there are multiple binding sites (with different binding constants) or phenanthroline causes oP-tRNA<sup>Glu</sup> to stick to the 30S subunit, the binding of oP-tRNA<sup>Glu</sup> in the competition reaction should not decrease linearly. oP-tRNA<sup>Glu</sup> bound at about 10%. In the competition reaction similar binding was seen.

The 10% binding of oP-tRNA<sup>Glu</sup> was considered questionable and not pursued. Attachment of phenanthroline to base 34 of tRNA<sup>Glu</sup> apparently prevents binding. This is not surprising, when one considers the fact that base 34 is the "wobble base" of the tRNA and involved in codon anticodon interaction. Attaching a bulky phenanthroline to base 34 of tRNA<sup>Glu</sup> possibly prevents proper codon anticodon interaction thereby preventing binding of the oP-modified tRNA, a simple case of simple steric hinderance.

A slightly different scenario was seen with tRNA<sup>Arg</sup>. The unmodified tRNA<sup>Arg</sup>, the oP-tRNA<sup>Arg</sup>, and the mock control tRNA<sup>Arg</sup> all bound at about 45%, indicating that the tethering reaction and oP-modification did not alter the ability of tRNA<sup>Arg</sup> to bind to

programmed 30S subunits. In the competition reaction oP-tRNA<sup>Arg</sup> binding dropped to nearly 8%, close to the expected value. This suggests oP-tRNA<sup>Arg</sup> was not binding to a non-specific binding site.

As discovered by experience, tRNA binding varied from tRNA to tRNA, and the presence of a homopolymer (poly-U) mRNA analog, a heteropolymer (poly-AG) mRNA analog, or a designed message affected tRNA binding. The binding of unmodified tRNA<sup>Glu</sup> (30%) may have been weaker than unmodified tRNA<sup>Phe</sup> (80%) because of the synthetic mRNA analogs used. Poly-U has the potential to slide in the mRNA binding track within the channel, and tRNA<sup>Phe</sup> will lock it into place. With poly-U as a messenger analog there are no sequence or frame constraints which inherently allow tRNA<sup>Phe</sup> to bind well. With tRNA<sup>Glu</sup>, the mRNA analog, poly AG, has to have the right sequence (GAA) and tRNA<sup>Glu</sup> has to find this sequence in the P-site to form the proper codon anticodon interaction. For this reason binding by tRNA<sup>Glu</sup> may never be as high as that of tRNA<sup>Phe</sup>. The use of designed messages typically leads to lower binding. This may be due to the fact that mRNA-A1 has only one base triplet that allows correct codon anticodon interaction. Thus, the odds of an unmodified tRNA<sup>Arg</sup> base pairing at the P-site were lower because it takes longer for the tRNA to find a properly aligned mRNA even though mRNA-A1 has an antiShine-Dalgarno sequence.

The first cleavage experiments were done with tRNA<sup>Glu</sup> using the free IoP controls. In these experiments no cleavages were seen in the 16S rRNA. Since oP-tRNA<sup>Glu</sup> does not bind to the P-site of programmed 30S, there should have been no

cleavages on the 30S subunit. Stops corresponding to nucleotides G198/A199 in the cleavage lanes and the control lanes in the autoradiograms of tRNA<sup>Glu</sup> cleaved 30S were seen. It was known from spectrophotometer readings that free IoP remained with the tRNAs through the purification process, and it was found that roughly 20 IoPs for every tRNA were coming through the purification. With the 4:1 ratio of tRNA to ribosomes, the ratio of IoP to 30S may have been as high as 80:1. An 80-fold excess of free IoP in the cleavage lane makes it quite possible for the cleavages with tRNA<sup>Glu</sup> to have been generated by free IoP. The free IoP in the control lane may have been present in sufficient quantity to generate cleavage at the 200 region of the 16S rRNA. It seems likely that the free IoP in the cleavage and control reactions may have caused cleavage at the 200 region. The free IoP control used in this set was a very crude control for subtracting cleavages due to free IoP. A series of titration experiments performed in our lab suggested increased amounts of copper would increase the rates of cleavage.

The free IoP control could not properly control for cleavages due to free IoP because the amount of IoP added to the cleavage reaction did not equal the amount of free IoP remaining with the oP-tRNA after butanol/chloroform extraction. For this reason the free IoP control was replaced with a nitrophenanthroline "mock" control in the next series of cleavage experiments. As mentioned above, "mock" tRNAs were sent through the tethering reaction with 5-nitro-1,10-phenanthroline instead of IoP. In theory equal amounts of unreacted IoP and NoP should have passed through the purification procedure. Cleavages in the mock control would be due to free NoP and,

by subtracting the mock cleavages from the oP-tRNA cleavages, the remaining cleavages should be due to oP tethered to a tRNA.

Cleavage experiments with oP-tRNA<sup>Arg</sup> and the NoP mock controls produced three sites of cleavage: G198/A199, C840/G846, and 923-930 on the 16S rRNA. From this set of experiments alone, it is impossible to definitively state whether oP tethered to the 8- or 32-position of the tRNA generated each cleavage. However, existing data provide strong clues as to which cleavages came from position 8 and position 32 (discussed below) (Fig 4.1). The C840/G846 cleavages were in best agreement with existing data. Wollenzien's group had identified a zero-length crosslink between base A845 and the 5' and middle segment of a s<sup>4</sup>-UTP substituted mRNA (110). Since tRNA<sup>Arg</sup> contains the thiol-modified base s<sup>2</sup>C at position 32, cleavages at the 840 region from phenanthroline tethered to position 32 of the tRNA are very reasonable.

Cleavages in the 930 region are also thought to be generated by phenanthroline tethered to base s<sup>2</sup>C at position 32 of tRNA<sup>Arg</sup>. This result also agrees with the existing knowledge base. The 930 region is base paired with the 1390 region. Modeling studies done by the Wollenzine group place the 930 region on the opposite side of the 930/1390 helix with regards to the tRNA. The width of an A-form helix is slightly greater than 20Å, and with the 10Å tether anchoring phenanthroline to base C32 of tRNA<sup>Arg</sup> the data fit quite well. The tethered phenanthroline would cleave the 930 region, but may not be able to fold back and cleave the 1400 region.

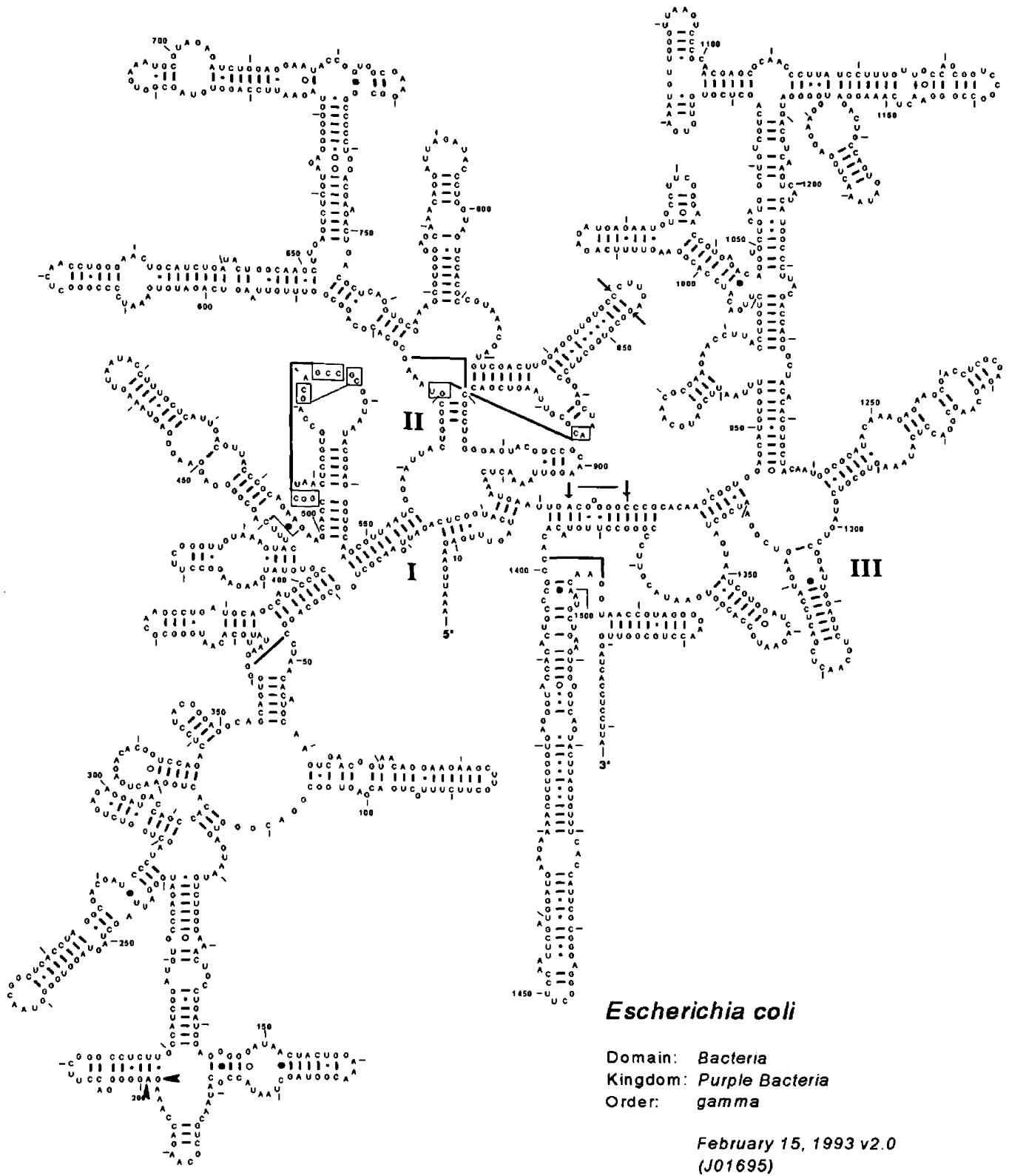


Figure 4.1 16S map showing the locations of cleavages generated by oP-tRNA<sup>Arg</sup>. Cleavages from position 32 are marked by solid arrows. Cleavages from position 8 marked by notched arrows.

No cleavages were seen at the 1400 region, thus lending further support to the validity of modeling studies placing the 930 region. Cleavages at G198/A199 are thought to be generated by phenanthroline tethered to position 8 on the tRNA<sup>Arg</sup> (discussed below).

Cleavage studies using oP-tRNA<sup>Phe</sup> and the NoP controls generated one set of cleavages in the 200 region. These cleavages were seen previously using s<sup>4</sup>-UTP-substituted transcribed tRNA<sup>Phe</sup> (8). Both tRNA<sup>Phe</sup> and tRNA<sup>Arg</sup> contain the modified base s<sup>4</sup>U at position 8. Cleavage of the 200 region of 16S rRNA by both oP-tRNA<sup>Arg</sup> and oP-tRNA<sup>Phe</sup> suggest the 200 region cleavages are due to a position 8 tethered phenanthroline. In all of the previous modeling studies the 200 region (helix 10) is located near the bottom of the 30S subunit near the cytoplasmic face along with helix 11 (4-6,53). However, there is little or no evidence localizing helix 10 at the bottom of the 30S near the cytoplasmic face. Two sets of protection studies by the Noller group are the major pieces of evidence shedding light on the location of this region. Protein S17 protected several bases within helix 11 (bases 240-290) from base modifying agents and from hydroxyl radical generating agents (70,75,96). Strong cross-links have been observed between S17 and bases within helix 11 (28,45). The neutron-scattering experiments showed protein S17 to be in the bottom of the 30S subunit closer to the cytoplasmic face (10) with helix 11.

Several bases within helix 10 and helix 11 have been protected by ribosomal protein S20 (70,75,96). But the location of S20 is currently under debate. The neutron scattering map has placed S20 in the head of the 30S subunit (13). Helix 10

and helix 11 cannot be separated by such a great distance, so some researchers want to move the placement of S20 further down in the body of the small subunit (96). There is a way to explain this discrepancy. Upon binding a protein to the naked 16S rRNA a conformational change may occur resulting in protection due to this change not a direct protein-rRNA interaction. It may also be possible for the protein to bind to an alternate site on the naked 16S rRNA, to which it does not normally bind in the intact 30S subunit.

The cleavages have been seen in the 200 region from position 8 tethered phenanthroline from three different tRNAs: thio-transcribed tRNA<sup>Phe</sup>, tRNA<sup>Phe</sup>, and tRNA<sup>Arg</sup>. Position 8 in the tRNA is in the elbow region of the tRNA, which is near the head of the 30S subunit and S20. The presence of these cleavages suggests helix 10 is located in the body near the head. If these results are true, this would constitute a major change to the previous ribosome models constituting the movement of an entire RNA domain into an already tightly packed region of the small subunit.

While the data from the cleavage experiments look great, and combined with the filter-binding assays the data look convincing, there are some problems. First, the electronic configuration of NoP differs from oP, meaning NoP may not cleave like IoP/oP or extract in the same manner as IoP. Subsequent experiments in our lab have shown differences in the patterns of cleavage by IoP, NoP, and AoP on naked 16S rRNA. The 100 region of the 23S and the 200 region of the 16S are cleaved more intensely by NoP compared to IoP and AoP. But the 840 and 920 regions of 16S were cleaved more strongly by IoP. With the observed differences in cleavage



patterns between IoP and NoP, combined with the possible differences in the extractability of IoP and NoP, serious questions as to the validity of the NoP mock control have been raised. Since approximately 20 IoPs pass through the extraction purification process along with the tRNA, there should have been enough free IoP or NoP in the cleavage reaction and controls to cause free IoP/NoP cleavage. Yet, stops were not seen in the control lanes indicating that the cleavages at the 200, 840, and 920 regions may have indeed been oP-tRNA<sup>Arg</sup> directed.

However, when oP-tRNA<sup>Phe</sup> was purified by dialysis, the 200 region cleavages disappeared. Cleavages have never been seen previously with dialyzed tRNA, but this was due to the low recovery of dialyzed oP-tRNA so that a proper experiment could not be run. Low recovery from dialysis was likely due to phenanthroline sticking to the dialysis membrane thus causing the tRNA tethered to the oP to also stick. Enough oP-tRNA<sup>Phe</sup> was recovered from the dialysis to check on an APM gel and perform a single cleavage experiment. The addition of small amounts of free IoP (4  $\mu$ M and 8  $\mu$ M) back to the cleavage reaction did not restore cleavage. This meant that there were one or two free IoPs for every tRNA. This is much less free IoP than in the extracted samples, which may have contained as many as 20 IoPs for every tRNA. The 200 region cleavages remained in the extracted oP-tRNA<sup>Phe</sup> cleavage reaction. This strongly suggests free IoP may be responsible for all cleavages seen in the previous cleavages reactions.

Dialysis proved to be a very inefficient method of tRNA purification due to poor recovery, so a new method of oP-tRNA purification had to be devised along with

updated controls. Switching to an aqueous tethering reaction followed by purification via ethanol precipitation produced oP-tRNAs with little free IoP. Removing the sulfhydryl groups from the tRNA and then utilizing them in the tethering reaction provided a very good mock control. The use of a noncognate mRNA would prevent oP-tRNA binding, but by providing a messenger RNA, cleavages due to non-specific tRNA binding could be controlled out. The two free IoP controls obviously controlled for cleavages due to free IoP on 30S with and without bound mRNA. In the cleavage experiments performed with all of these updated controls no, oP-tRNA directed cleavages of the 16S rRNA were seen. This was true for all three tRNAs used in this study. It is believed that ethanol precipitation, like dialysis, may have removed too much free IoP.

Most researchers working with phenanthroline believe that the *bis* complex (two phenanthrolines coordinated around one copper ion) is the phenanthroline species responsible for cleavage(12,23,88,89). If the *bis* phenanthroline complex is required for cleavage, there may not be enough free IoP remaining after ethanol precipitation or dialysis to form the *bis* phenanthroline complex and cause cleavage. The combined results from the cleavage experiments give no clear answers. One set of experiments (using the NoP controls) suggests that several regions of 16S rRNA are cleaved by oP tethered to a tRNA. The last set of experiments yielded no oP-tRNA directed cleavages, and the dialysis experiment suggested that cleavage may have been due to free IoP. A greater understanding of the mechanism of cleavage by phenanthroline is required before the results of these cleavage experiments can be fully understood.

This apparent lack of cleavages in no way suggests a lack of 16S rRNA at or near the decoding site. The massive amounts of cross-linking, chemical protection, and various other studies clearly and definitively show the presence of 16S rRNA at the decoding site. The mechanism of cleavage by phenanthroline is not known, and so the conditions under which maximal cleavage occur are also not known. The conditions used were designed to keep the ribosome in an active state and allow tRNA binding. If the reaction conditions could be optimized for phenanthroline cleavage from oP-tRNAs, this may provide valuable information concerning the tertiary structure of the ribosome.

Although no definite cleavages from the tRNA cleavage experiments were seen, sever conclusions can be drawn. First, phenanthroline can be tethered to naturally occurring thiol-modified bases within tRNA (Fig. 3.13 and Fig 3.14). These oP-modified tRNAs can bind to programmed 30S (Fig. 3.17). The reason for the lack of binding seen by oP-tRNA<sup>Glu</sup> is likely steric hinderance. The Cleavages seen in the experiment using the NoP control set may or may not be oP-tRNA directed.

## References

1. **Atkins, J. F., R. B. Weiss, and R. F. Gesteland.** 1990. Ribosome gymnastics--Degree of difficulty 9.5, style 10.0. *Cell* **62**:413-423.
2. **Brimacombe, R.** 1991. RNA-protein interactions in the *Escherichia coli* ribosome. *Biochimie* **73**:927-936.
3. **Brimacombe, R.** 1992. Structure-function correlations (and discrepancies) in the 16S ribosomal RNA from *Escherichia coli*. *Biochimie* **74**:319-326.
4. **Brimacombe, R.** 1995. The structure of ribosomal RNA: A three-dimensional jigsaw puzzle. *Eur.J.Biochem.* **230**:365-383.
5. **Brimacombe, R., J. Atmadja, W. Stiege, and D. Schueler.** 1988. A detailed model of the three-dimensional structure of *Escherichia coli* 16 S ribosomal RNA in situ in the 30 S subunit. *J.Mol.Biol.* **199**:115-136.
6. **Bucklin, D. J.** 1997. Mapping the mRNA binding track using phenanthroline. The University of Montana, Ph.D. dissertation.
7. **Bullard, J. M.** 1996. Mapping the ribosomal P and E sites with oP-tRNA, The University of Montana, Ph.D. dissertation.
8. **Bullard, J. M., M. A. Van Waes, D. J. Bucklin, and W. E. Hill.** 1995. Regions of 23 S ribosomal RNA proximal to transfer RNA bound at the P and E sites. *J.Mol.Biol.* **252**:572-582.
9. **Capel, M. S., D. M. Engelman, B. R. Freeborn, M. Kjeldgaard, J. A. Langer, V. Ramakrishnan, D. G. Schindler, D. K. Schneider, B. P. Schoenborn, I.-Y. Sillers, S. Yabuki, and P. B. Moore.** 1987. A complete mapping of the proteins in the small ribosomal subunit of *Escherichia coli*. *Science* **238**:1403-1406.
10. **Chen, C. B. and D. Sigman.** 1986. Nuclease activity of 1,10-phenanthroline-copper: sequence-specific targeting. *Proc.Natl.Acad.Sci.USA* **83**:7147-7151.
11. **Chen, C. B. and D. S. Sigman.** 1988. Sequence specific scission of RNA by 1,10 Phenanthroline-Copper linked to Deoxyoligonucleotides. *J.Am.Chem.Soc.* **110**:6570-6572.
12. **Corey, D. R. and P. G. Schultz.** 1987. Generation of a Hybrid Sequence-Specific Single-Stranded Deoxyribonuclease. *Science* **238**:1401-1403.

13. **Craigien, W. J., C. C. Lee, and C. T. Caskey.** 1990. Recent advances in peptide chain termination. *Mol.Microbiol.* **4**:861-865.
14. **Dahlberg, A. E.** 1989. The functional role of ribosomal RNA in protein synthesis. *Cell* **57**:525-529.
15. **Dahlberg, A. E., E. J. Murgola, H. U. Goringer, and K. A. Hizazi.** 1991. Mutations in 16S rRNA that affect UGA (stop codon)-directed translation termination. *Biochemistry* **88**:6603-6607.
16. **Dontsova, O., S. Dokudovskaya, A. Kopylov, A. Bogdanov, J. Rinke-Appel, N. Jünke, and R. Brimacombe.** 1992. Three widely separated positions in the 16S RNA lie in or close to the ribosomal decoding region; A site-directed cross-linking study with mRNA analogues. *EMBO J.* **11**:3105-3116.
17. **Dorsch, M., E. Moreno, and E. Stackebrandt.** 1989. Nucleotide sequence of the 16S rRNA from *Brucella abortus*. *Nucleic Acids Res.* **17**:1765
18. **Döring, T., P. Mitchell, M. Osswald, D. Bochkariov, and R. Brimacombe.** 1994. The decoding region of 16S RNA; a cross-linking study of the ribosomal A, P and E sites using tRNA derivatized at position 32 in the anticodon loop. *EMBO J.* **13**:2677-2685.
19. **Frank, J., P. Penczek, R. Grassucci, and S. Srivastava.** 1991. Three-dimensional reconstruction of the 70S *Escherichia coli* ribosome in ice: The distribution of ribosomal RNA. *J.Cell Biol.* **115**:597-605.
20. **Friederich, M. W., F.-U. Gast, E. Vacano, and P. J. Hagerman.** 1995. Determination of the angle between the anticodon and aminoacyl acceptor stems of yeast phenylalanyl tRNA in solution. *Proc.Natl.Acad.Sci.USA* **92**:4803-4807.
21. **Gallagher, J., C. B. Chen, C. Q. Pan, D. M. Perrin, and D. S. Sigman.** 1996. Optimizing the targeted chemical nuclease activity of 1,10-phenanthroline-copper by ligand modification. *Bioconjugate Chem.* **7**:413-420.
22. **Gluick, T.** 1994. Modification of oligodeoxyribonucleotides and application to the study of ribosomal RNA. Ph.D. thesis, University of Montana, Missoula, Montana.
23. **Gnirke, A., U. Geigenmüller, H. Rheinberger, and K. H. Nierhaus.** 1989. The allosteric three-site model for the ribosomal elongation cycle. XX Analysis with a heteropolymeric mRNA. *J.Biol.Chem.* **264**:7291-7301.
24. **Goringer, H. U. and B. Kleuvers.** 1990. The involvement of base 1054 in 16S rRNA for UGA stop codon dependant translational termination. *Nucleic Acids Res.*

18:5625-5632.

25. **Goringer, H. U., C. D. Prescott, and B. Kleuvers.** 1991. A rRNA-mRNA base pairing model for UGA-dependant termination. *Biochimie* 73:1121-1129.

26. **Graham, D. R., L. E. Marshall, K. A. Reich, and D. S. Sigman.** 1980. *J.Am.Chem.Soc.* 102:5419-5422.

27. **Greuer, B., M. Osswald, R. Brimacombe, and G. Stoffler.** 1987. RNA-Protein Crosslinking in *Escherichia coli* 30S Ribosomal Subunits; Determination of sites on 16S RNA that are Crosslinked to proteins S3, S4, S5, S7, S8, S9, S11, S13, S17, S19, S21 by Treatment with w-bis-(2-chloroethyl)-methylamine. *Nucleic Acids Res.* 15:3241-3255.

28. **Gutell, R. R., H. F. Noller, and C. R. Woese.** 1986. Higher Order Structure in Ribosomal RNA. *EMBO J.* 5:1111-1113.

29. **Gutell, R. R., B. Weiser, C. R. Woese, and H. F. Noller.** 1985. Comparative Anatomy of 16S-like Ribosomal RNA, p.155-216. In Anonymous Prog. Nucl. Acid Res. and Mol. Biol. Academic Press, New York.

30. **Gutell, R. R. and C. R. Woese.** 1990. Higher order structural elements in ribosomal RNAs: Pseudo-knots and the use of noncanonical pairs. *Proc.Natl.Acad.Sci.USA* 87:663-667.

31. **Hansen, P., B. F. C. Clark, and H. Petersen.** 1987. Interaction between non-formylated initiator Met-tRNA<sup>fMet</sup> and the ribosomal A-site from *Escherichia coli* *Biochimie* 69:871-877.

32. **Hartz, D., D. S. McPheeters, and L. Gold.** 1989. Selection of the initiator tRNA by *Escherichia coli* initiation factors. *Genes Dev.* 3:1899-1912.

33. **Heilik, G. M. and H. F. Noller.** 1996. Site-directed hydroxyl radical probing of the rRNA neighborhood of ribosomal protein S5. *Science* 272:1659-1662.

34. **Hill, W. E., D. J. Bucklin, J. M. Bullard, A. L. Galbraith, N. V. Jammi, C. C. Rettberg, B. S. Sawyer, and M. A. Van Waes.** 1995. Identification of ribosome-ligand interactions using cleavage reagents. *Biochem.Cell Biol.* 73:1033-1039.

35. **Hill, W. E., D. G. Camp, W. E. Tapprich, and A. Tassanakajohn.** 1111. Probing ribosome structure and function using short oligodeoxyribonucleotides, p.in pressAnonymousMeth. in Enz, ribosomes.

36. **Hill, W. E., D. G. Camp, W. E. Tapprich, and A. Tassanakajohn.** 1988. Probing

ribosome structure and function using short oligodeoxyribonucleotides. *Meth.Enzymol.* **164**:401-418.

37. **Hill, W. E. and R. J. Fessenden.** 1974. Structural studies on the 30 S ribosomal subunit from *Escherichia coli*. *J.Mol.Biol.* **90**:719-726.

38. **Hill, W. E. and A. Tassanakajohn.** 1987. Probing Ribosome Structure using Short Oligodeoxyribonucleotides: The Question of Resolution. *Biochimie* **69**:1071-1080.

39. **Holley, R. W., J. Aagar, G. A. Everett, J. T. Madison, M. Marquisee, S. H. Merrill, J. R. Penswick, and A. Zamir.** 1965. Structure of a ribonucleic acid. *Science* **147**:1462-1465.

40. **Huttenhofer, A. and H. F. Noller.** 1994. Footprinting mRNA-ribosome complexes with chemical probes. *EMBO J.* **13**:3892-3901.

41. **Hyde, E. L. and B. R. Reid.** 1985. NMR studies of ion binding to *Escherichia coli* tRNA<sup>Phe</sup>. *Biochemistry* **24**:4315-4325.

42. **Joseph, S. and H. F. Noller.** 1996. Mapping the rRNA neighborhood of the acceptor end of tRNA in the ribosome. *EMBO J.* **15**:910-916.

43. **Kim, S. H., F. L. Suddath, G. J. Quigley, J. L. McPherson, J. L. Sussman, A. H. J. Wang, N. C. Seeman, and A. Rich.** 1974. Three-dimensional tertiary structure of yeast phenylalanine transfer RNA. *Science* **185**:435-440.

44. **Kyriatsoulis, A., P. Maly, B. Greuer, R. Brimacombe, G. Stoeffler, R. Frank, and H. Bloecker.** 1986. RNA-protein cross-linking in *Escherichia coli* ribosomal subunits: localization of sites on 16S RNA which are cross-linked to proteins S17 and S21 by treatment with 2-iminothiolane. *Nucleic Acids Res.* **14**:1171-1186.

45. **Ladner, J. A. and J. E. Klug.** 1976. Crystallographic refinement of yeast phenylalanine transfer RNA at 2.5Å resolution. *J.Mol.Biol.* **108**:619-649.

46. **Lake, J. A.** 1985. Evolving ribosome structure: Domains in archaebacteria, eubacteria, eocytes and eukaryotes. *Annu.Rev.Biochem.* **54**:507-530.

47. **Lake, J. A. and L. Kahan.** 1975. Ribosomal proteins S5, S11, S13 and S19 localized by electron microscopy of antibody-labeled subunits. *J.Mol.Biol.* **99**:631-644.

48. **Lake, J. A. and W. A. Strycharz.** 1981. Ribosomal Proteins L1, L17 and L27 from *Escherichia coli* Localized at Single Sites on the Large Subunit by Immune Electron Microscopy. *J.Mol.Biol.* **153**:979-992.

49. **Lata, K. R., R. K. Agrawal, P. Penczek, R. Grassucci, J. Zhu, and J. Frank.** 1996. Three-dimensional reconstruction of the *Escherichia coli* 30 S ribosomal subunit in ice. *J.Mol.Biol.* **262**:43-52.
50. **Lodmell, J. S., W. E. Tappich, and W. E. Hill.** 1993. Evidence for a conformational change in the exit site of the *Escherichia coli* ribosome upon tRNA binding. *Biochemistry* **32**:4067-4072.
51. **Maitra, M., E. A. Stringer, and A. Chaudhuri.** 1982. Initiation factors in protein biosynthesis. *Annu.Rev.Biochem.* **51**:869-900.
52. **Malhotra, A. and S. C. Harvey.** 1994. A quantitative model of the *Escherichia coli* 16S RNA in the 30S ribosomal subunit. *J.Mol.Biol.* **240**:308-340.
53. **Marconi, R. T. and W. E. Hill.** 1988. Identification of defined sequences in domain V of *E. coli* 23S rRNA in the 50S subunit accessible for hybridization with complementary oligodeoxyribonucleotides. *Nucleic Acids Res.* **16**:1603-1615.
54. **Marshall, L., D. R. Graham, K. A. Reich, and D. S. Sigman.** 1981. *Biochemistry* **20**:244-250.
55. **Moazed, D. and H. F. Noller.** 1986. Transfer RNA shields specific nucleotides in 16S ribosomal RNA from attack by chemical probes. *Cell* **47**:985-994.
56. **Moazed, D. and H. F. Noller.** 1989. Transfer RNA shields specific nucleotides in 16S ribosomal RNA from attack by chemical probes Intermediate states in the movement of transfer RNA in the ribosome. *Cell* **342**:142-148.
57. **Moazed, D. and H. F. Noller.** 1989. Interaction of tRNA with 23S rRNA in the ribosomal A, P, and E sites. *Cell* **57**:585-597.
58. **Moazed, D. and H. F. Noller.** 1989. Intermediate states in the movement of transfer RNA in the ribosome. *Nature* **342**:142-148.
59. **Moazed, D. and H. F. Noller.** 1990. Binding of tRNA to the ribosomal A and P sites protects two distinct sets of nucleotides in 16 S rRNA. *J.Mol.Biol.* **211**:135-145.
60. **Moine, H. and A. E. Dahlberg.** 1994. Mutations in helix 34 of *Escherichia coli* 16 S ribosomal RNA have multiple effects on ribosome function and synthesis. *J.Mol.Biol.* **243**:402-412.
61. **Moore, P. B., D. M. Engelman, and B. P. Schoenborn.** 1975. A neutron scattering study of the distribution of protein and RNA in the 30S ribosomal subunit of *Escherichia coli*. *J.Mol.Biol.* **91**:101-120.



62. **Murgola, E. J., K. A. Hijazi, H. U. Göringer, and A. E. Dahlberg.** 1988. Mutant 16S ribosomal RNA: A codon-specific translational suppressor. *Proc.Natl.Acad.Sci.USA* **85**:4162-4165.
63. **Nekhai, S. A. and E. M. Saminsky.** 1994. On the binding of isolated yeast tRNA<sup>Phe</sup> anticodon arm to *Escherichia coli* 30S and 70S ribosomes. Guanosine-42 is important for the binding. *Biochim.Biophys.Acta* **1218**:21-26.
64. **Nierhaus, K., C. Prescott, and L. Krabben.** 1991. Ribosomes containing the C1054-deletion in *E.coli* 16S rRNA act as suppressors at all three nonsense codons. *Nucleic Acids Res.* **19**:5281-5283.
65. **Nierhaus, K. H.** 1990. The allosteric three-site model for the ribosomal elongation cycle: Features and future. *Biochemistry* **29**:4997-5008.
66. **Nierhaus, K. H., D. Beyer, M. Dabrowski, M. A. Schäfer, C. M. T. Spahn, J. Wadzack, J. U. Bittner, N. Burkhardt, G. Diedrich, R. Jünemann, D. Kamp, H. Voss, and H. B. Stuhmann.** 1995. The elongating ribosome: Structural and functional aspects. *Biochem.Cell Biol.* **73**:1011-1021.
67. **Nikonowicz, E., V. Roongta, C. R. Jones, and D. G. Gorenstein.** 1989. Two-dimensional <sup>1</sup>H and <sup>31</sup>P NMR spectra and restrained molecular dynamics structure of an extrahelical adenosine tridecamer oligodeoxyribonucleotide duplex. *Biochemistry* **28**:8714-8725.
68. **Noller, H. F.** 1991. Ribosomal RNA and Translation. *Annu.Rev.Biochem.* **60**:191-227.
69. **Noller, H. F., R. Green, G. Heilek, V. Hoffarth, A. Hüttenhofer, S. Joseph, I. Lee, K. Lieberman, A. Mankin, C. Merlyman, T. Powers, E. Viani Puglisi, R. R. Samaha, and B. Weiser.** 1995. Structure and function of ribosomal RNA. *Biochem.Cell Biol.* **73**:997-1009.
70. **Noller, H. F., V. Hoffarth, and L. Zimniak.** 1992. Unusual resistance of peptidyl transferase to protein extraction procedures. *Science* **256**:1416-1419.
71. **Noller, H. F., J. Kop, V. Wheaton, J. Brosius, R. R. Gutell, A. M. Kopylov, and W. Herr.** 1981. Secondary Structure Model for 23S Ribosomal RNA. *Nucleic Acids Res.* **9**:6167-6189.
72. **Osswald, M., T. Döring, and R. Brimacombe.** 1995. The ribosomal neighbourhood of the central fold of tRNA: Cross-links from position 47 of tRNA located at the A, P or E site. *Nucleic Acids Res.* **23**:4635-4641.

73. **Powers, T., G. Daubresse, and H. F. Noller.** 1993. Dynamics of *in vitro* assembly of 16 S rRNA into 30 S ribosomal subunits. *J.Mol.Biol.* **232**:362-374.
74. **Powers, T. and H. F. Noller.** 1995. Hydroxyl radical footprinting of ribosomal proteins on 16S rRNA. *RNA.* **1**:194-209.
75. **Prince, J. B., B. H. Taylor, D. L. Thurlow, J. Ofengand, and R. A. Zimmermann.** 1982. Covalent crosslinking of tRNA-val to 16S RNA at the ribosomal P site: identification of the crosslinked residues. *Proc.Natl.Acad.Sci.USA* **79**:5450-5454.
76. **Retberg, C. C.** 1995. Site-specific scission of ribosomal RNA by 1,10-phenanthroline linked to transfer RNA, The University of Montana, M.S. thesis.
77. **Rheinberger, H., U. Geigenmüller, A. Gnirke, T. Hausner, J. Remme, H. Saruyama, and K. H. Nierhaus.** 1990. Allosteric Three-Site Model for the Ribosomal Elongation Cycle, p.318-330. In W.E. Hill, A.E. Dahlberg, R.A. Garrett, P.B. Moore, D. Schlessinger, and J.R. Warner (ed.), *The Ribosome: Structure, Function and Evolution*, American Society for Microbiology, Washington, D.C.
78. **Rheinberger, H. and K. H. Nierhaus.** 1986. Allosteric interactions between the ribosomal transfer RNA-binding sites A and E. *J.Biol.Chem.* **261**:9133-9139.
79. **Rinke-Appel, J., N. Jünke, R. Brimacombe, S. Dokudovskaya, O. Dontsova, and A. Bogdanov.** 1993. Site-directed cross-linking of mRNA analogues to 16S ribosomal RNA; A complete scan of cross-links from all positions between '+1' and '+16' on the mRNA, downstream from the decoding site. *Nucleic Acids Res.* **21**:2853-2859.
80. **Rinke-Appel, J., N. Jünke, M. Osswald, and R. Brimacombe.** 1995. The ribosomal environment of tRNA: Crosslinks to rRNA from positions 8 and 20:1 in the central fold of tRNA located at the A, P, or E site. *RNA.* **1**:1018-1028.
81. **Rose, S. I. L. I., P. Lowary, and O. Uhlenbeck.** 1983. Binding of Yeast tRNA-phe Anticodon Arm to E. coli 30S Ribosomes. *J.Mol.Biol.* **167**:103-117.
82. **Roy, S. and A. G. Redfield.** 1983. Assignment of imino proton spectra of yeast phenylalanine transfer ribonucleic acid. *Biochemistry* **22**:1386-1390.
83. **Schaeffer, F., S. Rimsky, and A. Spassky.** 1996. DNA-stacking interactions determine the sequence specificity of the deoxyribonuclease activity of 1,10-phenanthroline-copper ion. *J.Mol.Biol.* **260**:523-539.
84. **Schwartz, I. and J. Ofengand.** 1978. Photochemical Cross-linking of Unmodified Acetylvalyl-tRNA to 16S RNA at the Ribosomal P Site. *Biochemistry* **17**:2524-2530.

85. **Shine, J. and L. Dalgarno.** 1974. The 3'-Terminal Sequence of *Escherichia coli* 16S Ribosomal RNA: Complementarity to Nonsense Triplets and Ribosome Binding Sites. *Proc.Natl.Acad.Sci.USA* 71:1342-1346.
86. **Shine, J. and L. Dalgarno.** 1975. Terminal-sequence analysis of bacterial ribosomal RNA. Correlation between the 3'-terminal-polypyrimidine sequence of 16-S RNA and translational specificity of the ribosome. *Eur.J.Biochem.* 57:221-230.
87. **Sigman, D. S.** 1986. Nuclease activity of 1,10-phenanthroline-copper ion. *Accounts of Chemical Research* 19:180-185.
88. **Sigman, D. S., A. Mazumder, and D. M. Perrin.** 1993. Chemical nucleases. *Chem.Rev.* 93:2295-2316.
89. **Simon, S. S., S. Grabowski, and G. M. Whitesides.** 1990. Convenient synthesis of cytidine 5'-triphosphate, guanosine 5'-triphosphate, and uridine 5'-triphosphate and their use in the preparation of UDP-glucose, UDP-glucuronic acid, and GDP-mannose. *J.Org.Chem.* 55:1834-1841.
90. **Smith, D. and M. Yarus.** 1989. Transfer RNA structure and coding specificity. II. A D-arm tertiary interaction that restricts coding range. *J.Mol.Biol.* 206:503-511.
91. **Smith, D. and M. Yarus.** 1989. Transfer RNA structure and coding specificity. I. Evidence that a D-arm mutation reduces tRNA dissociation from the ribosome. *J.Mol.Biol.* 206:489-501.
92. **Sprinzi, M., T. Hartmann, F. Meissner, J. Moll, and T. Vorderwulbecke.** 1987. Compilation of tRNA sequences and sequences of tRNA genes. *Nucleic Acids Res.* 15:r53-r188.
93. **Sprinzi, M., T. Hartmann, J. Weber, J. Blank, and R. Zeidler.** 1989. Compilation of tRNA sequences and sequences of tRNA genes. *Nucleic Acids Res.* 17:r1-r95.
94. **Stark, H., F. Mueller, E. V. Orlova, M. Schatz, P. Dube, T. Erdemir, F. Zemlin, R. Brimacombe, and M. Van Heel.** 1995. The 70S *Escherichia coli* ribosome at 23 Å resolution: Fitting the ribosomal RNA. *Structure* 3:815-821.
95. **Stem, S., T. Powers, L.-M. Changchien, and H. F. Noller.** 1989. RNA-protein interactions in 30S ribosomal subunits: Folding and function of 16S rRNA. *Science* 244:783-790.
96. **Stem, S., R. C. Wilson, and H. F. Noller.** 1986. Localization of the binding site for protein S4 on 16 S ribosomal RNA by chemical and enzymic probing and primer

extension. *J.Mol.Biol.* **192**:101-110.

97. **Stiege, W., K. Stade, D. Schuler, and R. Brimacombe.** 1988. Covalent cross-linking of poly(A) to *Escherichia coli* ribosomes, and localization of the cross-link site within the 16S RNA. *Nucleic Acids Res.* **18**:2369-2388.

98. **Stoffler-Meilicke, M. and G. Stoffler.** 1990. Topography of the ribosomal proteins from *Escherichia coli* within the intact subunits as determined by immunoelectron microscopy and protein-protein cross-linking. p.123-133. In W.E. Hill, A.E. Dahlberg, R.A. Garrett, P.B. Moore, D. Schlessinger, and J.R. Warner (ed.), *The ribosome: structure, function, and evolution*, American Society for Microbiology Press, Washington, DC.

99. **Sussman, J. L. and S. H. Kim.** 1976. Three-dimensional structure of transfer RNA in two crystal forms. *Science* **192**:853-858.

100. **Tam, M. F., J. A. Dodd, and W. E. Hill.** 1981. Physical Characteristics of 16S rRNA under Reconstitution Conditions. *J.Biol.Chem.* **256**:6430-6434.

101. **Tate, W. P. and C. T. Caskey.** 1981. Termination of protein synthesis, p.81-100. In G. Spedding (ed.), *Ribosomes and proteins synthesis: a practical approach*, Oxford University Press, Oxford, UK.

102. **Triana-Alonso, F. J., M. Dabrowski, J. Wadzack, and K. H. Nierhaus.** 1995. Self-coded 3' extension of run-off transcripts produces aberrant during in vitro transcription with T7 RNA polymerase. *J.Biol.Chem.* **270**:6298-6307.

103. **Van Waes, M. A.** 1997. tRNA-rRNA interactions in the *Escherichia coli* ribosome. The University of Montana,

104. **Watanabe, K., N. Hayashi, A. Oyama, K. Nishikawa, T. Ueda, and K. I. Miura.** 1994. Unusual anticodon loop structure found in *E.coli* lysine tRNA. *Nucleic Acids Res.* **22**:79-87.

105. **Watson, J. D.** 1964. The synthesis of proteins upon ribosomes. *Bull.Soc.Chim.Biol.* **46**:1399-1425.

106. **Weller, J. and W. E. Hill.** 1994. Probing the Interactions of Poly(U) and tRNA(Phe) with Nucleotides 1530-1542 and 1390-1417 of 16S rRNA of *Escherichia coli*. *J.Biol.Chem.* **269**:19369-19374.

107. **Weller, J. W. and W. E. Hill.** 1992. Probing Dynamic Changes in rRNA Conformation in the 30S Subunit of the *Escherichia coli* Ribosome. *Biochemistry* **31**:2748-2757.

108. **Woese, C. R., R. Gutell, R. Gupta, and H. F. Noller.** 1983. Detailed analysis of the higher-order structure of 16S-like ribosomal ribonucleic acids. *Microbiol.Rev.* **47**:621-669.
109. **Wollenzein, P. L.** 1997. Placement of the 930 region, B.S. Sawyer and W.E. Hill (ed.),
110. **Wollenzein, P. L., A. Expert-Bezancon, and A. Favre.** 1991. Sites of contact of mRNA with 16S rRNA and 23S rRNS in the *Escherichia coli* ribosome. *Biochemistry* **30**:1788-1795.
111. **Woo, N. H., B. A. Roe, and A. Rich.** 1980. Three-dimensional structure of *Escherichia coli* initiator tRNA<sup>Met</sup>. *Nature* **286**:346-351.
112. **Yarus, M. and D. Smith.** 1995. tRNA on the ribosome: a Waggle theory, p.443-469. In D. Söll and U. RajBhandary (ed.), tRNA. Structure, biosynthesis and function, ASM Press, Washington, D.C.
113. **Yokoyama, S., T. Watanabe, K. Murao, H. Ishikura, Z. Yamaizumi, S. Nishimura, and T. Miyazawa.** 1985. Molecular mechanism of codon recognition by tRNA species with modified uridine in the first position of the anticodon. *Proc.Natl.Acad.Sci.USA* **82**:4905-4909.
114. **Yonath, A., W. Bennett, S. Weinstein, and H. G. Wittmann.** 1990. Crystallography and Image Reconstructions of Ribosomes, p.134-147. In W.E. Hill, A.E. Dahlberg, R.A. Garrett, P.B. Moore, D. Schlessinger, and J.R. Warner (ed.), *The Ribosome: Structure, Function and Evolution*, American Society For Microbiology, Washington, D.C.
115. **Zimmermann, R. A., C. L. Thomas, and J. Wower.** 1990. Structure and function of rRNA in the decoding domain and at the peptidyltransferase center, p.331-347. In W.E. Hill, A.E. Dahlberg, R.A. Garrett, P.B. Moore, D. Schlessinger, and J.R. Warner (ed.), *The ribosome: structure, function, and evolution*, ASM press, Washington, D.C.